European wind turbine testing procedure developments. Task 1: Measurement method to verify wind turbine performance characteristics

Hunter, R.; Friis Pedersen, Troels; Dunbabin, P.; Antoniou, Ioannis; Frandsen, Sten Tronæs; Klug, H.; Albers, A.; Lee, W.K.

Publication date:
2001

Document Version
Publisher's PDF, also known as Version of record

Risø-R-1209(EN)

European Wind Turbine Testing Procedure Developments

Task 1: Measurement Method to Verify Wind Turbine Performance Characteristics

Raymond Hunter	RES	Task coordinator
Troels Friis Pedersen	RISØ	Project coordinator
Penny Dunbabin	RES	
Ioannis Antoniou	RISØ	
Sten Frandsen	RISØ	
Helmut Klug	DEWI	
Axel Albers	DEWI	
Wai Kong Lee	NEL	

Risø National Laboratory, Roskilde
January 2001

Abstract
There is currently significant standardisation work ongoing in the context of wind farm energy yield warranty assessment and wind turbine power performance testing. A standards maintenance team is revising the current IEC (EN) 61400-12 Ed 1 standard for wind turbine power performance testing. The standard is being divided into four documents. Two of them are drafted for evaluation and verification of complete wind farms and of individual wind turbines within wind farms. This document, and the project it describes, has been designed to help provide a solid technical foundation for this revised standard. The work was wide ranging and addressed 'grey' areas of knowledge, regarding existing methodologies or to carry out basic research in support of fundamentally new procedures.

The work has given rise to recommendations in all areas of the work. These cover:

- Improved definition of site calibration procedures using two met masts
- Procedures for using nacelle mounted anemometry for site calibration
- Methods for checking the consistency of site calibration results
- Advice on defining nacelle-to-free-wind-speed relationships to be used for power curve verification
- Advice on placement of nacelle anemometers to minimise errors
- Recommendations on how to account for and minimise the shortcomings of the nacelle anemometer method related to inflow, induction and wake influences
- Methods for checking the consistency of power curve verifications using nacelle anemometry
- Advice on exercising caution when making estimates of the in-service uncertainties associated with wind speed and electrical power monitoring equipment
- A step-wise procedure for applying multi-variate regression analysis methods using partial residuals for identifying the functional dependency of power performance on secondary parameters
- Suggestions for more sophisticated density normalisation for actively controlled turbines

The current work was supported partly by the European Union Fourth Frame-work research program through the SMT project: "European Wind Turbine Testing Procedure Developments" , contract no. SMT4-CT96-2116.

ISBN 87-550-2752-0
ISBN 87-550-2753-9 (Internet)
ISSN 0106-2840

Print: Danka Services International A/S, 2001

Contents

Preface

This report describes research work carried out by a research consortium with researchers from seven different research institutes from five different European countries. The European Commission supported the work partly through the Standards, Measurements and Testing (SMT) research program under the Fourth Framework program. This research project, ”European Wind Turbine Testing Procedures” SMT4-CT96-2116, was divided in four different tasks. This report describes results from one of the tasks. The four tasks are:

Part 1 ”Measurement Method to Verify Wind Turbine Power Performance Characteristics”
Part 2 ”Power Quality”
Part 3 ”Blade Testing Methods”
Part 4 ”Wind Turbine Load Measurement Instrumentation”

Project coordinator: Troels Friis Pedersen, RISØ, Denmark.
Task coordinators:
Part 1 Raymond Hunter, RES, UK
Part 2 Poul Sørensen, RISØ, Denmark
Part 3 Bernard Bulder, ECN, Netherlands
Part 4 E. Morfiadakis, CRES, Greece

Part 1 ”Measurement Method to Verify Wind Turbine Power Performance Characteristics”

This published report is based on the final task report: RES 071/RES/2002.
The work was carried out by the following researchers:
Raymond Hunter, Penny Dunbabin, RES, UK
Ioannis Antoniou, Troels Friis Pedersen, Sten Frandsen, RISØ, Denmark Helmut Klug, Axel Albers, DEWI, Germany
Wai Kong Lee, NEL, UK

In Chapter 2, the work on the Enercon turbines was carried out by DEWI. The work on nacelle anemometry of a parked wind turbine for site calibration wase carried out jointly by RISØ and DEWI. In Chapter 3, the work on the Enercon turbine was carried out by DEWI. RISØ carried out the work on anemometer behaviour and on nacelle anemometry on the Elkraft turbine. In Chapter 4, the work on instrument accuracy was carried out by NEL In Chapter 5, RES carried out the work on enhancement of performance assessment analysis methods. In Chapter 6, NEL carried out the work on air density correction, based on earlier work. The work on uncertainty analysis in Chapter 7 was collated, interpreted and reported by RISØ. The various chapter authors, following discussion with relevant project participants in the project, proposed the recommendations given in Chapter 8.

1 Introduction

The ‘European Wind Turbine Testing Procedure Developments’ contract, SMT4-CT96-2116, has three formal tasks, the first of which addresses a ‘Measurement Method to Verify Wind Turbine Power Performance Characteristics’. In this context, ‘characteristics’ relate both to power production and to power quality. This report addresses only the former characteristic.
The work as specified has seven elements, these being:

Site Calibration, the aim being to develop/identify an improved procedure for calibrating the wind flows over a site prior to conducting a performance test

Nacelle Anemometry, the aim being to identify and understand the factors which affect the uncertainty inherent in the use of nacelle-mounted anemometry to estimate the wind speed incident upon a test turbine

Instrument Accuracy, the aim being to define in particular the in-service uncertainties associated with measuring wind speed and power output in a semi-stochastic environment

Analysis to Verify and Enhance the Performance Assessment Method, the aim being to understand the secondary parameter dependencies which prevent power performance being a sole function of wind speed

Air Density Correction, the aim being to develop improved ways of normalising power performance characteristics to account for variations in the air density experienced throughout the test

Proposal of New Procedures, the aim being to interpret the results of the other sub-tasks to ensure that clear recommendations are made on improved procedures.

The following texts are based upon the sub-task reports provided by the leaders of the individual sub-tasks.

Formal performance evaluation of wind turbines to recognised or common procedures has been carried out for more than 10 years. There are a number of ‘grey’ areas of knowledge relating to various aspects of such evaluations and this project has been designed to address several of them. Although the various chapters of this document may in some cases seem to be unrelated to one another, the topics of study all have particular significance in helping improve performance assessment methodologies and to allowing better evaluation of uncertainty.

2 Site Calibration

The work reported in this chapter has the following elements:

- Site Calibration in Simple Terrain
- Site Calibration in Complex Terrain
- Alternative Site Calibration in Complex Terrain
- Comparison of Methods

A more comprehensive report is to be found in Ref 2.1.
Site calibration conventionally (i.e. according to the IEC 61400-12 Ed 1 standard for Wind Turbine Performance Testing) requires the deployment of a temporary meteorological mast at the turbine position prior to erection of the turbine to allow wind conditions at the location to be correlated with those at a reference position roughly 2.5 to 4 wind turbine rotor diameters distant.

Logistical and cost considerations do not always allow or encourage such a test and it would be very useful were it to be demonstrated that the parked host wind turbine could itself be used as a temporary meteorological mast.

The work described here examines this possibility.

The vehicles for the study have been the Enercon 40 wind turbine and the Nordtank NTK 550/41 machine.

The performance of the Enercon turbine in flat terrain has been determined in strict accordance with IEC 61400-12 Ed 1.

Additionally, the relationship between the wind speed as measured by the nacelle anemometer when the turbine is parked and the free field wind speed as monitored at the reference position meteorological mast has been determined and verified at another site in flat terrain.

At a location of moderately complex terrain a conventional site calibration has been carried out using two meteorological masts. For the same site, a theoretical site calibration has been obtained using the Wind Atlas and Analysis Program (WAsP).

The flow field around a scale model of the nacelle of the Enercon turbine (rotor parked) has been examined in the wind tunnel using Laser Doppler Anemometer and the correction factor between the free wind speed and the wind speed at the nacelle anemometer position determined. This then allows a site calibration to be performed with one meteorological mast (the reference mast) and the parked wind turbine instead of two meteorological masts.

Similar wind tunnel tests have also been conducted using a model of the Nordtank turbine.

Finally, a plausibility check method for site calibrations has been examined, which is based on determining incident wind conditions from readings of the electrical power and the nacelle anemometer wind speed.

2.1 Locations of the Measurements

The topography of the measurement sites are summarised in the following sections. Fuller details are to be found in Ref 2.1.

2.1.1 Inte Wind Farm - Flat Terrain Site, Enercon 40

Inte Wind Farm is located near the German North Sea coast. The site is characterised by flat farm land with single housings. The wind farm consists of 14 Enercon 40 turbines.

Turbine 2 has been the focus of the investigation. A meteorological mast (mast 1) is located north-west of the turbine. As this mast is affected by flow distortion caused by houses and trees in a large wind direction sector a second mast has been erected south of turbine 2.

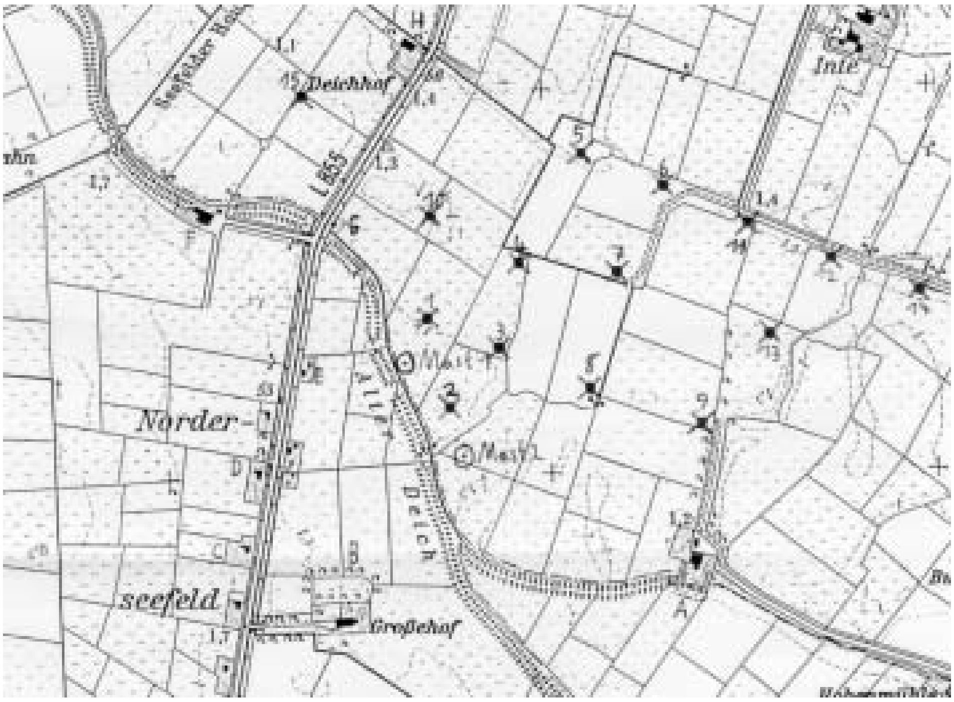

Fig. 2.1. Inte wind farm (flat terrain)

2.1.2 Schmidt - Complex Terrain Site, Enercon 40

Measurements in complex terrain were performed near the German town Schmidt in the Eifel mountains. An Enercon 40 wind turbine as well as a met mast are located at a hill top 493 m above sea level. The hill top is afforested. The largest terrain slope of about 13 % is found in south-easterly and north-easterly directions. About 700 m south-west of the turbine location is a second hill (altitude 495 m) which leads to significant differences between the wind conditions at the mast and turbine location. Very close to the Enercon 40 machine at a distance of 84 m is a second turbine, a Nedwind 44 of 500 kW rated power and 44 m rotor diameter.

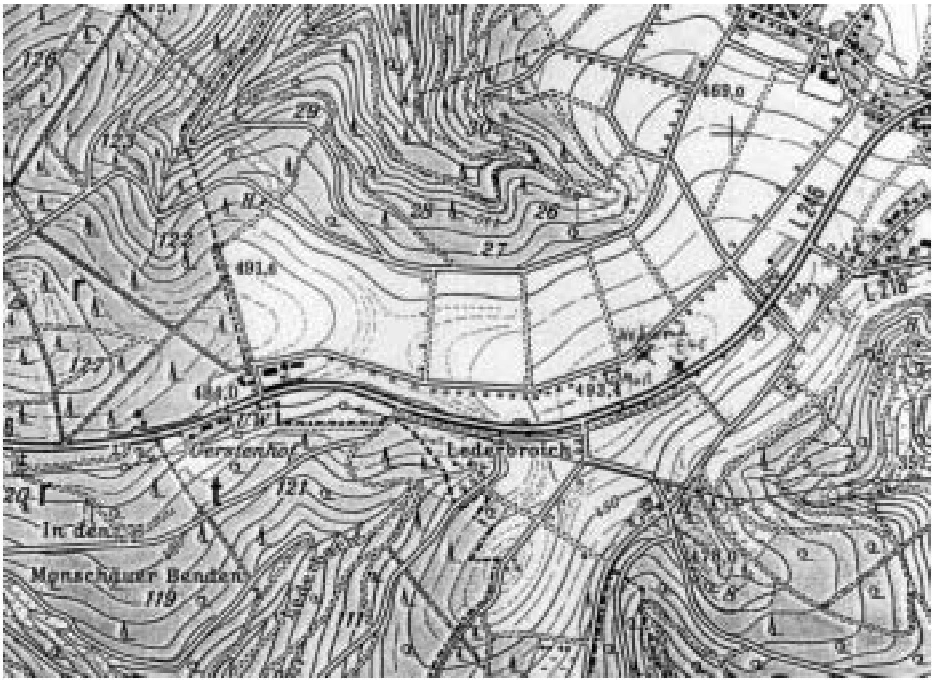

Fig. 2.2. Location of Enercon wind turbine at Schmidt in the Eifel Mountains in moderately complex terrain

2.1.3 The Enercon Turbine

The specification of the test turbine is as follows:

Rotor:

Position of Rotor:	Upwind
Direction of Rotor Axis:	Horizontal
Number of Blades:	3
Rotor Diameter:	40.3 m
Tilt Angle:	3°
Airfoil:	Enercon
Material:	GRP/Epoxy
Chord Length (Tip/Root):	0.45 m/1.92 m

Control Design:

Rotor Speed:	Variable, 18-40 min-1
Power Control:	Active Pitch
Yaw Control:	Active, Electromechanical
Cut In Wind Speed:	3 m/s
Rated Wind Speed:	12 m/s
Cut Out Wind Speed:	25 m/s
Survival Wind Speed:	70 m/s

Generator:

Type:	Synchronous Ring Generator
Power Transmission from Rotor:	Gearless, Direct Drive
Rated Power:	500 kW
Rated Voltage:	500 V
Frequency:	Variable
Speed Range:	18-40 min-1
Tower:	
Material:	Reinforced Concrete (Inte) Steel Tube (Eifel)
Hub Height:	42 m (Inte) 50 m (Eifel)

2.2 Nacelle Anemometer (Enercon 40)

A combined anemometer/wind vane manufactured by Thies is installed on the wind turbines' nacelles. The mounting arrangement on the nacelles is shown in Fig 2.3. For lightning protection the anemometers are placed within a wire lattice, Fig 2.4. As this wire lattice may have a significant influence on the anemometer's behaviour, it has been ensured that the lightning protection is aligned in the same way at all investigated turbines.

The turbine's control system provides a correction to convert the nacelle anemometer signal to ambient wind conditions, which consists of two linear equations for different wind speed ranges. As the behaviour of the pure nacelle anemometer is of interest in this project, the evaluation of the nacelle anemometer is based only on such periods in which the correction was cut off.

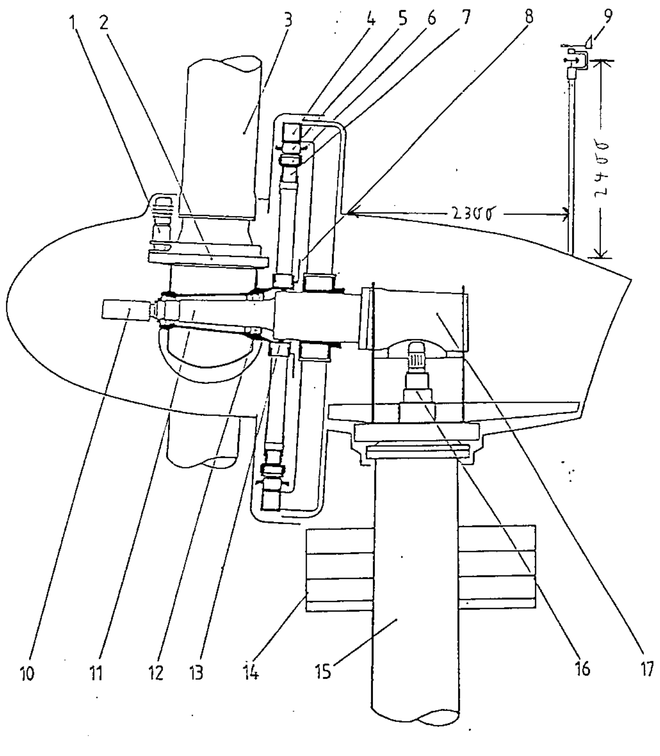

Fig. 2.3. Position of the anemometer on the Enercon nacelle

Fig. 2.4. Enercon nacelle anemometer with lightning protection

2.3 Site Calibration in Moderately Complex Terrain Using Two Met Masts

At the Schmidt site in the Eifel mountains, to get the relationship between the wind speeds at the turbine location and the location of the reference meteorological mast 170 metres distant, a wind flow calibration using two met masts was carried out over a period of three months prior to installation of the turbine. The wind speed was measured with two identical masts at 50 m height.

Fig 2.5 shows the bin averaged ratio of the two wind speeds (sorting according to 10 degree sectors, and wind speed ranges 4-16 m/s and 5-10 m/s). Although the site does not look very complex, a significant influence is recognisable at 190 degrees. This influence is probably caused by a small hill south-west of the met mast.

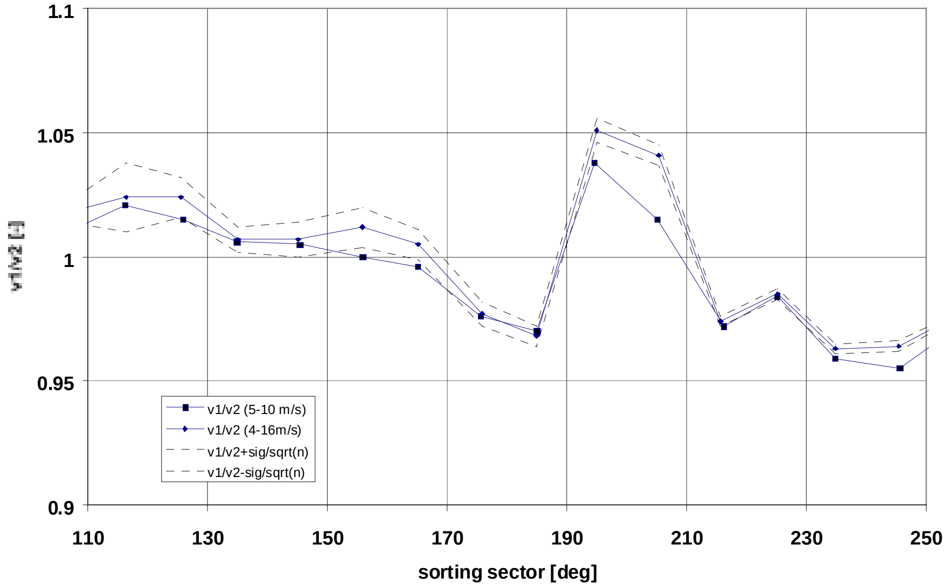

Fig. 2.5. Result of the site calibration using two met masts over a period of 3 months

IEC 61400-12 Ed 1 recommends a measuring period of at least 24 hours for each 30 degree sector. To justify these figures, we need to ask how long should the measurement period be and how small should the sorting sector be to get agreement with the long-term (assuming a period of 3 months is sufficient to get the real site conditions). For this case the site calibration was carried out for different sorting sectors from 5 to 30 degrees and different measuring periods from 4 to 36 hours (for each sector).

Fig 2.6 shows the result of the calculation for different sector sizes. Wind direction sectors of 10° seem to represent the conditions sufficiently.

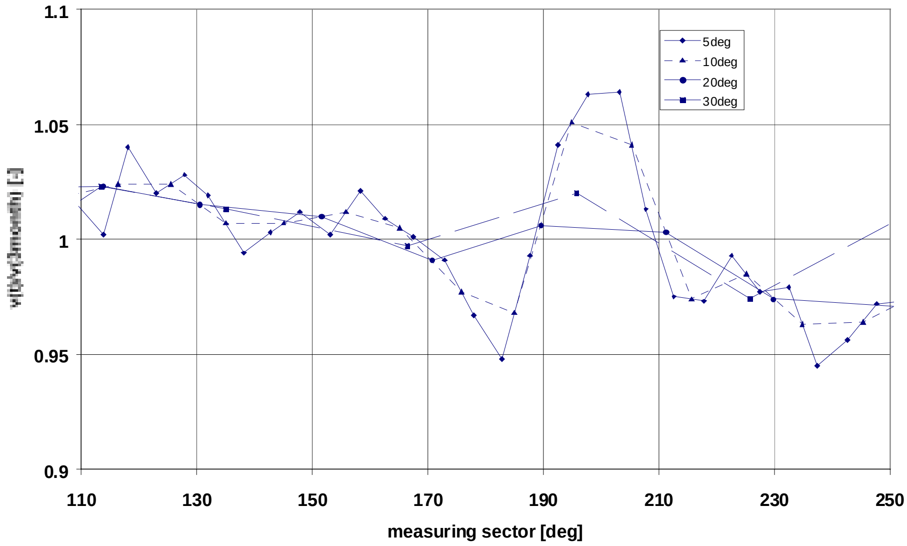

Fig. 2.6. Result of the site calibration using different wind direction sizes (4-16 m/s)

Fig 2.7 shows the results for different measuring periods. For most sectors the results of short time measuring already fit the long time average after eight hours (for each sector) with a deviation of approximately one percent.

Only for two sectors (185 ° and 195 °) is the deviation less than one percent after 24 hours (per sector). However, these are the sectors with the largest corrections to the wind speed.

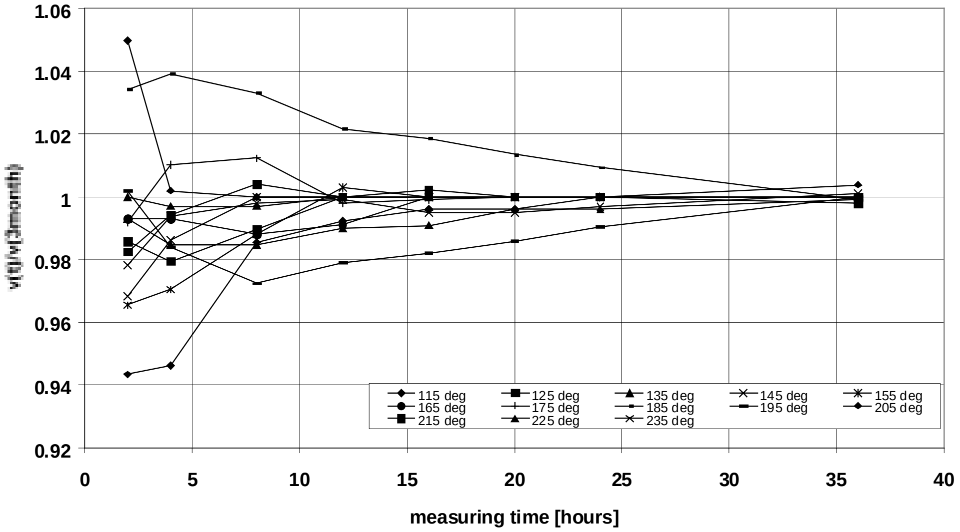

Fig. 2.7. Result of the site calibration using different measurement periods (for each sector)

To investigate if the site correction is dependent on the meteorological conditions, the collected data was sorted according to wind speed and turbulence intensity. Fig 2.8 and Fig 2.9 indicate that both wind speed and turbulence intensity influence the correction factors systematically. As not much data were available for turbulence intervals of 0-10% and 20-30%, the finding regarding the effect of turbulence intensity must be treated carefully.

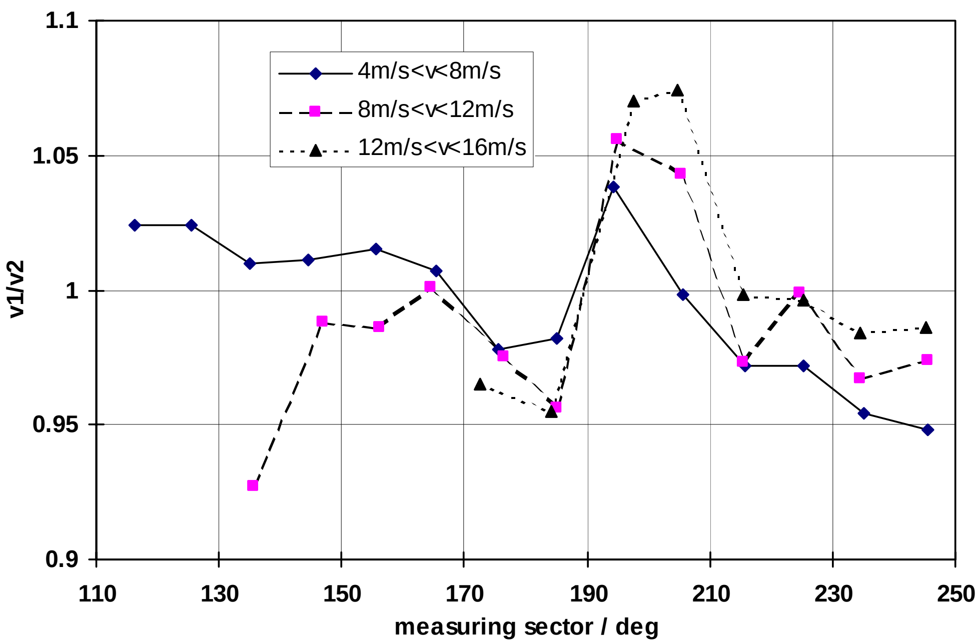

Fig. 2.8. Result of site calibration for different wind speed intervals

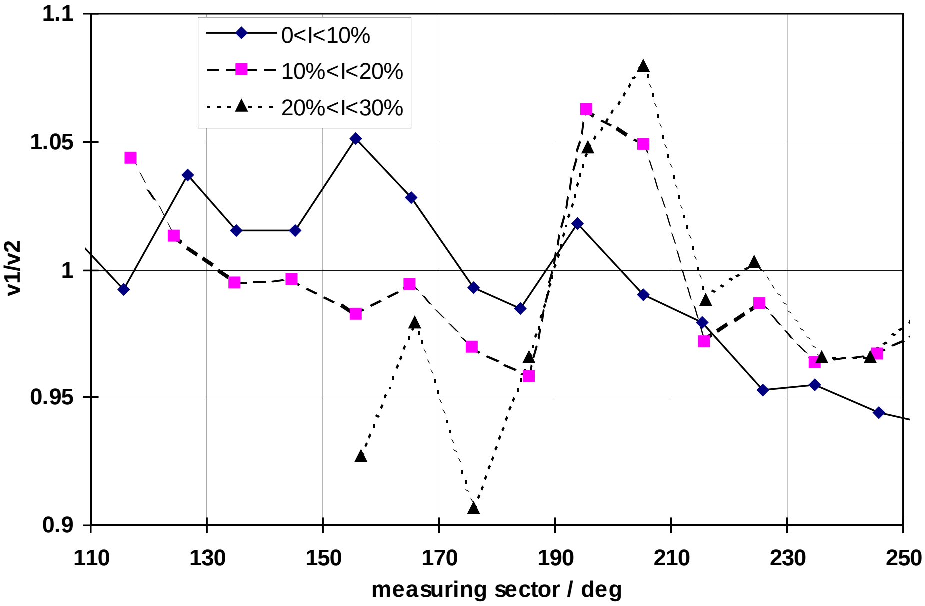

Fig. 2.9. Result of site calibration for different turbulence intensity intervals

An interesting question relates to how the apparent site calibration affects the power curve of the investigated Enercon 40 turbine. The bin-averaged power curves evaluated with the site calibration shown in Fig 2.5 (4-16m/s, 10° sectors), without site calibration and with wind speed dependent site calibration are compared in Fig 2.10. The non wind speed dependent site calibration has almost no effect on the bin averaged power curve, while the wind speed dependent site calibration shows a small effect at the particular location.

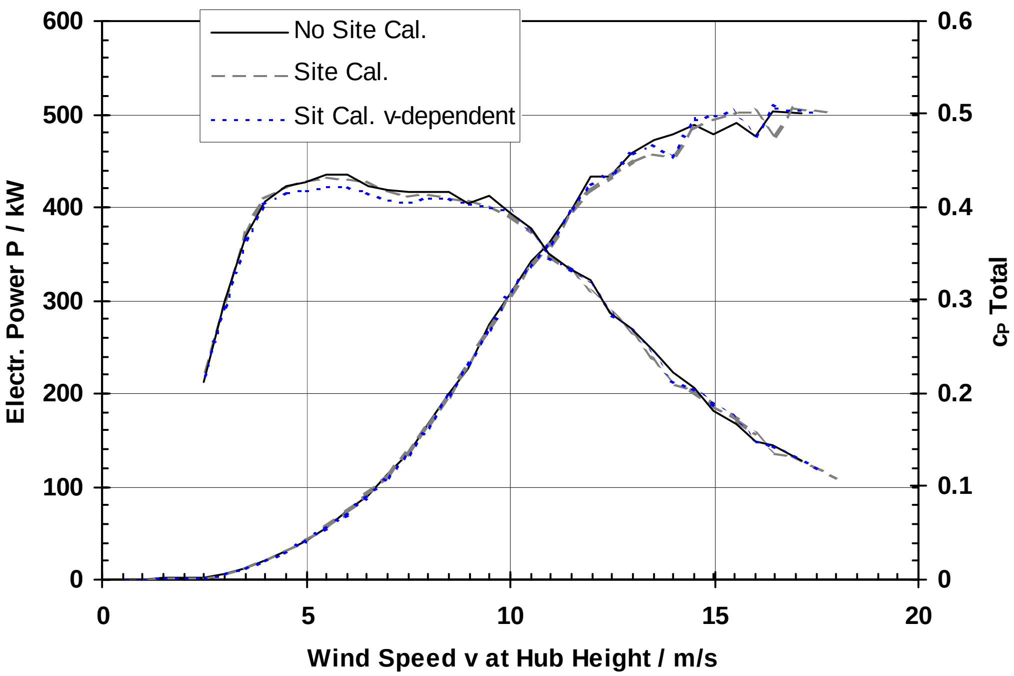

Fig 2.10. Power curves in moderately complex terrain evaluated without site calibration, with site calibration and with wind speed dependent site calibration.

Figures 2.11 and 2.12 show the raw power curve data for the flat Inte site and the semi-complex Schmidt, Eifel Mountain site.

It is clear that the scatter of the measurements is much larger in moderately complex terrain. The reason for the large data scatter is most probably due to a low correlation of the wind speed measured at the met mast and the wind speed representative of the turbine. Figures 2.13 and 2.14 show that the scatter of the power curve data is not lowered by applying the non wind speed dependent site calibration or the wind speed dependent site calibration.

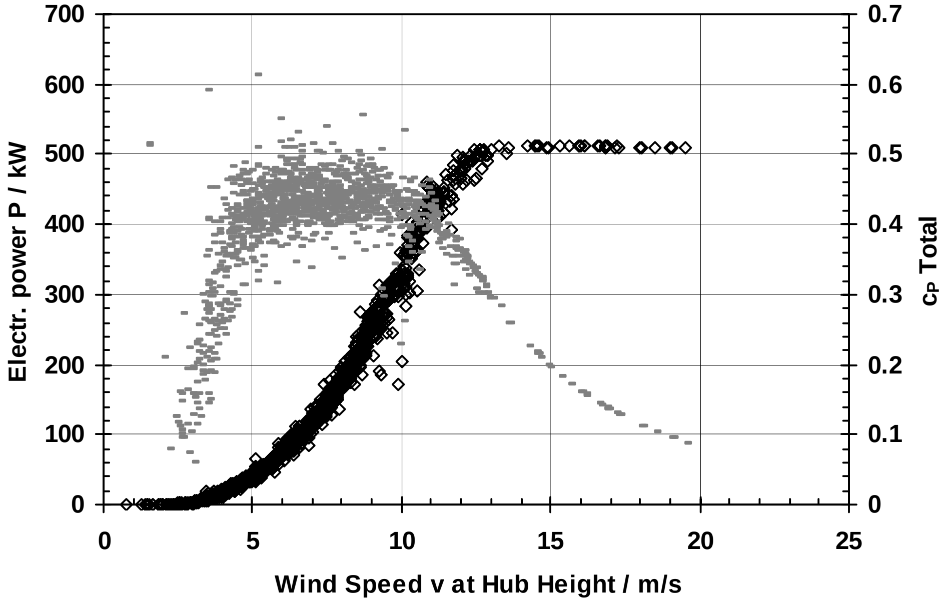

Fig 2.11. Raw power versus wind speed data for the flat site at Inte

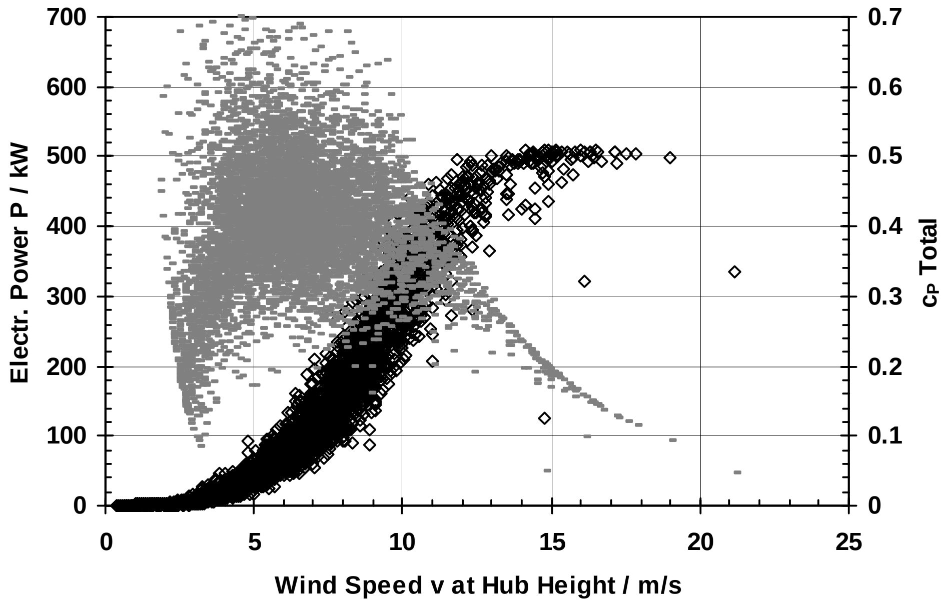

Fig 2.12. Power curve raw data in moderately complex terrain at Schmidt, Eifel Mountains evaluated with met mast without site calibration

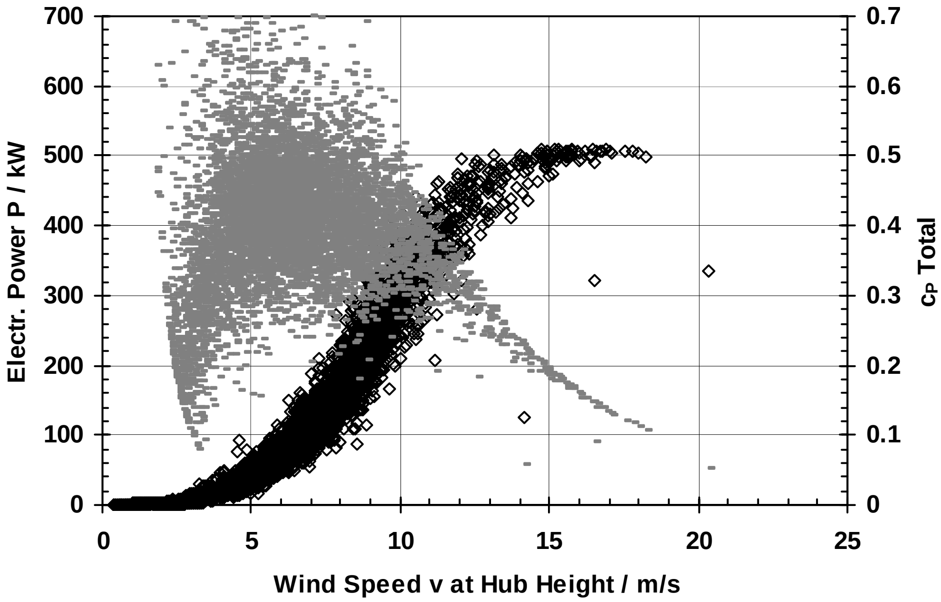

Fig 2.13. Power curve raw data in moderately complex terrain at Schmidt based on met mast and site calibration

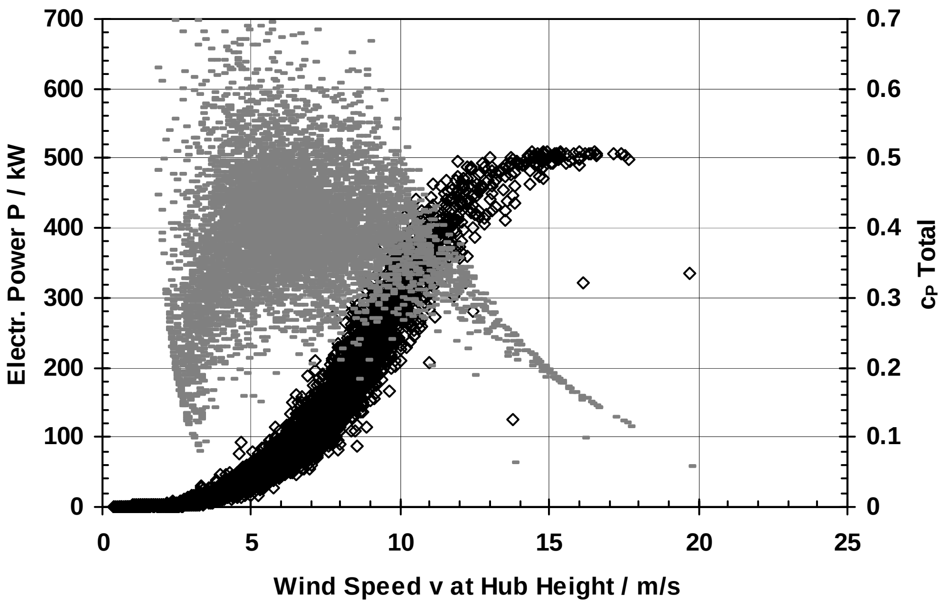

Fig 2.14. Power curve raw data in moderately complex terrain at Schmidt based on met mast and wind speed dependent site calibration

From the measurement results it can be concluded, that 10° sectors and a measurement period of 24 hours per sector (wind speed range 4-16 m/s) should be recommended for site calibrations. The site calibration technique as recommended in IEC 61400-12 Ed 1 does not reduce the typical large scatter of power curve raw data in complex terrain. An influence of the wind speed and turbulence intensity on the site calibration results is indicated.

2.4 Site Calibration via Flow Modelling

An attempt was made to establish a wind flow site calibration for the location of the test turbine in moderately complex terrain at Schmidt in the Eifel Mountains on the basis of the Wind Atlas and Analysis Program (WAsP). For the mast location as well as for the turbine location WasP predicts a wind histogram for each 30° sector (30° is the resolution of WasP). To gain more detailed information about possible site effects the WAsP application was repeated with the roughness and orography maps turned by 10° and 20°. This yields wind speed distributions for 30° sectors around each integer multiples of 10°. The ratio of the average wind speeds derived from the wind speed distribution at the turbine location and at the mast location finally results in the correction factor for the wind speed for each wind direction sector (Fig 2.15).

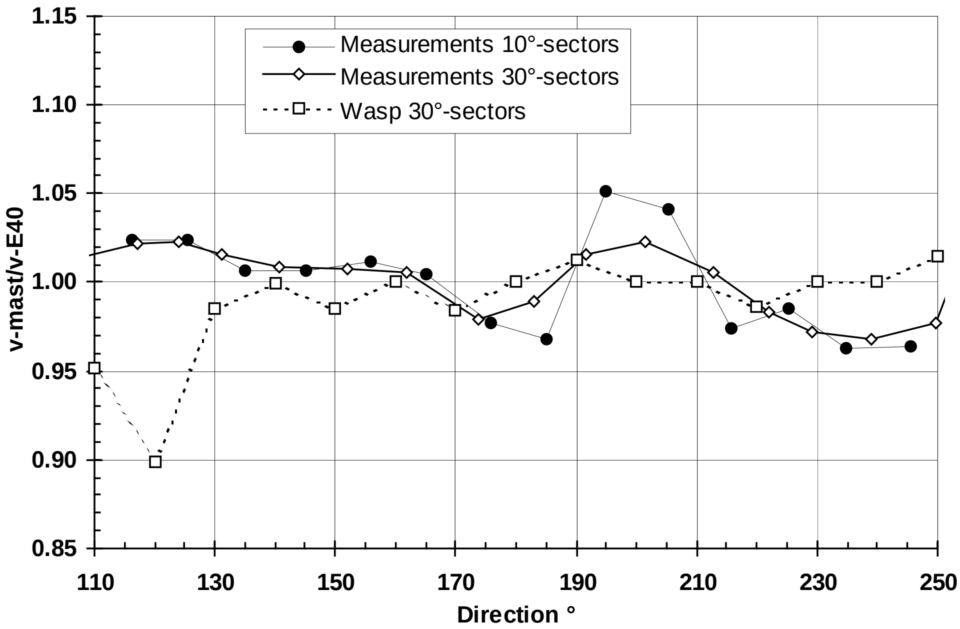

Fig. 2.15. Wind speed correction factors evaluated via WASP compared to measurements in the selection sector for the power curve measurements in the Eifel mountains.

To gain a comparable site calibration from the measurements with two masts, the measured data were also sorted into 30° sectors around each integer multiple of 10° (Fig 2.15). In the wind direction sector between 180° and 200°, a site effect caused by a nearby hill cannot be resolved by averaging over 30° sectors. Nevertheless, the wave shape of the correction factors between 180° and 220° according to the WAsP analysis shows some similarities to the measured correction factors averaged over 30° sectors. Between 230° and 250°, where the terrain is nearly flat, WAsP predicts correction factors near unity, which cannot be confirmed by the measured values of around 0.97 and 0.98. The agreement between the model and measurements is disappointing between 110° and 120°, where the terrain at the turbine location is characterised by steep slopes. Here, either the flow modelling in WAsP fails, or the measurements are misleading. The latter could possibly originate from the steeper terrain at the turbine location compared to the mast location. Due to the steeper slope, the vertical flow inclination is probably greater at the turbine location and hence the ratio between the horizontal wind speed component as measured by the cup anemometer and the magnitude of the wind speed vector might be smaller at the turbine location, which indeed could result in a measured correction factor larger than unity. Also, the sensitivity of cup anemometers to inclined inflow can be an error source for site calibrations if steep slopes are present.

As a result it must be stated, that the directional resolution of the open-release WAsP code seems to be insufficient for site calibrations, because site effects are likely to be cancelled out by directional averaging.

2.5 Self Consistency Test

A site calibration, e.g. derived from measurements with two masts can be checked by using data measured directly at the turbine during the power curve measurements. Below rated power the wind speed incident to the wind turbine can be derived from the momentary time averaged mean value of the electrical power by use of the measured power curve. Alternatively, the turbine’s incident wind speed can be derived from the corrected nacelle anemometer (nacelle anemometry as a separate topic is discussed in Chapter 3). The ratio of the wind speed estimated from the electrical power or the nacelle anemometer and the wind speed measured at the met mast can be bin averaged according to the wind direction. Ideally this wind speed factors should be identical to the wind speed correction factor established from the site calibration before the erection of the wind turbine.

As can be seen from Fig 2.16 at the moderately complex terrain site in the Eifel mountains the wind speed correction factors derived from the electrical power, compare well with those based upon the nacelle anemometer and the site calibration with 2 masts, even in the wind direction sector between 180° and 200° where a significant site effect occurs. In the sector 110°-150° the correction factors gained from the nacelle anemometer are smaller than the factors established from the second mast, which could be due to an overestimation of the wind speed by the corrected nacelle anemometer due to the large terrain slope present in this sector.

The proposed self-consistency testing procedure can also be used to verify the valid sector for power curve evaluation. If no site effects or flow effects induced by obstacles or neighbouring wind turbines are present, the ratio between mast measured wind speed and wind speed derived from the electrical power or the nacelle anemometer should be unity.

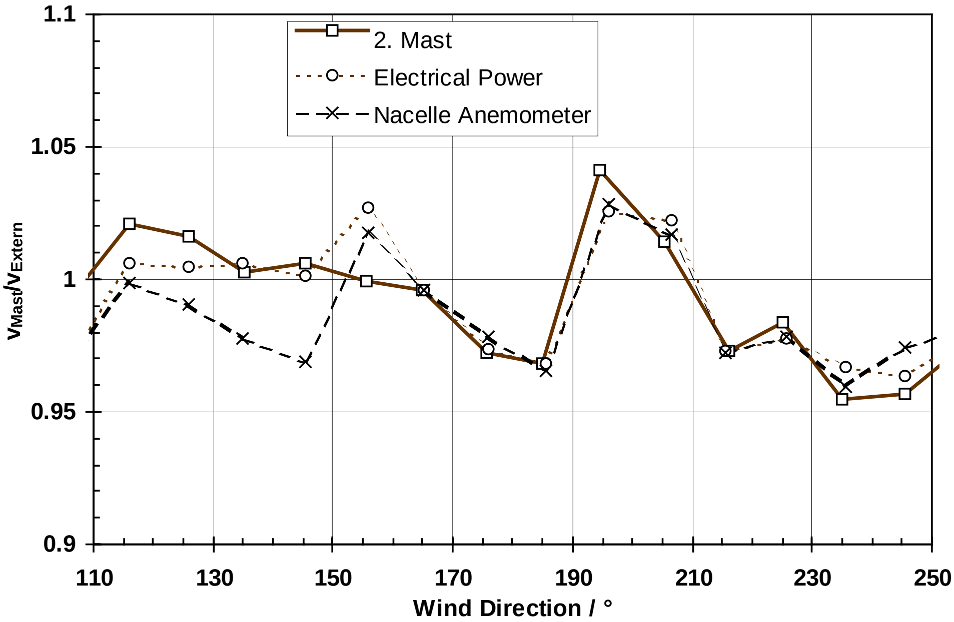

Fig 2.16. Check of site calibration in moderately complex terrain with wind speed data derived from electrical power and corrected nacelle anemometer (wind speed range 5-10 m/s)

This is indeed the case in the wind direction sector for the power curve evaluation of turbine 2 in the Inte wind farm chosen according to IEC 61400-12 Ed 1 (see Fig 2.17, 273°-316°), while in the other sectors the influence of nearby agriculture farm buildings and nearby wind turbines on the air flow at the met mast or the measured wind turbine are reflected in average wind speed ratios different from unity. For most wind directions the wind speed ratios derived from the corrected nacelle anemometer and the electrical power are very similar, which indicates that both the corrected nacelle anemometer as well as the wind speed derived by the electrical power are good measures for the wind speed incident to the turbine. If the turbine operates directly in the wake of a neighbouring wind turbine (directions 330°-360°), the wind speed measured by the nacelle anemometer (corrected) is significantly higher than the wind seen by the turbine. It is hypothesised that the nacelle anemometer is located in the wake centre, where the wind speed reduction is largest, while the rotor average exceeds the wake centre value.

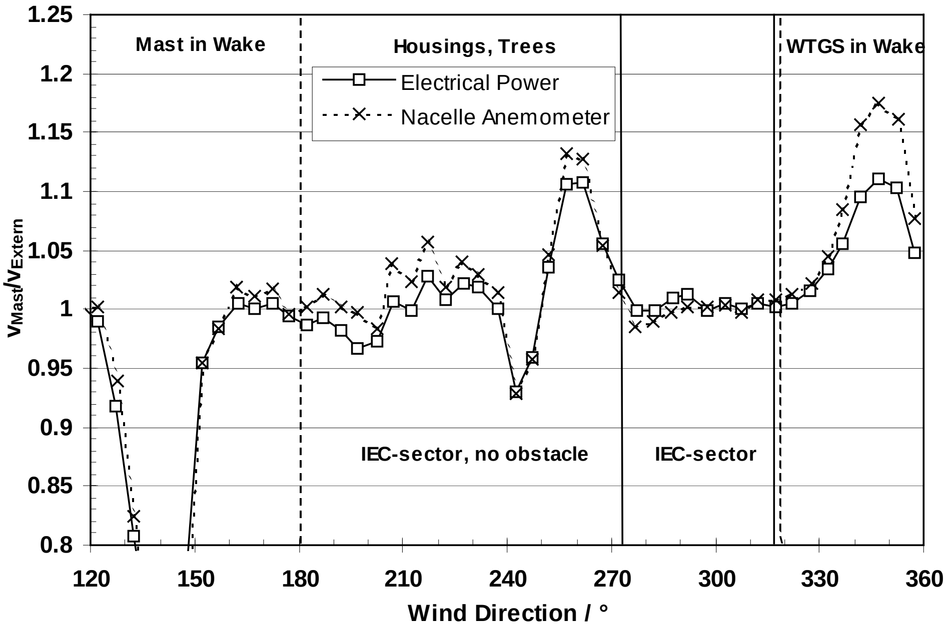

Fig 2.17. Sector check at turbine 2 in Inte (flat terrain) with wind speed data derived from electrical power and corrected nacelle anemometer (wind speed range 5-10 m/s)

A further test method for establishing the valid wind direction sector for a power curve evaluation is based on looking at the turbulence intensity. The turbulence intensity seen by a turbine can be established from the nacelle anemometer or from measurements of the electrical power with the help of the power fluctuation coefficient as described in Ref. 2.2. In the sector valid for power curve evaluations the ratio of the turbulence intensity measured at the met mast and the turbulence intensity evaluated from measurements of the electrical power or the corrected nacelle anemometer should be unity.

For turbine 2 at Inte the turbulence ratios are near unity in the sector deemed valid according to the IEC (Fig 2.18). In the other sectors the turbulence ratios are larger than unity where the associated wind speed ratio (Fig 2.17) is lower than unity and vice versa, indicating that a wind speed reduction at the turbine’s location or the met mast caused by obstacles or other turbines is linked with increased wake turbulence. The turbulence ratios derived by the electrical power are overall very similar to the ratios gained from the corrected nacelle anemometer. However, between 170° and 270° the turbulence ratio derived from the electrical power tends to be higher than the turbulence ratios derived from the nacelle anemometer. The wind obstacles in this wind direction region consist of dwellings and trees with a height much lower than the hub height of the measured turbine and hence they will induce a higher turbulence only in the lower part of the rotor. As a consequence the turbulence intensity indicated by the nacelle anemometer at hub height is higher than the turbulence intensity seen by the turbine averaged over the whole rotor. This is in good agreement with the slightly lower average values of the nacelle anemometer wind speed (higher ratios) compared to the wind speed derived from the electrical power in this wind direction (Fig 2.17).

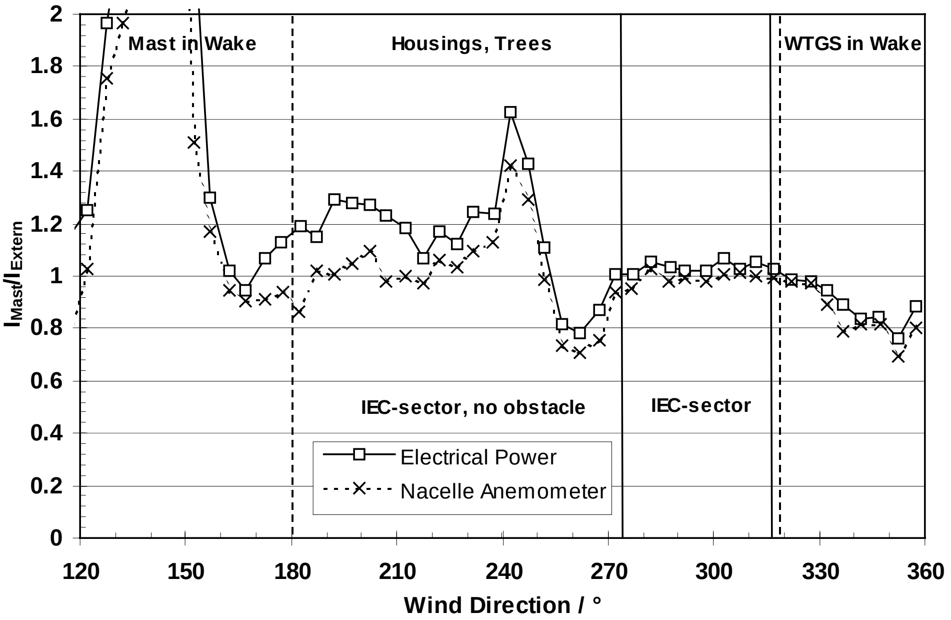

Fig 2.18. Sector check at turbine 2 in Inte (flat terrain) with turbulence data derived from electrical power and corrected nacelle anemometer (wind speed range 5-10 m/s)

Generally the proposed method has the following potential applications:

- as a check of site calibration carried out using two masts,
- as a check of valid wind direction sectors for a met mast based power curve evaluation,
- as a check and determination of useful wind direction sectors for nacelle anemometer based power curves by comparing wind speed derived from electrical power with wind speed derived from corrected nacelle anemometer wind speeds for each wind direction interval,
- for site calibration by applying the average ratio between wind speed derived from electrical power and mast measured wind speed as a correction factor within each wind direction interval. For this purpose a preliminary power curve must be derived within a wind direction sector without site effects, which later serves to evaluate the wind speed from the electrical power. The technique can be applied in an iterative way by first evaluating a power curve without site calibration, then using this power curve to calculate the wind speed seen by the turbine and from this the site correction factors, then evaluating a power curve based on the site calibration, then calculating a new site calibration from the new power curve and so on. This iterative process can be repeated until the site calibration or the power curve converges to a certain limit.
- if a nacelle anemometer correction is available for the type of turbine to be measured, for instance from a flat terrain site, the ratio between corrected nacelle anemometer readings and mast measured wind speed can serve to determine the site correction factors. As a first step the wind direction dependent site calibration factors have to be calculated from the corrected nacelle anemometer wind speed and the mast measurements. Then a power curve can be evaluated based on the corrected mast wind speed. From this power curve and recordings of the electrical power a further site calibration can be calculated. Wind directions in which the site calibration derived from the nacelle anemometer is not confirmed by the site calibration via electrical

power should be eliminated from the process. Finally a new power curve has to be evaluated from the shortened wind direction sector.

Overall the presented method can be a useful tool for site calibrations, at least as a plausibility check. Determining wind speed from readings of the electrical power has the general advantage of providing the incident wind speed representative for the whole rotor area rather than a single point at hub height.

2.6 Concluding Summary

Measurements on an Enercon 40 turbine were performed in moderately complex terrain at a site in the Eifel Mountains. Wind flow site calibration data obtained using two masts were analysed to identify an appropriate wind direction resolution and the necessary time period per wind direction sector. It was concluded that a wind speed correction factor for each 10° wind direction sector over a measuring period of at least 24 hours is needed. It must be pointed out, that the site calibration technique as recommended in IEC 61400-12 Ed 1 does not reduce the large scatter of raw power data normal in complex terrain. An influence of the wind speed and turbulence intensity on the site calibration results is indicated by the recorded data.

An attempt was made to derive a site calibration for the test location in the Eifel mountains with the Wind Atlas and Analysis Program (WAsP). Although the site calibration with two masts could be verified to some extend, the low directional resolution of 30° was found to be insufficient for a site calibration.

A consistency test procedure for power curve evaluations was presented based on determining the wind speed via the electrical power output of the turbine and the nacelle anemometer. The site calibration in the Eiffel Mountains obtained using two masts and the selection sector for the power curve data in flat terrain could be verified successfully with this method. The presented technique is very useful in identifying and quantifying site effects on the basis of the power curve measurement data themselves and hence complements very well the rules for the selection of the wind direction sector described in the existing standards, which are based on the terrain description.

2.7 Site Calibration Using Nacelle Mounted Anemometry

Although the technical justification for site calibration is well accepted, there can often be cost and logistical impediments to carrying it out. Additionally, for an existing wind turbine, site calibration is clearly not viable.
These problems could be solved if a suitable way could be found of using an anemometer mounted to the parked wind turbine structure.
The flow field around a 1:15 scale model of a wind turbine has been determined using Laser Doppler Anemometer techniques in the wind tunnel. This relates the wind conditions at the nacelle anemometer position to the free-field flow.
A site calibration using the real wind turbine has been carried out using the nacelle mounted anemometer and an upwind met mast.
The LDA results provide a correction factor which can be applied to the site data to yield what is believed to be the true site calibration.
The turbine model is shown in Figure 2.19 and the position of the nacelle anemometer in Figure 2.20.

Fig 2.19. The wind tunnel model

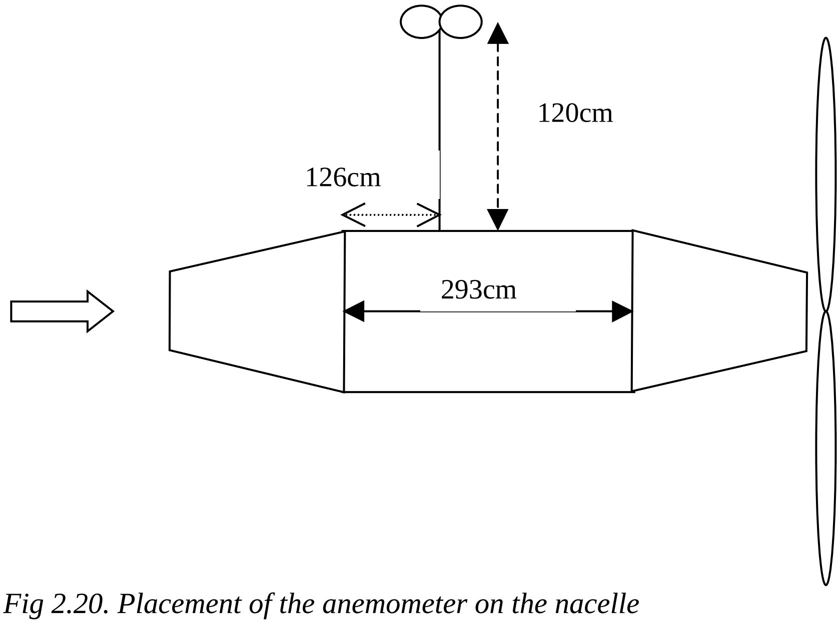

Fig 2.20. Placement of the anemometer on the nacelle

The real turbine was placed on test pad 4 of the Risø Test Station, Figure 2.21. The met mast is placed at a distance of 92.5m and in the direction 284°. The sector that conforms to the standards is 264° to 330°, while for wind directions below 264° the terrain is characterised as moderately complex.

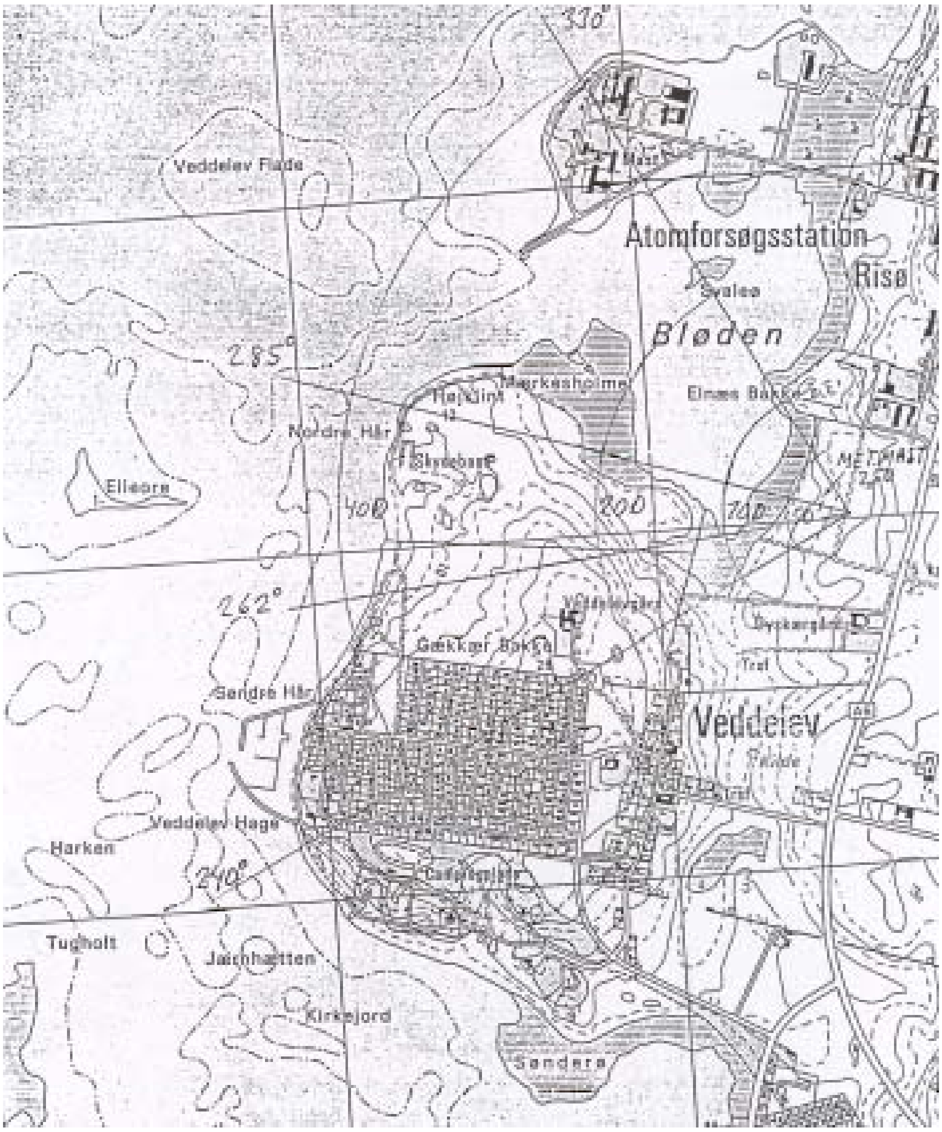

Fig 2.21. Layout of the test site

Calculations using the WAsP wind flow model code reveal that the wind speed at the met. mast relative to the wind speed at the wind turbine is of the order of -2% for the sector 240° to 330°.

Before any attempt to compare the full scale and the wind tunnel data the following should be kept in mind:

First the wind tunnel and the full-scale measurements refer to different positions on the nacelle and therefore an interpolation is necessary. Secondly the full-scale data does not allow the comparison to take place for the same wind speed as in the wind tunnel. This problem is however resolved, since similarity is assumed as the nacelle of the turbine closely resembles a 'bluff body'. Finally, although the atmospheric turbulence has not been simulated in any way during the wind tunnel measurements, no significant influence in the results is expected.

Figures 2.22 and 2.23 show the raw and binned relationship between wind speed ratio and wind direction.

As the wind direction deviates from the mast-turbine direction and to both sides, the spreading of the data points and the value of the ratio increases. This confirms the influence of the nacelle on the data. In fact the ratio of the two anemometers increases almost symmetrically around the mast-turbine direction and this cannot be attributed to the influence of the terrain.

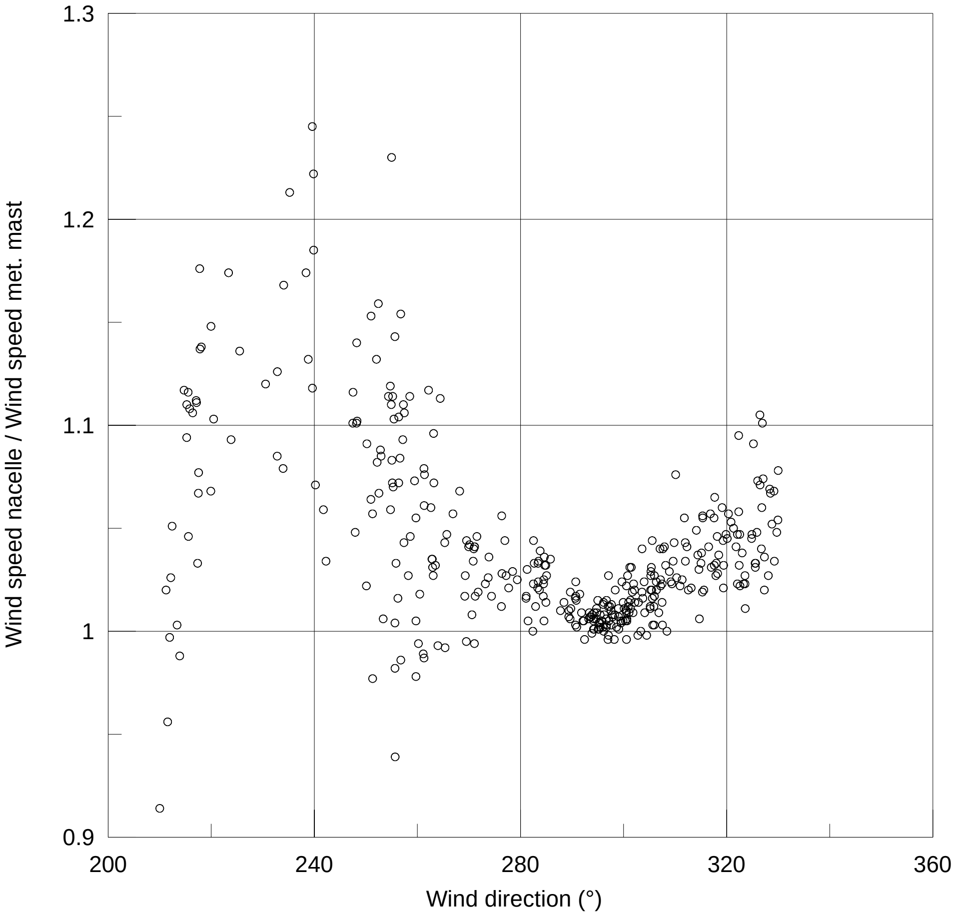

Fig 2.22. The ratio of the nacelle to the mast data as a function of the wind direction

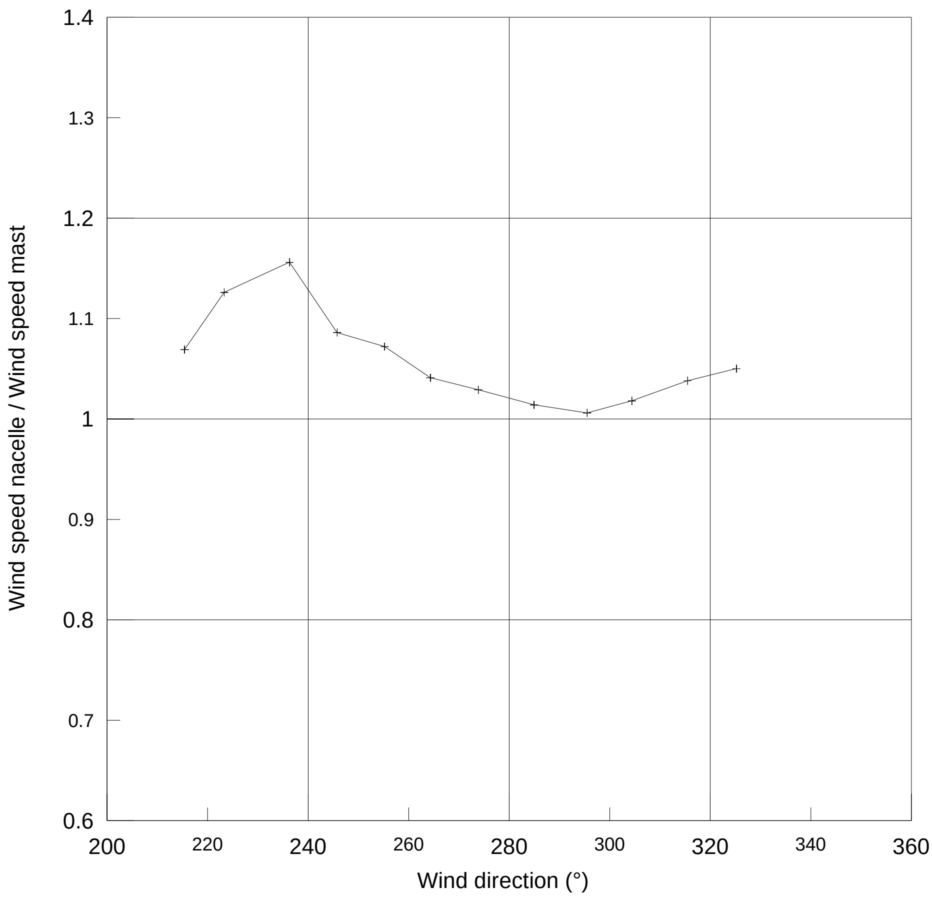

Fig 2.23. The ratio of the nacelle to the mast data as a function of the wind direction bin values

A comparison of the above results to the wind tunnel results shows good qualitative agreement as the lateral flow to the nacelle exhibits the same trends both according to the wind tunnel and the full scale results. Actually as the flow angle deviates from the mast-nacelle direction, the flow measured on top of the nacelle exhibits a 'speed-up' which is observed both in the full scale and the wind tunnel data. The least influence from the presence and the shape of the nacelle is seen to be in mast-tower direction.

The quantitative evaluation and the comparison to the wind tunnel results are unfortunately not conclusive. This is mainly due to the lack of more detail in both the wind tunnel and the full-scale data and to the fact that the terrain corrections due to topography are of the same order, or smaller, than the corrections due to the presence of the nacelle. Based on the existing data and by limiting ourselves to the sector around the mast-turbine direction, the speed-up of the flow at the turbine position is 1.7%. This is in good agreement to the wind tunnel results (1.3%) if the prediction of the WasP model which predicts a 2% acceleration is considered.

3 Nacelle Anemometry For Performance Verification

The purpose of this part of the work has been to research the limitations of the corrected nacelle anemometer method to identify the free-field wind speed incident on an operational wind turbine.

The basis of the nacelle anemometer method is the hypothesis that if a relationship can be established between the wind speed indicated by the nacelle anemometer and the free-field wind speed, then it is possible to estimate a wind turbine's power curve without using a reference meteorological mast and without going through the site calibration procedures of IEC 61400-12 Ed 1. In practice this might mean establishing the nacelle to free wind speed relationship for a reference turbine in a wind farm and then assuming that the same relationship holds for all other turbines in the development. A basis of verifying the performance of every individual turbine is thus established.

In the current project, some work was once again carried out using data from the Enercon 40 wind turbines described in Section 2.

Additionally, data from a similarly sized stall regulated turbine (model not declared), from the Elkraft 1 MW wind turbine on Jutland and from a Nordtank 550/41 turbine at the Risø test station in Denmark were also analysed.

Before looking at these analyses and results, some more fundamental studies are reported which look at the flow regime in the vicinity of wind turbine nacelles and the (inability) of conventional anemometers to provide good absolute measurements.

Fuller details of the work are outlined in Refs 3.1 and 3.2.

3.1 Nacelle Anemometry - Instrumentation Considerations

3.1.1 The Response of Cup Anemometers to Angle of Attack in the Vertical Plane

The importance of knowing how a cup anemometer behaves in non-horizontal wind is now being recognised. To determine the nature of the sensitivity to inclined flow, two identical cup anemometers were deployed on a boom with one support pillar being vertical and the other being at an angle to the vertical.

The experimental arrangement also comprised a wind vane, which was mounted on another meteorological mast at 60 m away in the 180°direction. The direction normal to the boom iwass 198° and the tilt of the anemometer was considered positive when the anemometer was tilted towards the wind direction.

The ratio of tilted to normally mounted anemometer output is shown in Figures 3.1 and 3.2 for a tilt angle of 5°. Figure 3.1 clearly shows the influence of the lattice support mast. For figure 3.2, the sectors used are ±18° for the positive and ±25° for the negative angles.

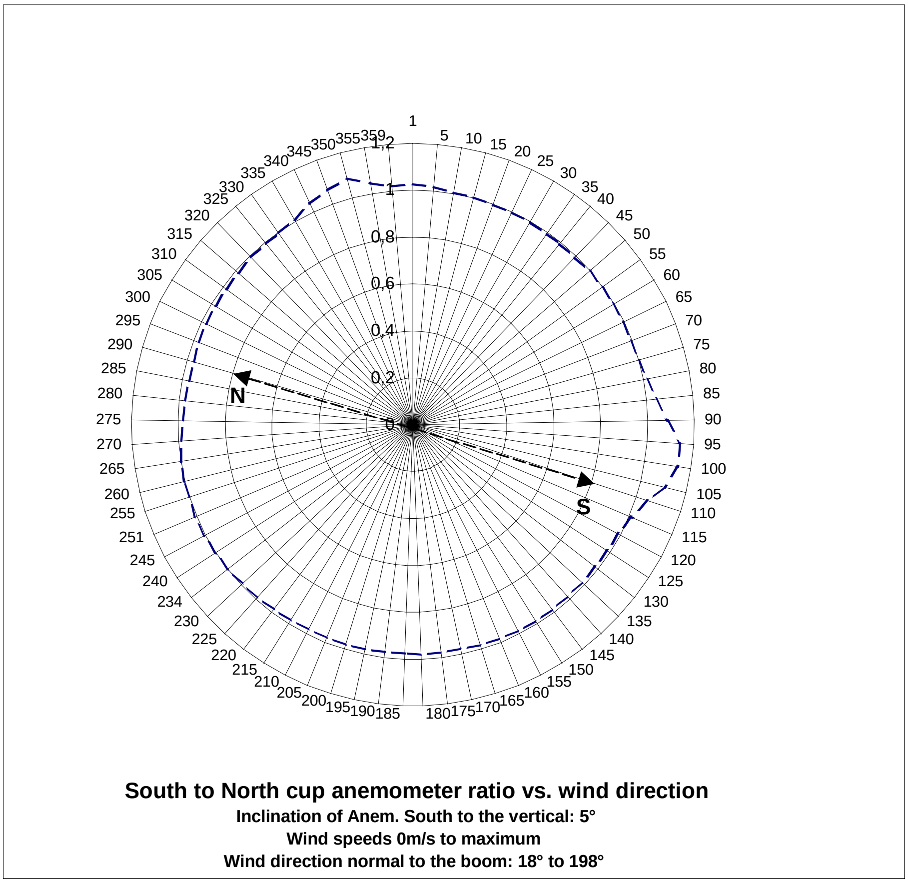

Fig 3.1. Ratio of tilted to vertical anemometer outputs for a tilt angle of 5 °

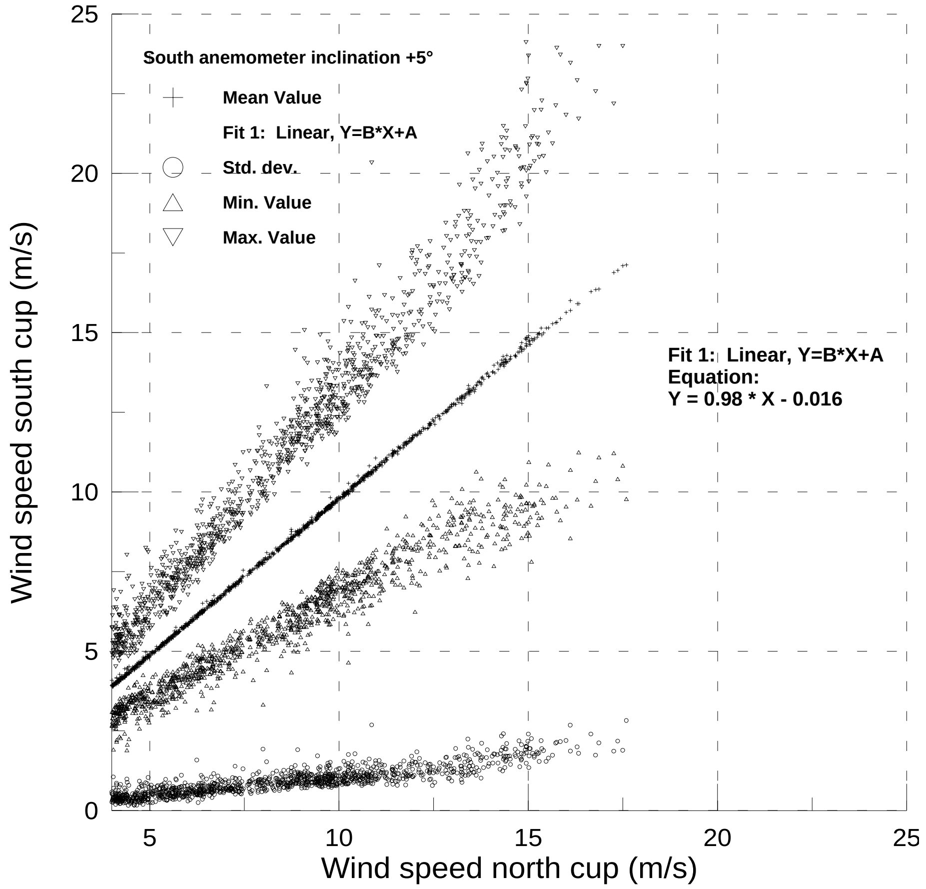

Fig 3.2. 10 minute statistics of tilted anemometer output as a function of vertical anemometer output for a tilt angle of 5 °

The tests were conducted at a range of tilt settings (-15°, -10°, -5°, 0°, +5°, +10°, +15°). The angular characteristics for these settings are shown in Figure 3.3. The normal and inverse triangular points correspond to data from opposite wind directions (180° difference) and equal but opposite inclinations of the cup anemometer. In the same figure wind tunnel results (circular points) along with the theoretically expected ‘cosine response’ curve, are also presented.

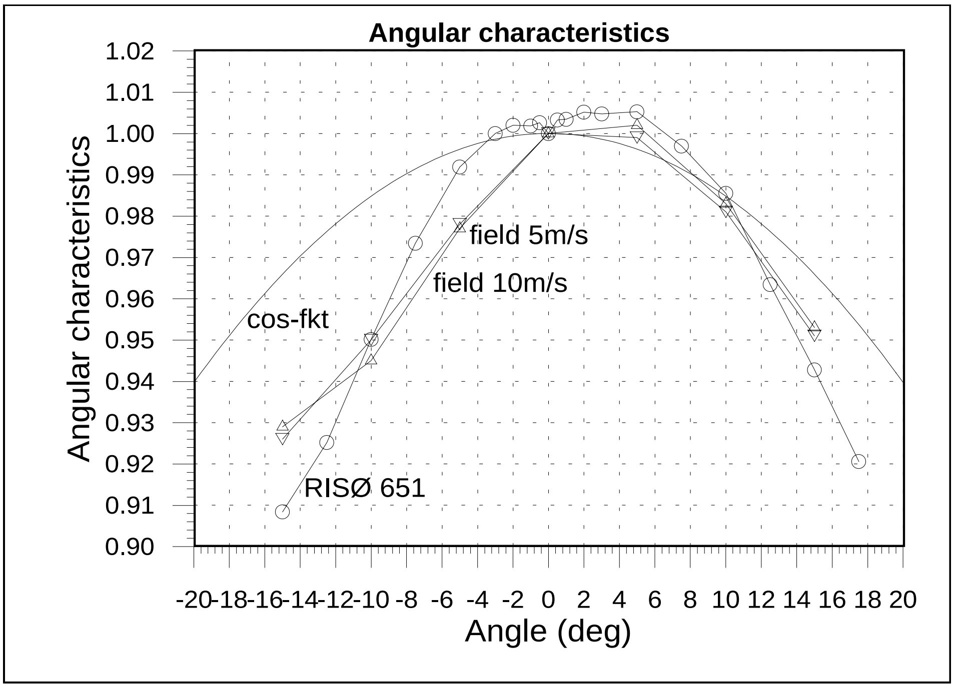

Fig 3.3. Comparison of the response of the inclined anemometer to the cosine function

The behaviour of the anemometer deviates from the cosine and it is not symmetric relative to the vertical position. Open air and wind tunnel data are in good agreement for positive tilt angles, while differences are observed for negative ones.

The implication is that on a wind turbine nacelle where the flow is liable to be highly distorted and to have vertical components, the anemometer is unlikely to measure a true wind speed, be it either the total wind speed or the horizontal wind speed in which interests lie.

This in itself of course is not a problem as long as the behaviour is consistent.

3.1.2 Replacing Nacelle Mounted Cup Anemometers with Sonic Instruments

In the present report the results from a measurement campaign are presented where a sonic anemometer has replaced the nacelle cup anemometer. The purpose is to study the flow field at the position where the nacelle anemometer is mounted in order to get some more detailed information of the velocity field to which the nacelle cup is exposed. These tests are related to the effort of finding the ‘best position’ on the nacelle for the placement of the cup anemometer.

The velocity field on the nacelle is of interest for a number of reasons. One is the use of the nacelle anemometer as an alternative to verify the turbine’s power curve. The response of the nacelle anemometer depends on its placement on the nacelle, on the pitch settings of the blades and the incoming wind profile. The mast-nacelle anemometer relation is complicated and the desired result would be to find a position on the nacelle that is as much as possible insensitive to the influences of the aforementioned factors.

One equally important reason is to find out whether the presence of the rotor induces, at the specific position, a vertical velocity component which can, as seen previously, influence the anemometer response. This is important in the case of verification of the turbine's power curve in complex terrain where site calibration is not possible and only the nacelle anemometer is only available.

The tests took place on the Elkraft 1MW turbine in Jutland and data were selected to come from a flat sector. The reference mast anemometer was at 55 metres elevation whilst the sonic anemometer was deployed at 1.2 metres above the nacelle.

Figure 3.4 shows the vertical component of nacelle anemometer wind speed as a function of met mast wind speed.

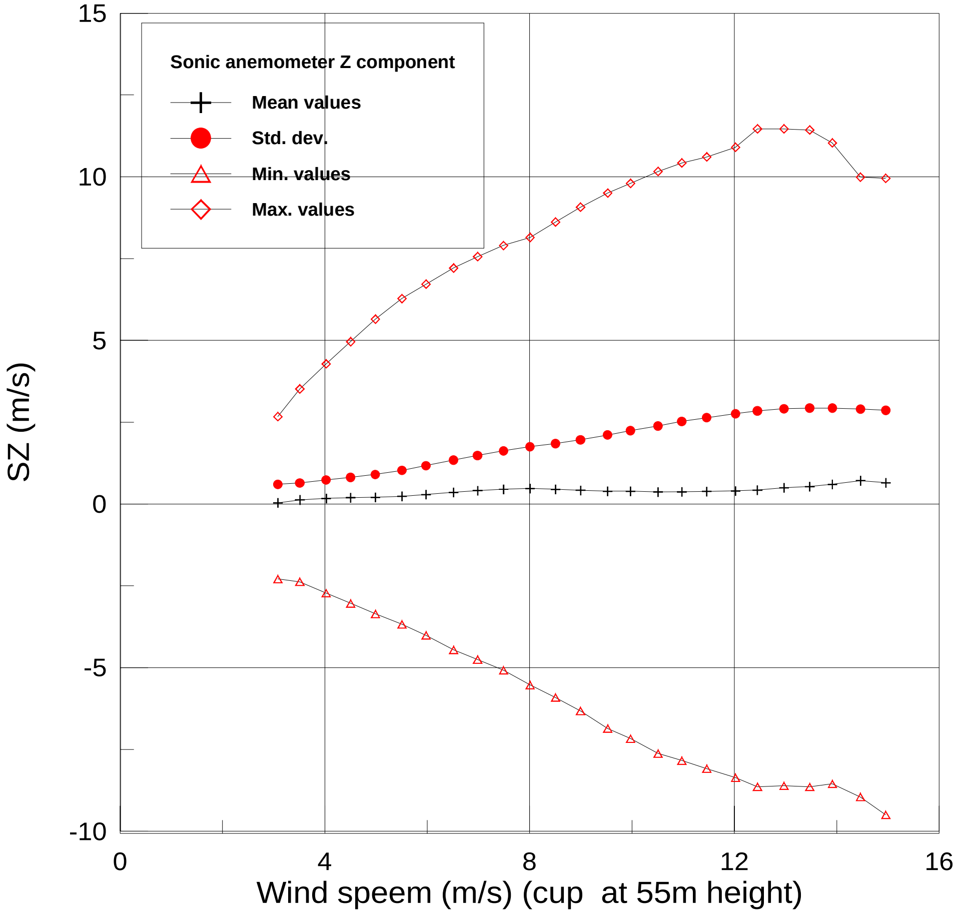

Fig 3.4. The w-component as a function of the mast anemometer

The maximum and minimum velocities observed are almost of the same magnitude and they increase with the wind speed. Since changes in the pitch angle take place above wind speeds of 12 m/s, the changes in the maximum and minimum values are not due to the pitch activity and can be considered a result of the interaction of the wind and the blade passage. The mean value of the w-component though almost shows no changes and remains positive throughout the wind speed interval measured, indicating a possible influence from the presence of the nacelle or a minor vertical misalignment. Whatever the case, the mean value of the vertical component is independent of wind speed. By looking later at the minimum and maximum angles of attack of the flow to which the cup anemometer is exposed, it is seen that these also remain relatively constant with increasing wind speed. Thus it can be argued that flow inclination on the nacelle should only be expected to depend on terrain conditions, provided the nacelle anemometer is placed at a certain distance from the nacelle.

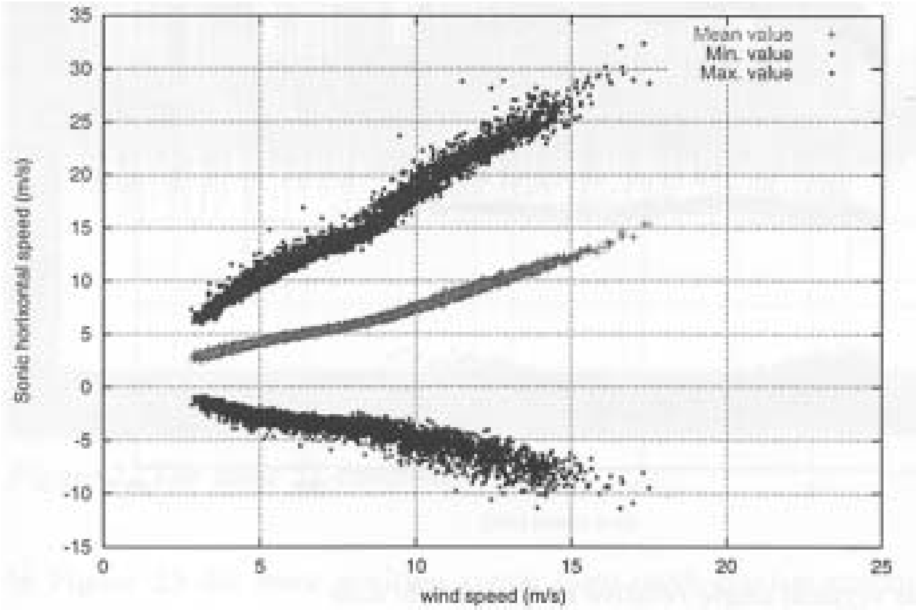

Fig 3.5. Horizontal nacelle wind speed as a function of met mast wind speed

In Figure 3.5, the sonic horizontal velocity is shown as ten-minute average values. Note that the minimum value is consistently negative confirming the existence of re-circulation at the specific position.

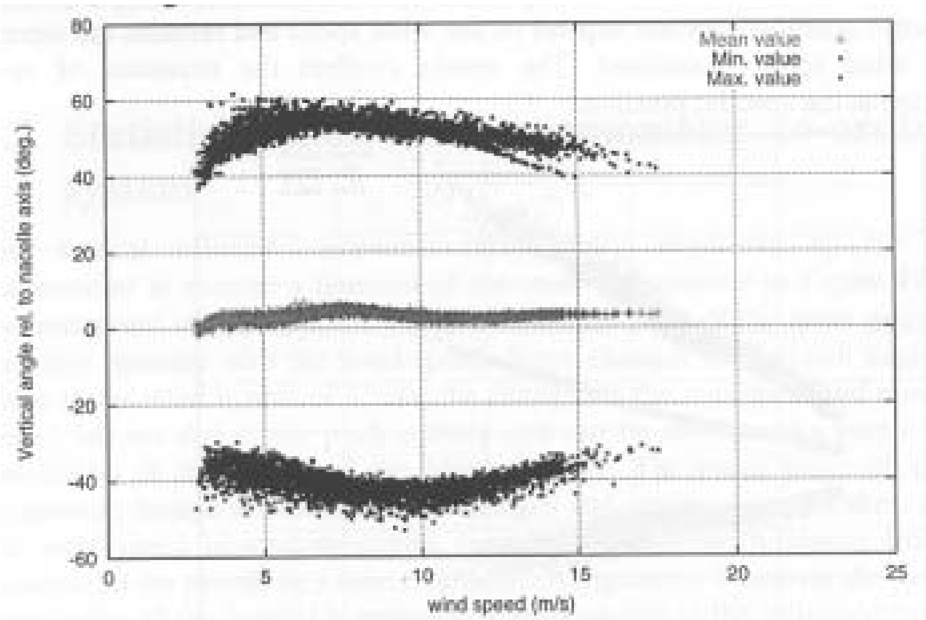

Fig 3.6. Vertical angle of attack of the nacelle wind speed relative to the met mast wind speed

In Figure 3.6, the flow angle in the vertical plane is shown. This shows very wide spreading confirming the degree of turbulence being experienced.

A study of the time series from the sonic anemometer confirms that the velocity variations are highly stable and correlated with rotor position as might be expected.

In summary, it can be concluded that significant deviations of the flow occur relative to the horizontal direction and the nacelle's longitudinal axis. Since the cup anemometer is based on the drag principle, only changes in the vertical direction are expected to affect its response. The influence of the blade passage on the velocity component signals has been documented by looking at both the statistical and time series data. The cup anemometer, which normally measures the wind speed on top of the nacelle at the place where the sonic anemometer was installed, is exposed to harsh operating conditions.

3.2 Studies Using the Enercon Wind Turbine

The same turbines as used for the site calibration studies reported in Chapter 2 were also used for the work on nacelle anemometry.

The purpose of the work was to investigate:

- The general nature of the relationship for the operational wind turbine between wind speed indicated by the nacelle anemometer and the free wind speed
- The best way of representing the relationship
- The general advantages of using corrected nacelle wind speeds to produce power curves
- The robustness or otherwise of the method when operating in wake flow
- The variation in the nacelle to wind speed relationships between turbines
- The dependency of the relationship to control settings
- The variation in nacelle to wind speed relationships depending upon topographic conditions.

Each of these is studied in turn below, but firstly it is worth reviewing some pertinent details of the Enercon turbines used for the tests and appraisals.

In the Enercon 40 rotor speed is adjusted according to the wind speed to optimise the power output. The rpm-power curve used for tracking the actual wind conditions not only affects the power output but may also influence the nacelle anemometer readings. For turbine 1 and turbine 2 in the Inte wind farm the rotor speed was reduced during part of the measurement campaign in order to lower the sound power emission of the turbines. The control setting with the reduced rotor speed is referred to as P35 in this report while the normal turbine mode is called P38. Fig 3.7 shows that at Inte in the power range above approximately 150 kW, the rotor speed in the P35-mode was lower than at the complex Eifel site. When the turbines in Inte were operated in the P38-mode there were still small differences compared with Eifel, which might result from the terrain complexity at the Eifel (e.g. higher turbulence intensity) as well as from the lower air density caused by the difference in altitude. Turbines 1 and 2 have the same control curve in the P38-mode.

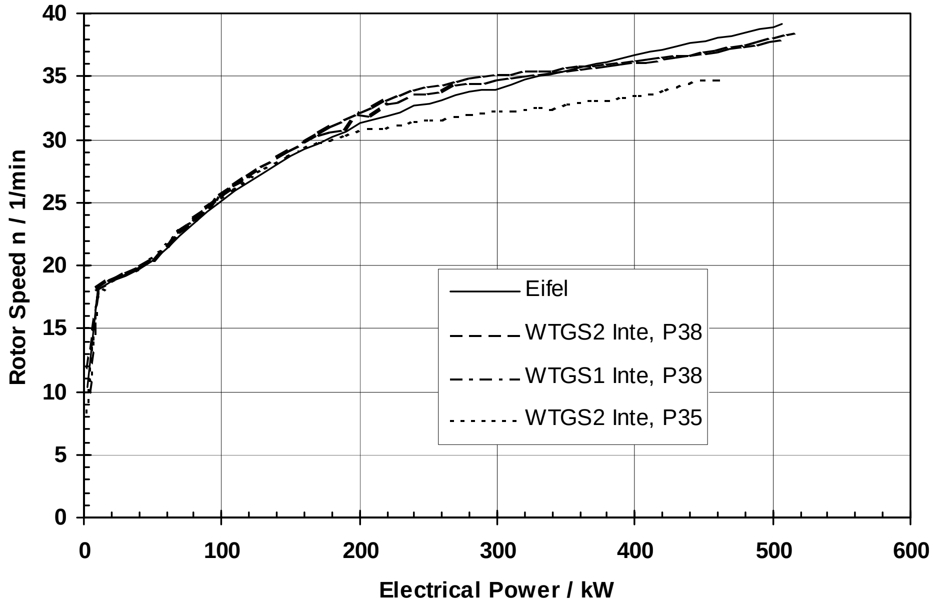

Fig. 3.7. Rotor speed versus electrical power at the Eifel (complex terrain) and at turbine 2 in Inte (flat terrain)

3.2.1 Nature of the Relationship Between Wind Speed Indicated by the Nacelle Anemometer and the Free Wind Speed

For these tests, the nacelle anemometer was calibrated, inflow conditions were monitored at mast 1, the directional sector was confined to 273°-316° to ensure that IEC 61400-12 conditions were satisfied.

As can be seen from the raw data plot of Fig 3.8 the wind speed at the met mast is clearly overestimated by the nacelle anemometer. Furthermore, the wind speed measurements show a high correlation (R=0.99467).

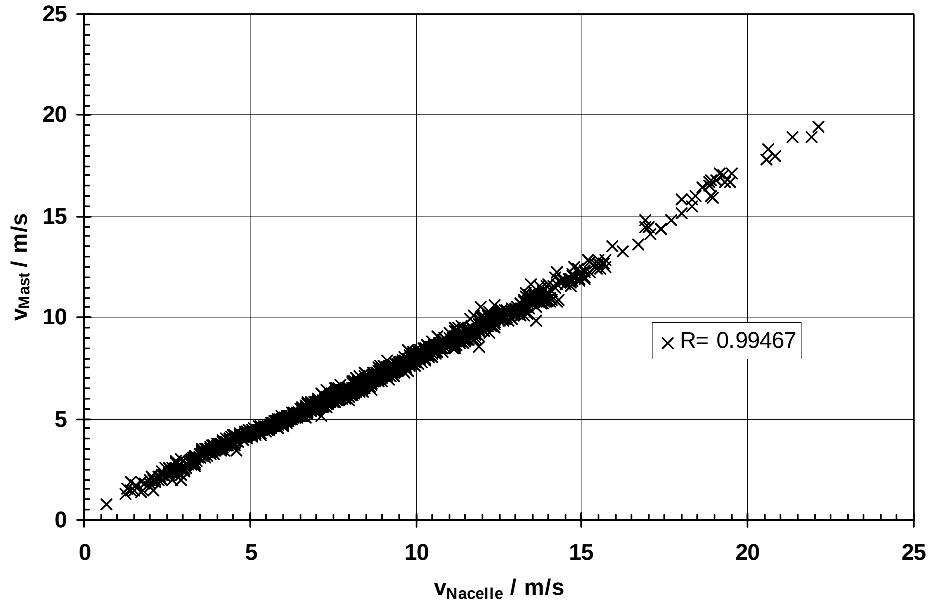

Fig. 3.8. 10-minute averages of the wind speed measured at the met mast in Inte versus the nacelle anemometer readings from turbine 2 (flat terrain).

In Fig 3.9 the raw data are bin averaged according to the wind speed at the met mast. From the bin analysis a linear correction as well as a 5th order polynomial correction to the nacelle anemometer is derived by regressing data in the wind speed range 1.25-17.25 m/s. The wind speed range of the regression is limited according to the availability of data per wind speed bin.

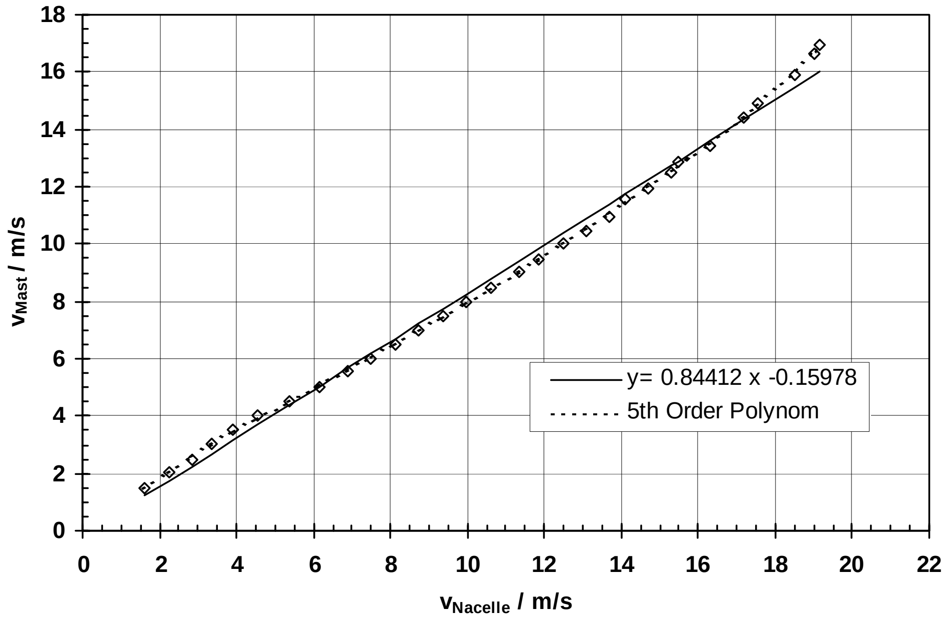

Fig. 3.9. Nacelle wind speed versus mast measurements bin averaged according to the wind speed at the met mast (bin width 0.5 m/s) at Inte (flat terrain)

3.2.2 Representing the Nacelle-to-Free-Wind-Speed Relationship

Fig 3.10 and Table 3.1document the accuracy of different nacelle anemometer corrections. Due to the non-linear behaviour of the nacelle anemometer the linear regression method for correcting the nacelle anemometer leads to a clear overestimate of the ambient wind speed of more than 3 % in the wind speed range between 6 m/s and 11 m/s and to a distinct underestimate of more than 3 % below 4 m/s and for wind speeds higher than 16 m/s. This is reflected in a high standard error of 0.36 m/s and a high uncertainty of the regression constant of 93 %.

The 5th order polynomial regression correction shows a difference from the mast measured wind speed of below 1 % for wind speeds higher than 4 m/s. The standard error is below 0.1 m/s which indicates, that this is a suitable method for power curve assessments. However, the statistical uncertainty of the single regression coefficients shows high values of between 13 % and 53 % which is due to the large number of regression parameters (6) compared to the number of wind speed bins (32).

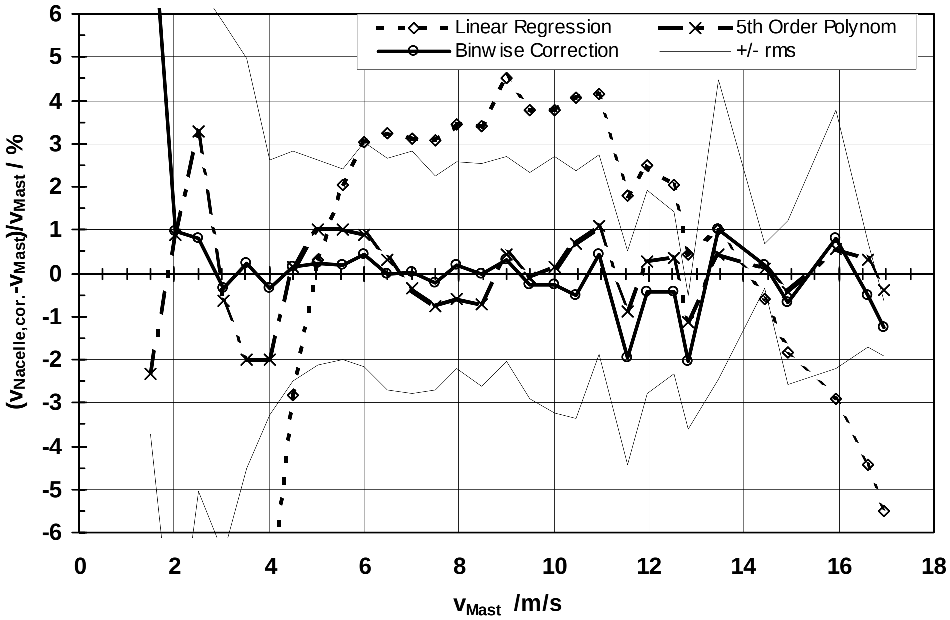

Fig. 3.10. Difference between the corrected nacelle anemometer readings and mast measurements as a function of wind speed for turbine 2 in Inte. For the binwise correction of the nacelle anemometer also the standard deviation of the wind speed difference within each bin is shown.

A more decisive method of correcting the nacelle anemometer is to evaluate a correction for each wind speed bin individually. For this purpose the ratio of the wind speed measured at the met mast to the wind speed measured at the nacelle is bin averaged according to the nacelle wind speed giving a binwise correction factor (Fig 3.11). This correction factor is then applied to each 10 minute average value of the nacelle anemometer. Again, the accuracy of this correction procedure is illustrated in Fig 3.10. The difference in wind speed between the corrected nacelle anemometer and the mast measured data averaged for each bin is now below 1 % for most wind speed bins and no systematic errors occur like with the linear correction. The standard error of the binwise correction method is below 0.1 m/s and the average binwise error is below 1 %.

The average wind speed difference between the corrected nacelle anemometer and mast measurements plus/minus the standard deviation of the wind speed differences in each wind speed bin can be interpreted as the uncertainty associated with the correction of the nacelle anemometer for wind speed determinations within single 10 minute intervals. From Fig 3.10 it can be seen, that the standard deviation of the wind speed difference is in the region of 2-3 % for wind speeds higher than about 4 m/s if the binwise correction method is used.

When using the nacelle anemometer for power curve evaluations the statistical uncertainty of the correction method regarding single 10-minute intervals decreases with the number of 10-minute values per wind speed bin. Principally, this uncertainty converges to the average difference between mast measurements and corrected nacelle readings in each wind speed bin if sufficient data per bin are available.

Table 3.1. Statistical performance of different correction procedures. The regressions are derived from the wind speed range 1.25-17.25 m/s.

Method	Binwise	Linear Regression	5th Order Polynom
	Performance (Bins)		
Mean Error	-0.018 m/s	0.052 m/s	0.004 m/s
Standard Error	0.091 m/s	0.358 m/s	0.064 m/s
R	0.9998	0.9982	0.9999
	Statistical Uncertainty of Coefficients		
a0		+/-93 %	+/53 %
a1		+/-1.5 %	+/-13 %
a2			+/-31 %
a3			+/-33 %
a4			+/-35 %
a5			+/-36 %
Average (Binwise)	0.7 %		

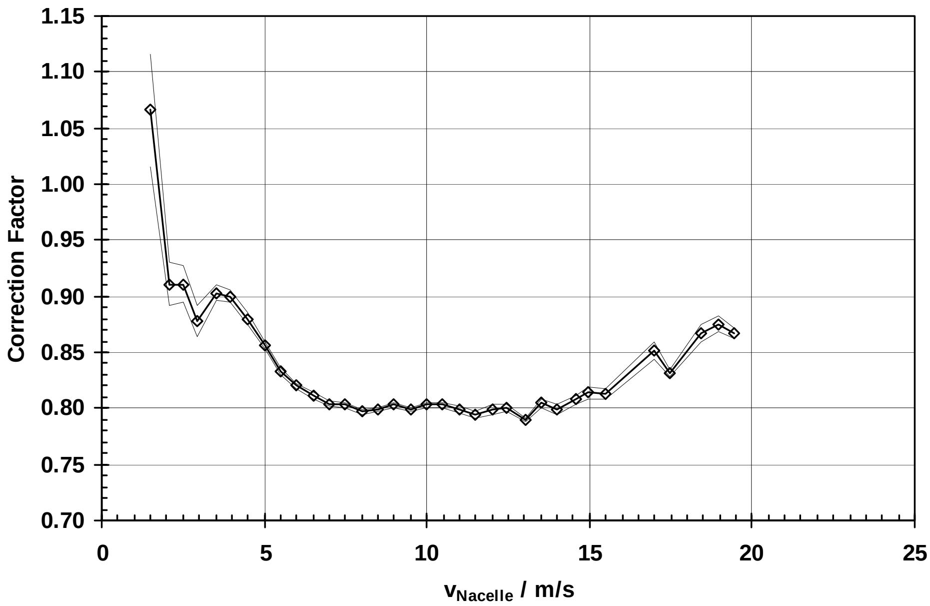

Fig. 3.11. Binwise correction factor for the nacelle anemometer for turbine 2 in Inte. The average values and the standard deviation divided by the square root of number of values within each bin (statistical uncertainty) are shown.

Overall it seems possible to use nacelle anemometry for power curve verification due to the high correlation between mast measurements and nacelle anemometer readings. The choice of the correction method should preferably be based on a statistical comparison of the corrected nacelle anemometer readings and the mast measurements. A criterion for an appropriate correction procedure might be a standard error below 0.1 m/s in the most important wind speed range (e. g. 4-16 m/s). In case of the Enercon 40 turbine this criterion can be fulfilled with a 5th order polynomial regression or the binwise correction. In the following only the binwise correction of the nacelle anemometer is investigated further due to its low and non-systematic uncertainty, and also from the point of ease of application.

3.2.3 The General Features of a Power Curve Produced Using the Nacelle Anemometer Method

The nacelle anemometer correction established in the previous section can be used to evaluate the power curve of the same turbine

Fig 3.12 and 3.13 compare the power curves of the turbine (turbine 2 at Inte) evaluated with the met mast and with the binwise corrected nacelle anemometer. The difference between these power curves in almost all wind speed bins is below 2% for the bulk of the energy productive part of the power curve. This is smaller than the uncertainty of the met mast based power curve itself. This is all the more impressive as for the calculation of the uncertainty of the met mast based power curve no site effects are assumed in order to gain an optimistic estimation of the uncertainty. According to the IEC standard an uncertainty of 3 % in the wind speed determination must be taken into account if no site calibration is performed.

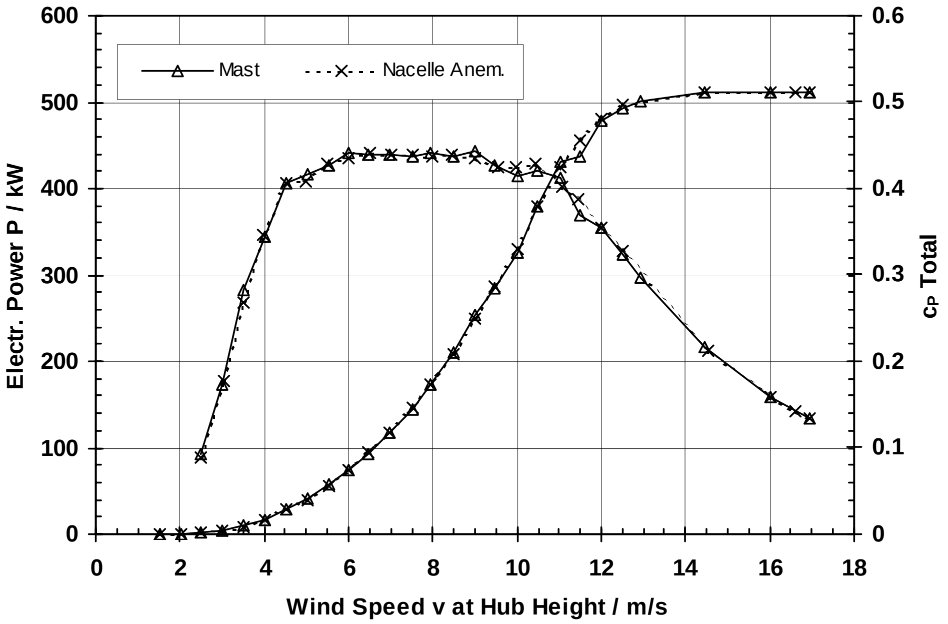

Fig. 3.12. Bin averaged power curves of WTGS 2 based on met mast and on the corrected nacelle anemometer

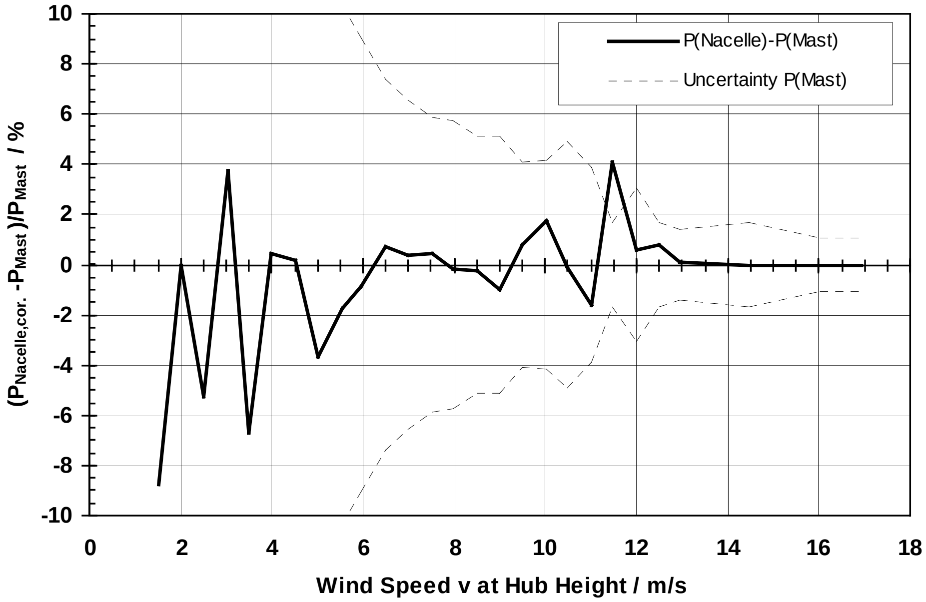

Fig. 3.13. Bin averaged difference between power curves of turbine 2 at Inte evaluated with the wind speed data from the met mast and with the binwise corrected nacelle anemometer. The uncertainty of the met mast based power curve is illustrated for comparison reasons.

As can be expected from the relative small differences of the power curves the resulting annual energy production (AEP) calculated according to IEC 61400-12 Ed 1 is nearly equal. The difference in AEP between the mast based power curve and the power curve evaluated from the binwise corrected nacelle anemometer is below 0.5 %. Furthermore, the differences in AEP are much smaller than the uncertainty of the AEP associated to the mast based power curve.

The raw data of the power curves evaluated with the mast measured wind data and the binwise corrected nacelle anemometer data are shown in Fig 2.11 and 3.14. The data scatter is lower in case of the nacelle anemometer power curve, which indicates a better correlation between power data and the nacelle wind speed than between power data and mast measured wind speed.

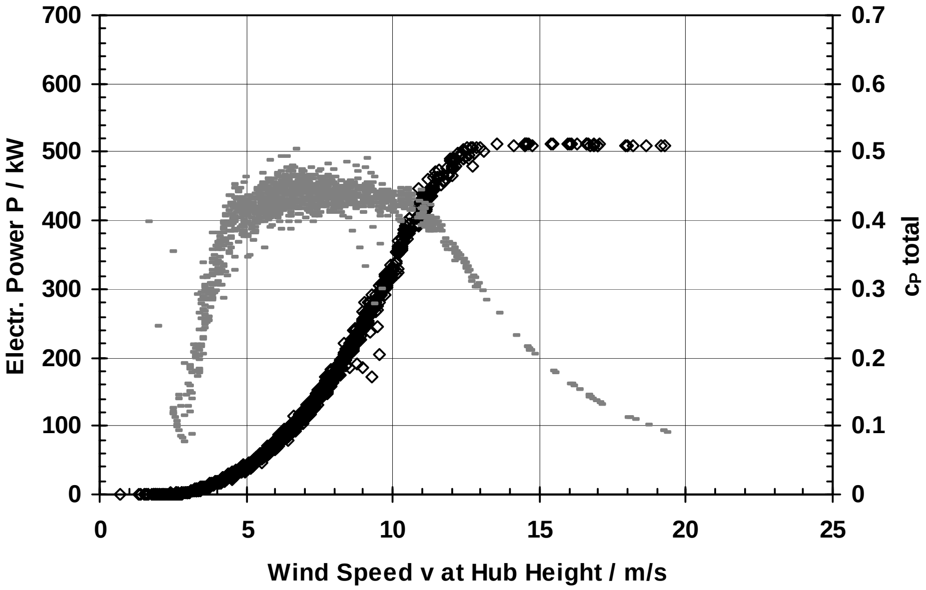

Fig. 3.14. Power curve raw data of turbine 2 at Inte evaluated with the corrected nacelle anemometer

3.2.4 Robustness of Nacelle Anemometry when Operating in Wake Flow

Using the nacelle anemometer approach, power curves can readily be produced for different sectors. In the case where turbine 2 operates in the wake centre of the neighbouring turbine 1 (5.5 rotor diameters distant in wind direction sector 330°-360°), the power curve appears too optimistic when compared with the non-wake sectors as shown in Fig 3.15. The difference in the AEP ranges from 2% at high annual average wind speeds up to 12% at low annual average wind speeds. It would seem that the nacelle anemometer correction derived for the turbine in free air flow leads to too low wind speeds in wake flow. The reason is probably, that the nacelle anemometer is placed in the wake centre, where the wind speed reduction due to the upstream turbine is largest, while the rotor average exceeds the wake centre and hence is under impact of stronger average wind speeds than the nacelle anemometer. This effect is compensated in large part, if the power curve is derived over all wind directions whereupon the overestimation of the power coefficient is much reduced and the effect on the associated AEP is only between 1 % and 4 %.

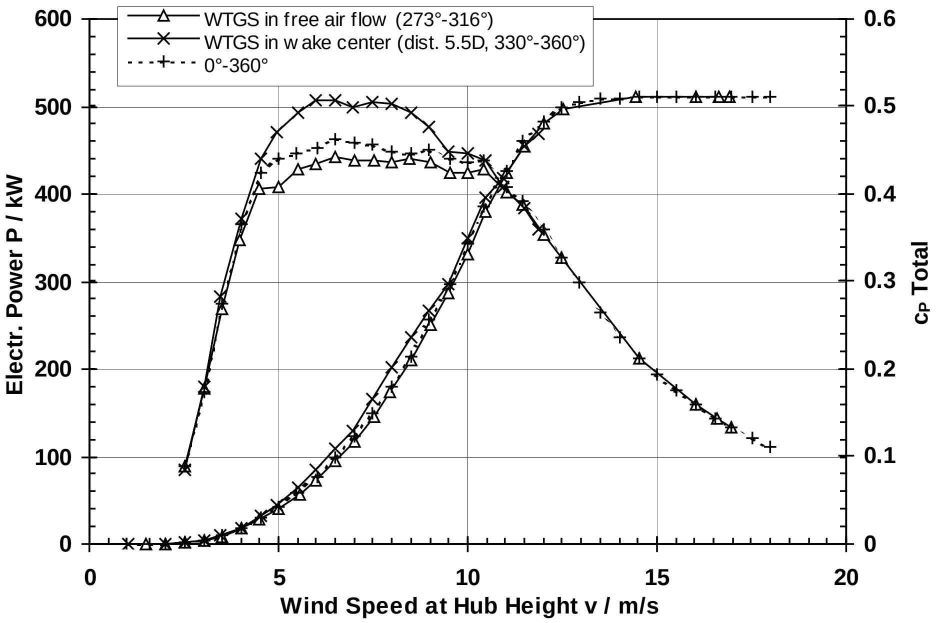

Fig. 3.15. Bin averaged power curves of turbine 2 at Inte based on the corrected nacelle anemometer for different wind direction sectors.

As a general outcome it is implied, that the presented correction method for the nacelle anemometer is well suited for the application of power performance tests. Wind direction sectors in which the investigated turbine operates in the wake centre of nearby wind turbines should be excluded from power curve evaluations.

3.2.5 Verification of the Nacelle Anemometer Correction at Another Turbine in Flat Terrain

The integrity of the nacelle anemometer correction gained from turbine 2 in Inte can be tested by comparison with a second turbine of the same type also in the Inte wind farm. Turbine 1 is located in a way that its power performance can be derived as a reference from met mast 1 in accordance with IEC 61400-12 Ed 1. First, the properties of the nacelle anemometer of turbine 1 can be investigated directly using mast 1 and compared to those of turbine 2. Unfortunately, the nacelle anemometer of turbine 1 could not be calibrated in a wind tunnel. In order to make this task possible, the wind tunnel calibration of the nacelle anemometer of turbine 2 was assumed to be valid also for turbine 1. For comparison reasons only data with the turbines controlled in the PM38-mode are used in this section.

The relation between the wind speed measured at the nacelle of turbine 1 and the wind speed measured at mast 1 is compared to the relation between the wind speed measured at the nacelle of turbine 2 and the wind speed measured at mast 1 in Fig 3.16. Both nacelle anemometer readings behave in a similar way compared to the mast data. The difference in the nacelle readings is below 2 % relative to the wind speed measured at the nacelle of turbine 2 for wind speeds higher than 4 m/s measured at the mast. This difference seems to be reasonable considering the fact that different uncertainty sources may add up, as the nacelle anemometer at turbine 1 is not calibrated in a wind tunnel and site effects might play a role.

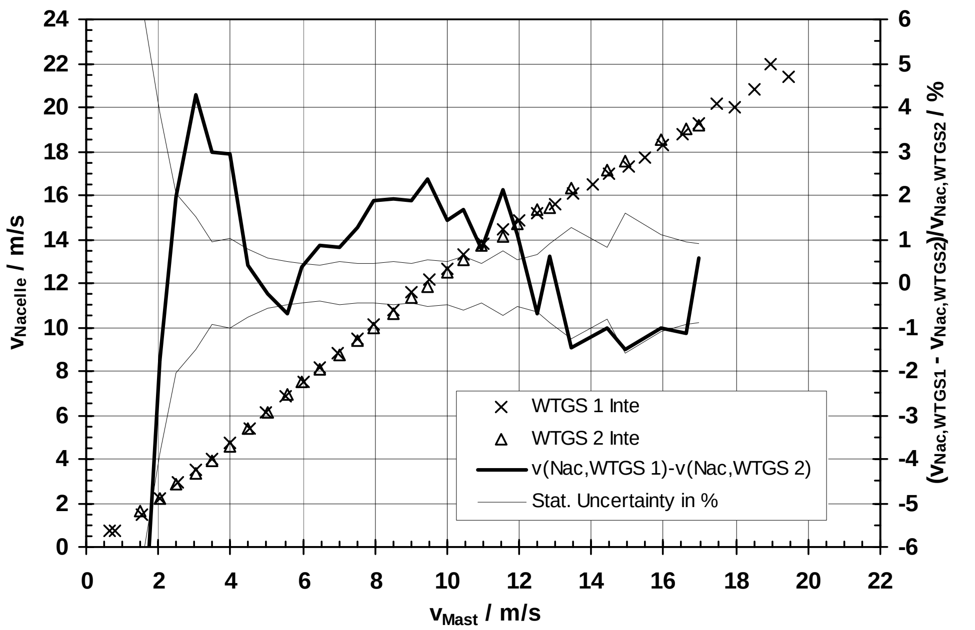

Fig. 3.16. Nacelle anemometer data from turbine 1 and turbine 2 at Inte bin averaged according to the met mast data (bin width 0.5 m/s). The combined statistical uncertainty of the nacelle anemometer readings in each wind speed bin is compared to the relative difference between the nacelle anemometer measurements.

The difference in the AEPs for turbine 1 calculated using firstly the IEC power curve and secondly the nacelle relationship defined using turbine 2 (ie the wrong turbine) turn out to be well within the uncertainty of the AEP.

This confirms in principle the justification of extending the nacelle to free wind speed relationship to other turbines within the same wind farm which notionally are in the same environment and are set up in a similar manner.

3.2.6 Verification of the Nacelle Anemometer Correction in Flat Terrain for Different Control Settings

The rotor speed of turbine 2 at Inte was reduced during part of the test (mode P35), so allowing the effect on the nacelle to free wind speed relationship to be tested.

The reduction in rotor speed was applied in the power range beyond 150 kW, corresponding to a wind speed of about 8 m/s, and was increased with the electrical power. Below 150 kW only slight changes in rotor speed control occurred. At rated power the rotor speed was reduced to 35 rpm compared to 38 rpm in the mode without speed reduction.

The reduction in speed led to a reduction in power regulation from in excess of 500 kW down to approximately 450 kW. Notwithstanding this, there was surprisingly little influence on the nacelle to free-wind-speed relationship as shown in Fig 3.17.

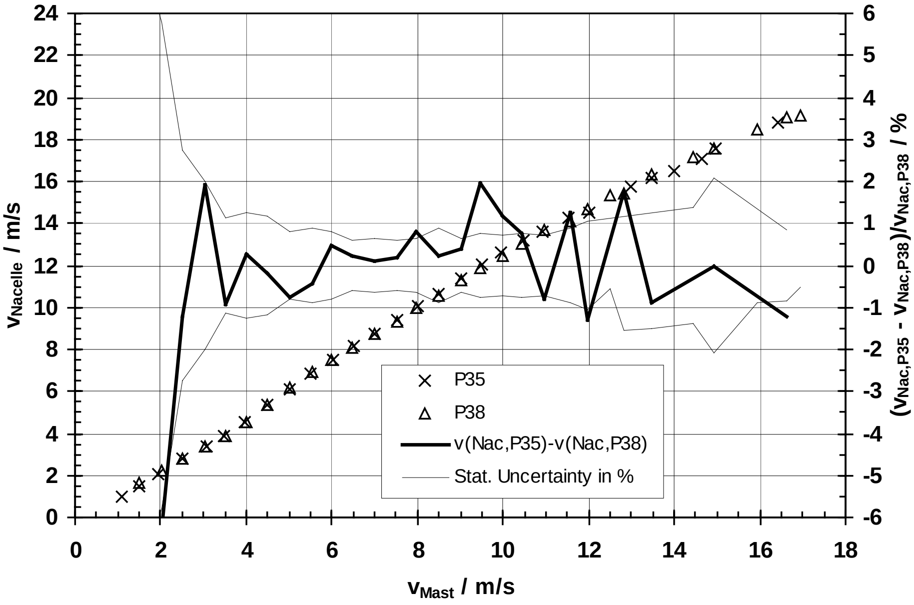

Fig. 3.17. Nacelle anemometer data from turbine 2 at Inte for two different turbine modes bin averaged according to the met mast data (bin width 0.5 m/s). The combined statistical uncertainty of the nacelle anemometer readings in each wind speed bin is compared to the relative difference between the nacelle anemometer measurements.

This clearly indicates that the nacelle to free-wind-speed relationship derived in the initial mode can still be used with low uncertainty to produce a power curve based upon corrected nacelle wind speed in the modified speed mode (in fact the error in AEP in so doing is smaller than 1 % and is by far lower than the uncertainty of the AEP associated with the mast based power curve.

A general conclusion of this investigation is that the properties of the nacelle anemometer are not influenced significantly by a change of rotor speed setting of up to 10 %. Thus, a nacelle anemometer correction derived when the turbine's rotor speed is controlled e.g. to higher levels can also be used for other rotor speed settings to evaluate the power performance.

3.3 Stall Regulated Turbine (Model Not Declared)

From the actively controlled Enercon tests it appears that the nacelle-to-free-wind-speed relationship appears to be independent of control setting. This conclusion does not automatically transfer to stall regulated turbines for reasons that will be suggested later.

A series of tests were carried out to study the sensitivity of the nacelle-to-free-wind-speed relationship for a stall-regulated turbine at different pitch settings.

The turbine had the following specifications:

Rotor:

Position of Rotor:	Upwind
Direction of Rotor Axis:	Horizontal
Number of Blades:	3
Rotor Diameter:	42 m

Control Design:

Rotor Speed	Fixed, at low power variable
Power Control:	Stall
Yaw Control:	Active

Generator:

Type:	Asynchron
Power Transmission from Rotor:	Gear
Rated Power:	600 kW
Rated Voltage:	690 V
Frequency:	50 Hz

Tower:

Material:	Conical Steel Tube (Eifel)
Hub Height:	45 m (Inte)

During the measurements the wind turbine was operated with different rotor bade settings:

- pitch angle set differently for each blade between –2.3° and –3.3°,
- pitch angle set to –2.1° for all blades
- pitch angle set to –0.8° for all blades, stall strips installed

Fig 3.18 shows that the nacelle-to-free-wind-speed relationship changes depending upon the rotor configuration. The relationship for the -2.1º setting is used as the benchmark against which differences for the other rotor settings are judged.

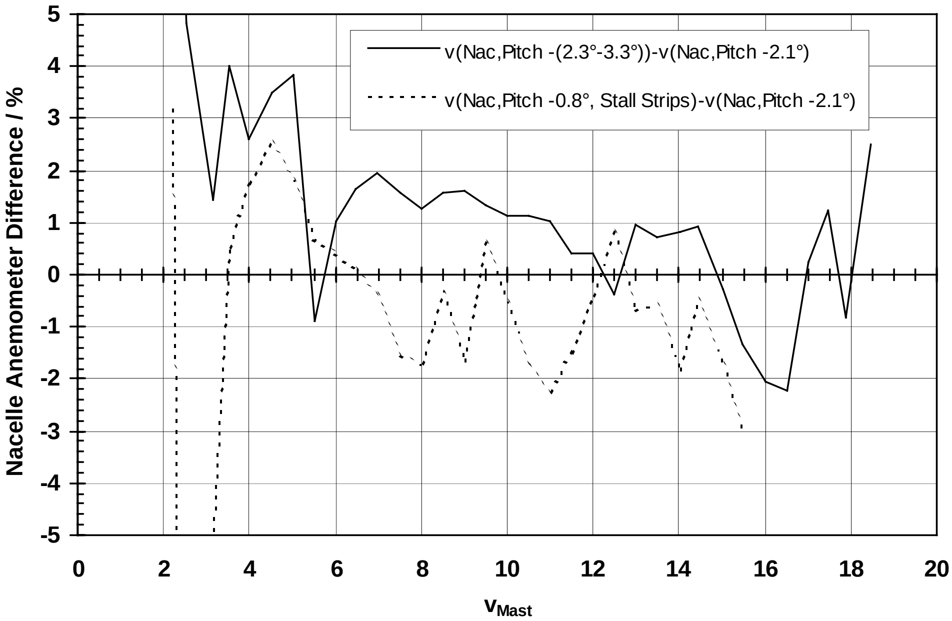

Fig. 3.18. Difference in nacelle anemometer readings due to different rotor blade configurations classified according to the mast measured wind speed. All values are related to the Pitch setting –2.1°.

There is a clear change in the relationship according to rotor setting. The key question then becomes how well will it be possible to judge the power curve of a machine in one configuration using a nacelle-to-free-wind-speed relationship established in another. Figure 3.19 provides an indication.

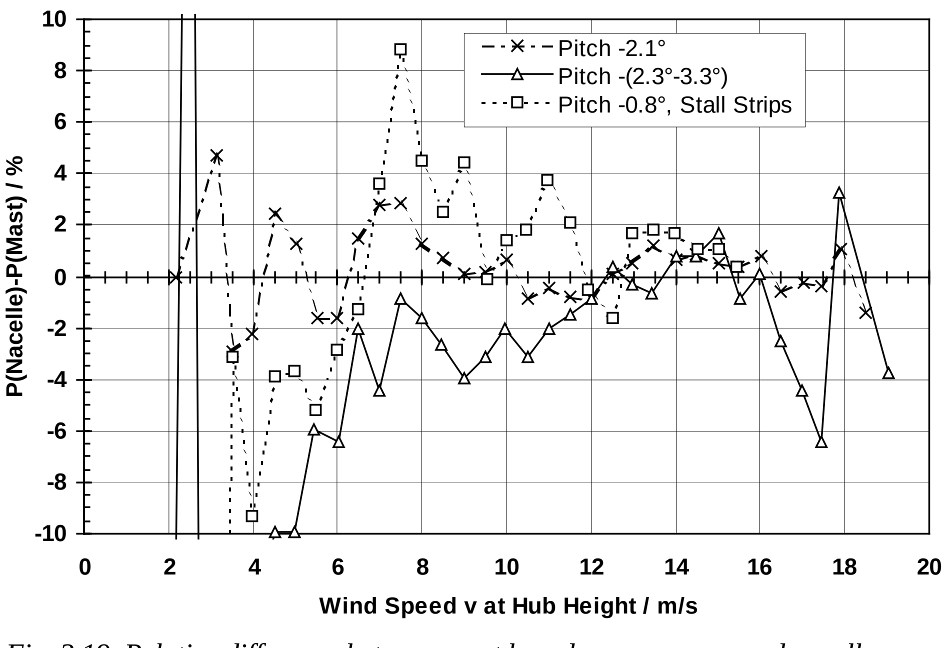

Fig. 3.19. Relative difference between mast based power curves and nacelle anemometer based power curves for all three rotor blade configurations of the investigated stall controlled WTGS. In each case the same nacelle anemometer correction was applied which was derived for the pitch angle –2.1°.

The impact of these differences on apparent Annual Energy Production are appreciable (varying depending upon rotor configuration from 3% to 7% under-prediction for a mean wind speed of 7 m/s). However, the apparent AEP always moved in the same direction as the true AEP i.e. using the ‘wrong’ nacelle to free-wind-speed relationship tended to amplify rather than mask real performance changes. This has practical use. Fuller details of the results are provided in Ref 3.1.

One might ask why seemingly small changes in pitch setting can have such a dramatic impact on the nacelle-to-free-wind-speed relationship whereas a significant change in control algorithm for the actively controlled Enercon turbine did not. The answer may lie in the nature of the change in induction which there changes bring about. In changing the speed of the Enercon turbine, the induction was not altered dramatically (all that happened was that the operational point moved along the top of a fairly flat C_p-λ curve), whereas with the pitch change it was (the turbine dropped to a new C_p-λ curve having lower C_p values.

3.4 Elkraft 1 MW Turbine

The aim of the work on the Elkraft turbine on Sealand was to determine whether the nacelle wind speed to free wind speed relationship is influenced by the rotor setting i.e. whether there is an induction sensitivity present.

Or the purposes of the test three turbine configurations/settings were adopted as indicated in Table 3.2 below. For the last setting, two alternative positions for the nacelle cup anemometer were considered.

Table 3.2. The four measurement periods for the Elkraft turbine

Measurement phase→	1	2	3a	3b
Pitch settings	+0.5°	+0.5°	-1.0°	-1.0°
Nacelle anemometer height	1.2m	1.2m	1.2m	3.m
Yaw error at 10m/s	+12	+7	+7	+7
VG on the blades	No	no	yes	Yes

Fig 3.20 shows the power curves for phase 1 and 2 based upon the met mast wind speed together with the power curve for phase 2 based upon the nacelle wind speed corrected according to the relationship determined during phase 1.

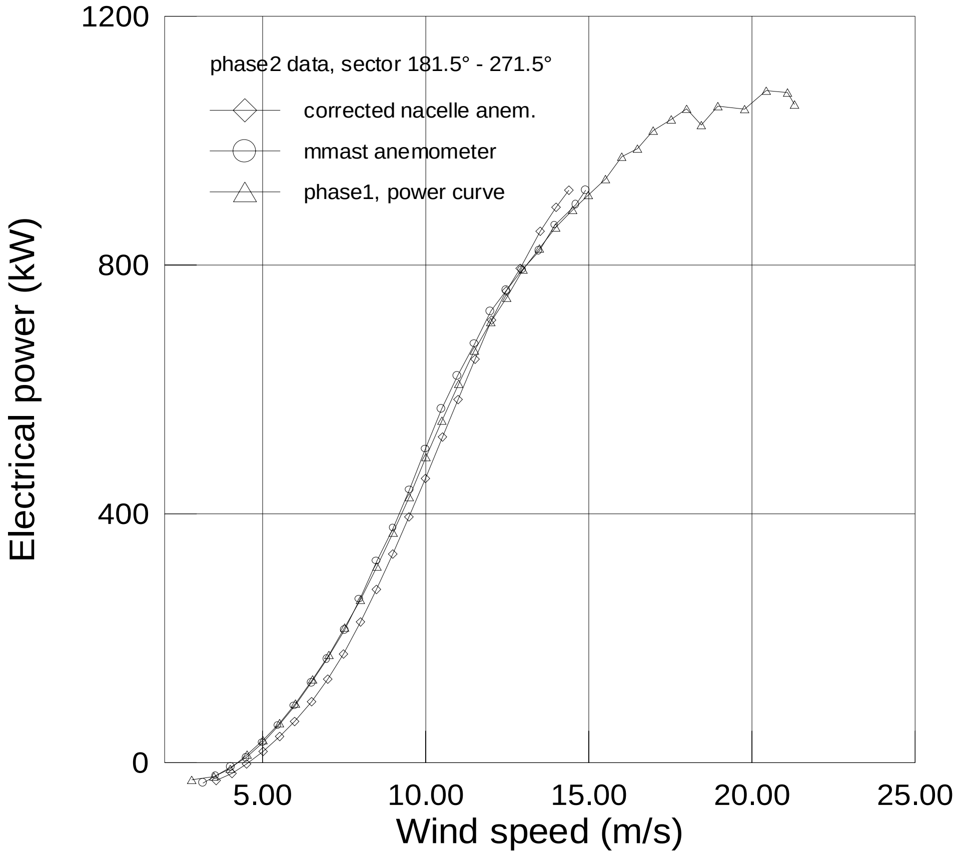

Fig. 3.20. Real and inferred power curves for the Elkraft turbine in two different configurations.

The simple nacelle method gives totally misleading indications of how the turbine performance changes relative to the stage 1 benchmark. For the bulk of the power curve, the true performance actually improves marginally whereas the nacelle approach would suggest a major decrease in productivity.

In Fig 3.21 the mast-nacelle anemometer relation for the various measurement phases is presented. The large differences between the phase1 and the phase2 data, and the small differences between the phase2 and the phase3a data, are surprising when the differences in the rotor aerodynamics are considered. The largest deviation from the original relation happens in the case of the phase3b data.

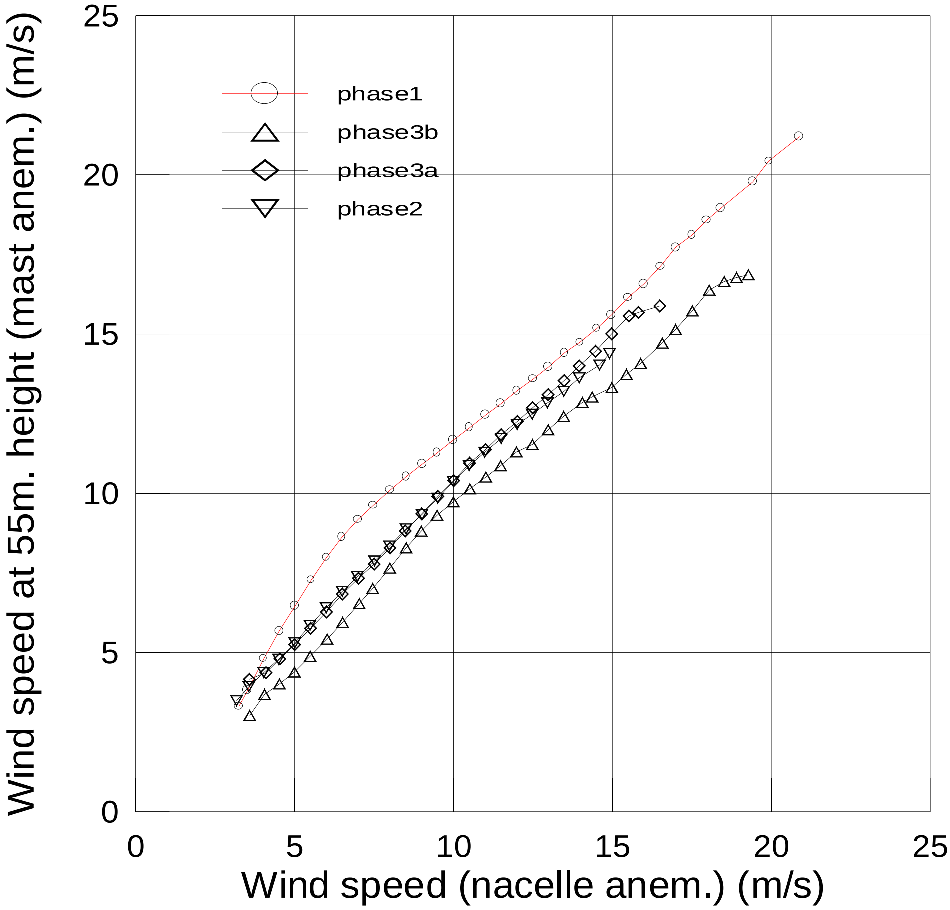

Fig. 3.21. Comparison of met mast to nacelle based wind speed relationships for various measurement phases

The case of the Elkraft turbine shows very clearly the dangers of transferring the nacelle-to-free-wind-speed relationship from one turbine to another recognising that a change in performance may also be accompanied with a change in the nacelle-to-free-wind-speed relation itself.

4 Instrument Accuracy

In defining a power curve, the key variables to be monitored are of course wind speed and electrical power. Much work has been carried out in recent years in understanding the dynamics and characteristics of cup anemometers. The aim of the current investigation is to look at what this knowledge implies for attainable in-service accuracy. Similarly, for power monitoring devices, the aim, in the context of power quality and power variability typical of wind turbines, is to look at to what degree uncertainty classifications still apply.

The work reported here:

- Reviews uncertainty sources for cup anemometers and defines characteristics for particular instruments
- Uses this knowledge to assess in-service errors, and
- Looks at uncertainties in non-wind-speed transducers.

The work is reported in greater detail in Refs 4.1, 4.2 and 4.3

4.1 Characterisation Tests for Specific Anemometers

In order to derive anemometer-specific parameter values for subsequent use in ‘in-service’ modelling, three series of tests were carried out using two models of cup anemometer.

The tests were designed to look at:

- Dynamic Response
- Vertical Sensitivity
- Horizontal Shear Sensitivity

The anemometers used were the Vector A100 and the NRG Max 40, both of which are extensively used by the wind energy community. Photographs are shown in Figures 4.1 and 4.2 below.

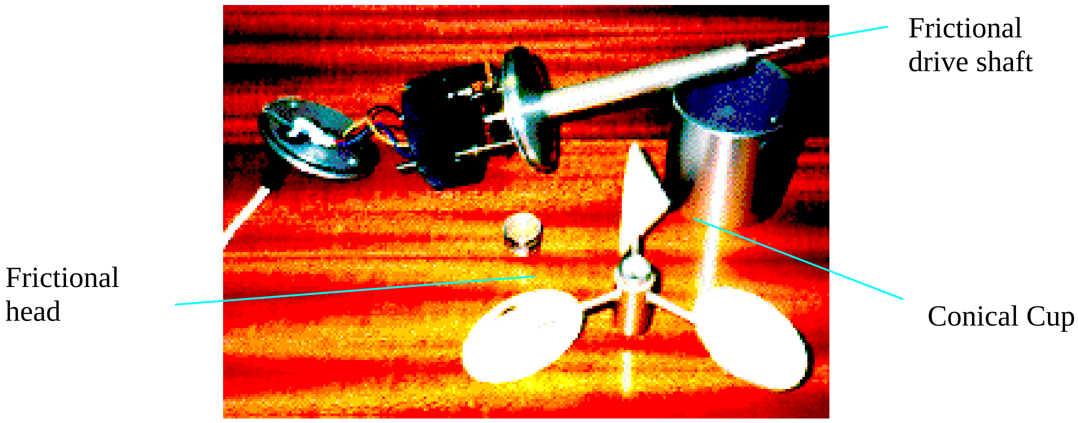

Fig. 4.1. Vector A100 cup anemometer

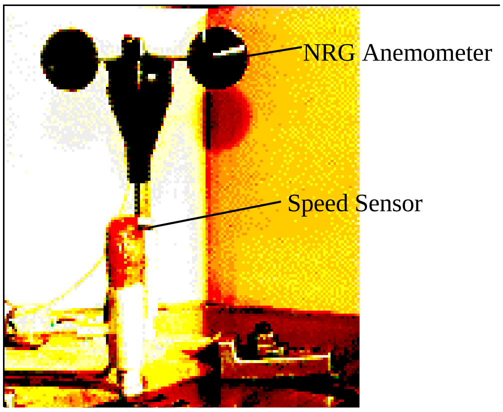

Fig. 4.2. NRG Max 40 cup anemometer

4.1.1 Dynamic Response Tests

The response of the anemometers to step changes in wind speed (with speed falling to zero) were monitored both with and without rotors attached. This gives information on both the aerodynamic and frictional (including internal windage) damping of the instruments.

The results of the tests are as shown in Table 4.1 below.

Table 4.1. Distance constants for the NRG and Vector anemometers

	Distance Constant	
Step Input –Rad/sec	NRG- Rad (m)	Vector- Rad (m)
35 (with cups)	30 (2.1)	42.8 (2.27)
260 (without cups)	1097	268.7

Both anemometers are seen to be responsive (in fact the Vector is much more responsive than claimed by the manufacturer which quotes a 5 metre distance constant). In the case of the NRG instrument, the frictional drag is much lower than in the case of the Vector.

4.1.2 Static Calibration and Linearity

Tests were conducted to identify to what degree the calibration coefficient of the anemometer was sensitive to cup and rotor orientation. Tables 4.2 and 4.3 summarise the results.

Table 4.2. Sensitivity of calibration factor to angle of attack (rotor tilt)

Rotor Angle	VECTOR A100	NRG Maximum 40
-15°	y = 1.0227x + 0.092	y = 1.0053x + 0.2239
-10°	y = 1.0099x + 0.1257	y = 1.0258x + 0.3175
-5°	y = 0.9987x + 0.1112	y = 0.9994x + 0.3368
0°	y = 1.0089x + 0.0416	y = 0.9903x + 0.069
5°	y = 1.0134x - 0.0608	y = 0.9889x + 0.0958
10°	y = 1.04x + 0.0022	y = 0.989x + 0.1769
15°	y = 1.061x +0.0316	y = 1.0104x + 0.0806

Table 4.3. Sensitivity of calibration factor to cup angle

Cup Angle	VECTOR A 100	NRG Maximum 40
-15°	y = x + 0.2055	N.A.
-10°	y = 1.0003x + 0.2638	N.A.
-5°	y = x + 0.2459	N.A.
0°	y = 1.0089x + 0.0416	N.A.
5°	y = x + 0.1965	N.A.
10°	y = x + 0.5039	N.A.
15°	y = x + 0.3679	N.A.

The rotor tilt results are presented graphically in Figures 4.3 and 4.4 below.

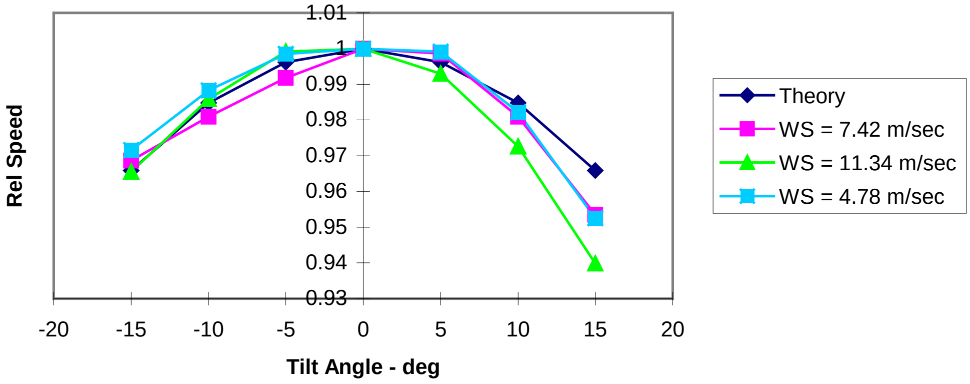

Fig. 4.3. Sensitivity of Vector A100 anemometer to angle of attack in the vertical plane at various wind speeds.

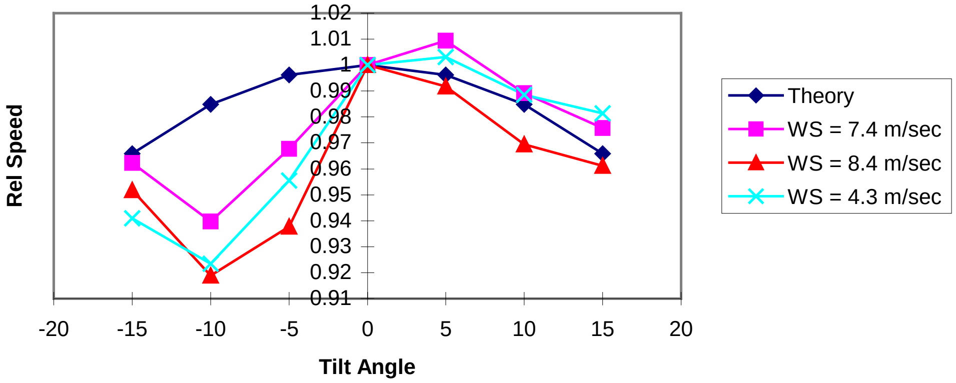

Fig. 4.4. Sensitivity of NRG Max40 anemometer to angle of attack in the vertical plane at various wind speeds

These show that the Vector anemometer behaves in a manner which approximates the simple cosine sensitivity, albeit that the deviations are not inconsiderable and are not wind speed independent.

The NRG on the other hand does not follow a cosine pattern, and has very marked wind speed dependency.

In the free atmosphere, there will be clear errors in monitoring wind which has a vertical component.

4.1.3 Sensitivity to Horizontally Sheared Flow

It is readily shown in a horizontally sheared flow where one half of the anemometer rotor sees a wind speed lower than the mean whilst the other half sees one that is correspondingly higher, that the net response of the rotor will not be to average out the distortion. Any shear rather than being averaged out is likely to result in the mean flow being erroneously logged with the error margin being three times the shear amplitude. Whether the error is positive or negative is determined by whether the concave sides of the cups see the positive shear or the negative shear.

To determine whether this expectation is borne out in reality, the test anemometers were mounted on a lever arm that was alternately rotated clockwise and then anti-clockwise, so simulating negative and then positive horizontal shear. A vertical-boring machine was used for the test. Using this arrangement has the advantage of imposing a very severe horizontal shear on the wind speed seen by the rotor, but has the disadvantage of imposing a very strong self-wake flow regime on the rotor. Nevertheless, it was hoped that the expected general trend should be discernible.

The results shown in Figures 4.5 and 4.6 do not support the hoped-for corroboration.

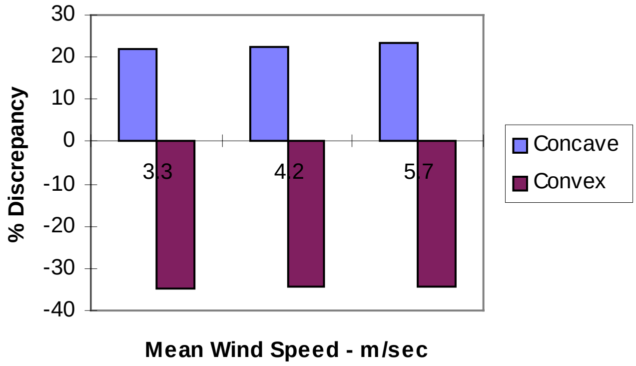

Fig. 4.5. Discrepancy between mean wind speed and mean wind speed indicated by the Vector A100 cup anemometer

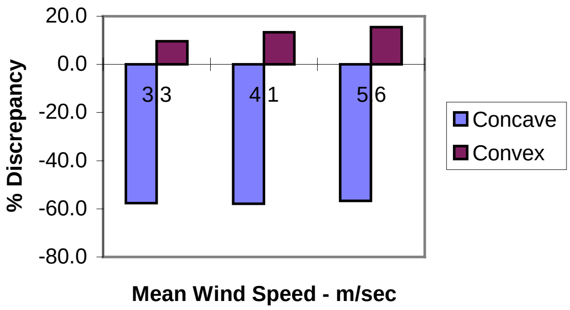

Fig. 4.6. Discrepancy between mean wind speed and wind speed indicated by the NRG Max40 cup anmeometer

4.2 Assessment of In-Service Errors and Uncertainties

It had been intended to use the results of the above tests as input parameters to two simulation models, the first describing the 3-dimensional flow in the vicinity of a meteorological mast and the other describing the flow over a parked wind turbine nacelle.

The complexity of including disturbance effects from the mast and nacelle obstructions in the model proved to be too great, and as a result the modelling has only addressed free field wind conditions.

4.2.1 Method

The dynamic responses of the two cup anemometers, NRG Max 40 and Vector A100, have been assessed under a simulated 3 dimensional wind regime.

Derivation of the most of the instrument parameters is described above. Other parameter values have been provided by the instrument manufacturers.

The wind regime was generated using a wind model described in Refs 4.4 and 4.5.

The anemometer model is as described in Ref 4.6.

The simulation tool used was VisSim/32.

The aim of the investigation was to generate a 3-dimensional wind field of known characteristics, to pass this through a comprehensive model of the anemometers and to derive the statistics of the anemometer outputs which could then be compared with the original ‘true wind inputs.

4.2.2 Anemometer Model

To analyse the dynamic responses of the two anemometers, the model proposed in Ref 4.6 is given below.

Rotor inertia torque = Rotor aerodynamic torque - Frictional torque

where

Rotor inertia torque = $I_{ZZ}\alpha_r$

Aerodynamic torque = $\frac{1}{2}R\rho AC_{dv}(U - R\omega_r)^2 - \frac{1}{2}R\rho AC_{dx}(U + R\omega_r)^2$

Frictional torque = $B_0 + B_1\omega r^1 + B_2\omega r^2 + \ldots$

Symbols are as follows:

I_{ZZ}	Moment of inertia of the rotor assembly.
α_r	Angular acceleration of the rotor assembly.
ω_r	Angular velocity of the rotor assembly.

R Radius (from centre line of the rotor axis to centre line of the cup).
 Air density.
C_{dv} Drag coefficient for the concave faces of the anemometer cup.
C_{dx} Drag coefficient for the convex faces of the anemometer cup.
A Frontal area of the anemometer cup.
B_0,B_1..; Coefficients determined by rotor frictional tests.
U Instantaneous resultant wind vector impinging the cup anemometer

For a 3-D wind regime, $U = \sqrt{u^2 + v^2 + w^2}$, where u, v, w are wind components.

Under steady state conditions and assuming no friction, the aerodynamic balance can be rewritten as:

$$C_{dv}(U-R\omega r)^2 = C_{dx}(U+R\omega r)^2$$

Typical C_{dv} and C_{dx} values are 1.4 and 0.4 respectively.

4.2.3 Simulation Results

Figure 4.7 shows the wind vector used as input to the model whilst Figures 4.8 and 4.9 show extracts from the simulation results for the two anemometers.

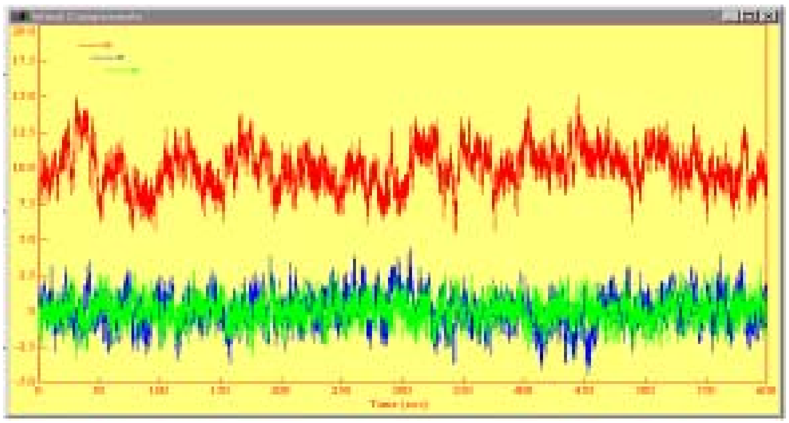

Fig. 4.7. 3-dimensional wind description used as input to the model

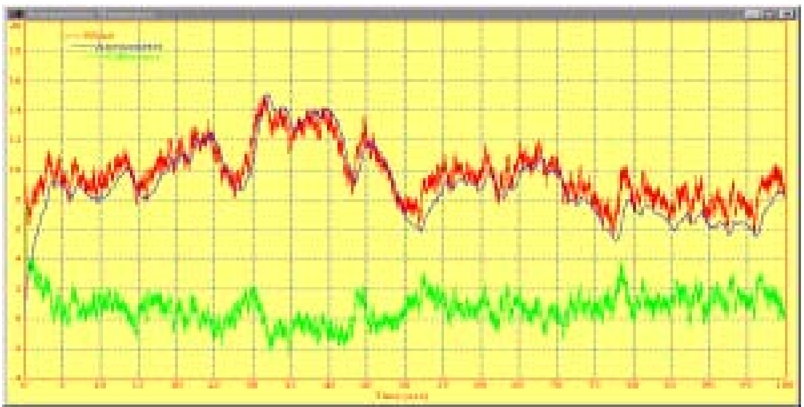

Fig. 4.8. Simulation result for vector A100 anemometer

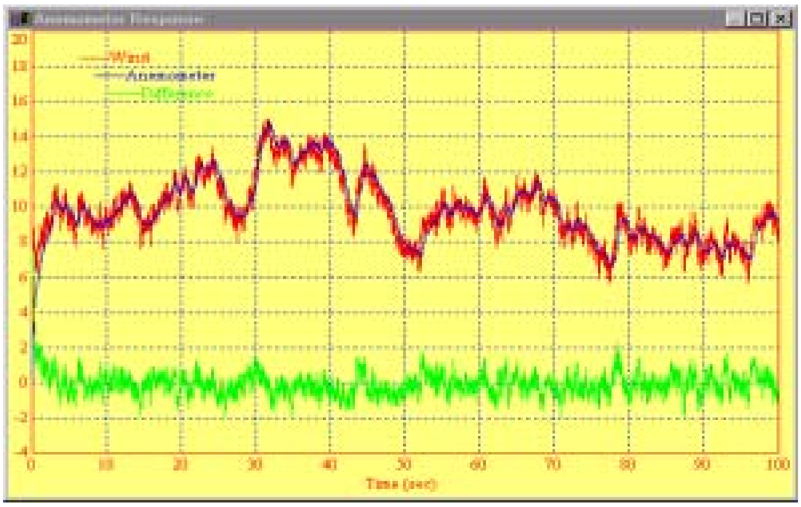

Fig. 4.9. Simulation result for NRG Max40 anemometer

In Figures 4.8 and 4.9, the wind speed is defined as the quadrature of the uvw components. From the tests of sensitivity in the vertical plane, it was shown that the Vector anemometer has a sensitivity which is close to cosine, implying that the anemometer will provide a good indication of the uv wind speed but not of the uvw. The NRG anemometer on the other hand has a highly asymmetric sensitivity, but in a turbulent wind, this may well average out to produce a good estimate of the uvw mean value. This may explain the apparent better following of the NRG.

The simulations were carried out using 60,000 data points at 0.01 second resolution (10 minutes total duration).

The input wind had a mean u component value of 10 m/s and a turbulence intensity I_u (= σ_u/U) of 15%. A Kaimal spectrum was assumed. A friction velocity of 0.687 m/s was used together with a longitudinal length scale, L_u, of 100 metres.

4.3 Uncertainties in Non-Wind Transducers

Wind turbines have a semi-stochastic power output which depending upon wind speed and wind turbine control can fluctuate greatly over short periods of time. On a weak grid, this can result in variations in power quality.

In specifying a power transducer for a power performance test of a wind turbine, the test engineer should look critically at whether the claimed uncertainty classification of the measurement system, particularly the power transducer, can be retained given the nature of the measurand and its effect on related variables.

To address these issues, investigations have been carried out into:

- instrument accuracy and possible operational limits of transducers using information provided by instrument suppliers.
- the effect of response filtering on average, rms and standard deviations of output signals generated by these transducers.

The International Electrotechnical Commission has published class indices for power monitoring and related equipment.

Power transducers are covered by CEI/IEC 688: 1992, Voltage transformers by CEI/IEC. 186, 1993 and current transformers by IEC 44-1 1996.

In the case of a Power Transducer (PT) a classification of 0.1, 0.2, 0.5 or 1 indicates that the limits of intrinsic error will be within ±0.1%, ±0.2%, ±0.5% or ±1.0% where the 'feduciary' value is the span.

In the case of Current and Voltage Transformers (VTs and CTs), similar classifications apply.

Manufacturers will typically present technical specifications for their VT and CT products as shown in Table 4.4 below.

Table 4.4. Typical specifications for voltage and current transformers

Operational Limit	Class 0.5 AC Current Transducer	Class 0.5 AC Voltage Transducer
Max. Current or Voltage	10 amps	480 volts
Preferred input	1, 5 or 10 A a.c.	63.5, 100, 110, 120, 220, 240, 250, 380, 400, 415, 440 and 480 V a.c.
Average Sensing RMS Calibrated	1 DC current output	1 DC current output
Distortion Factor	1%	1% of 3rd harmonic
Range	Not specified	20 to 125%
Temperature Range (operating)	0°C to 60°C calibrated at 23°C	0°C to 60°C calibrated at 23°C
Temperature Coefficient	0.03% per °C	0.03% per °C
Stability	±0.25%/annum (reducing with time)	±0.25%/annum (reducing with time)
Response Time	<400 ms from0 to 99% 250 ms to 90%	<400 ms from0 to 99% 250 ms to 90%
Output Ripple	<0.5% of full rated output	<0.5% of full rated output
Overload Capacity	2 x rated current	1.5 x rated voltage for 10 second
Input Impedance	10 k ohms/volt	10 k ohms/volt
Min. Test Voltage	2kV rms for 1 min.	2kV rms for 1 min.

It should be noted that none of the standards referred to above make any mention of errors being introduced by transients and harmonics. Wind turbine power output and the stability of the voltage waveform vary over a range of frequencies as shown in Figure 4.10.

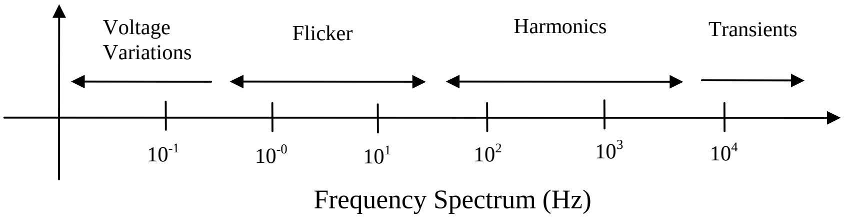

Fig. 4.10. Spectrum of Typical Power Quality Attributes

4.3.1 Sources of Uncertainty

The principal generic sources of uncertainty are:

- Uncertainties introduced by random data
- Uncertainties introduced by transient response
- Data logger impedance matching
- Aliasing in digital data acquisition systems

The second source is of the greatest concern in the current context.

Looking specifically at the effect which filtering of harmonics might have, Figure 4.11 shows measurements made on a 300kW variable speed wind turbine.

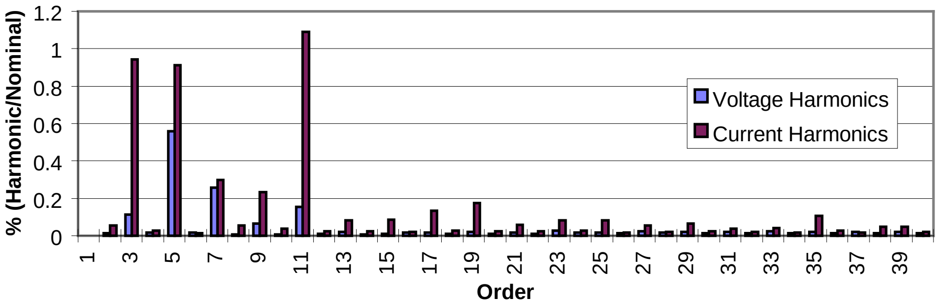

Fig. 4.11. Voltage and current harmonics from a variable speed wind turbine

These harmonics account for approximately 0.2% of turbine power. Filtering of them by the measurement device will introduce a corresponding error.

4.3.2 Thermal Effects on Transducer Performance

As electrical instruments are normally housed in shelters without air conditioning, the accuracy of instruments is certainty affected by the variation of environmental temperature. To look at the impact of such effects, an assessment of the Class 0.5 CT and VTs specified in Table 4.2 was undertaken.

The following parameters were assumed:

- Resistance of copper wire was R(T)Ω±0.3% at room temperature (ie 23°C)
- Length of copper wire was estimated to be around 20 m.

- Temperature coefficient of resistivity was 0.00393/°C±0.1%.
- Temperature of wire was varying between 5±1°C and 35±1°C.
- Parameters measured by the current and voltage transducer was A±0.5% or V±0.5%
- The average RMS current from the wind turbine was 112 A.
- The average RMS voltage from the wind turbine was 248 v.

The resistance of a certain size of copper wire is given by

$$R(T) = R_0 \{1+\alpha(T-23)\}$$

where R & R_0 are resistance of copper wire; α is temperature coefficient of resistivity and T is temperature of copper wire.

The power output measured by current and voltage transducer is given by:

$$P = I^2 R \text{ or } V^2/R$$

This equation can be written as

$$P = I^2 R_0 \{1+\alpha(T-23)\}$$

or

$$P = V^2/ R_0 \{1+\alpha(T-23)\}$$

Individual parametric uncertainty can be estimated by:

For current:	$\frac{\partial P}{\partial I} w_1$
For voltage	$\frac{\partial P}{\partial V} w_2$
For resistance	$\frac{\partial P}{\partial R_0} w_3$
For resistivity	$\frac{\partial P}{\partial \alpha} w_4$
For temperature	$\frac{\partial P}{\partial T} w_5$

where $w_{1\text{-}5}$ describe uncertainty propagation coefficients.

Combined uncertainty can be obtained by adding these contributions in quadrature. The combined uncertainty as a function of temperature is shown in Figure 4.12.

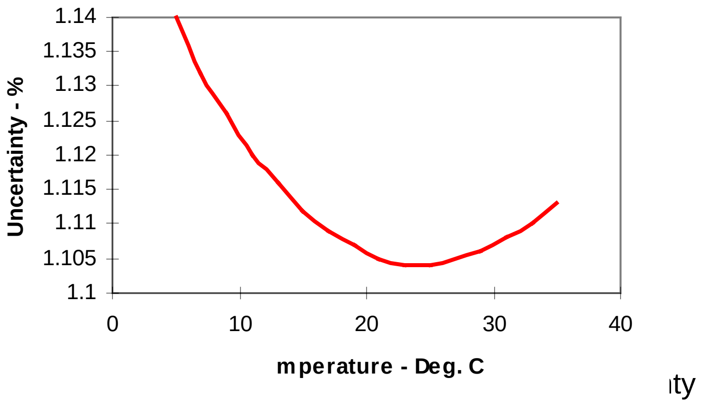

Fig. 4.12. Power measurement uncertainty

4.3.3 Conclusions on Uncertainty of Power Measurement

From the work reported and from the more comprehensive sub-task report, Ref 4.3, the following conclusions can be drawn.

- Transducer errors are expressed in terms of percentage of the fiduciary value, which can only be used when the transducer is operating in a deterministic steady state conditions.
- Instrument transducers are designed not to be excited by frequency lower than several kHz. However, they will be affected by harmonic and transient frequencies.
- The average power loss due to filtering was estimated to be around 0.2%. This would be significant in the long run.
- The overall system response is significantly slower than the response of the current and voltage transducers, around 1000 to 1.
- The category B uncertainty for typical current and voltage transducers under thermal effects is estimated to be around 1%; this is higher than would be expected from uncertainty classifications.

5 Enhancement Of Performance Assessment Analysis Methods

Current power performance assessment methods make the overt assumption that wind turbine performance only depends appreciably on hub height wind speed and upon air density. Brief reflection suggests that this may not be so and that other parameters of secondary importance, such as turbulence intensity, turbulence length scale and wind shear should also have an influence.

Should a performance test span a sufficiently long time, then a range of conditions typical of the long-term will be experienced and there will be no particular bias introduced by ignoring such dependencies. However, performance evaluation codes recommend quite short test durations, certainly too short for an annual range of weather conditions to be experienced. Additionally, unless these hypothesised parameter dependencies can be identified and quantified, there is no basis for making confident predictions of turbine performance in 'real' commercial sites based upon limited type testing.

The variability of performance likely to be experienced at a site and how it can be explained by such parameter dependencies has been studied as part of this and related projects. A number of reports have already presented the key studies and results (Refs 5.1 and 5.2), so a very abbreviated version is given here. However, some limited work, not previously published is also included.

Firstly, it will be demonstrated that wind farm power performance characteristics have a seasonal dependence.

Thereafter, it will be illustrated that ensemble averaging can confirm that performance dependencies exist which are normally ignored in performance tests.

Multi-variate regression analysis methods are then described which in principle could be used to extract the relevant functional relationships. Emphasis will be placed on satisfying the basic requirements of the mathematical method.

The results and implications will then be examined.

Finally a brief presentation of work not yet reported will be given.

For the purposes of this report, data from the wind farms at Coal Clough and Carland Cross in England will be used unless otherwise stated. These wind farms are equipped with 24 and 15 off 400 kW Windane 34 turbines respectively. This model of turbine is of fixed speed, pitch regulated design. Just over four years worth of data have been used in both cases. Note that this is a much more comprehensive data base than would ever be used for a conventional performance assessment. Both wind farms lie in complex terrain.

The nacelle anemometer method, as outlined in Chapter 3, and involving calibration of the nacelle-to-free-wind-speed relationship using a reference turbine, has been used throughout.

Finally, the use of the term Weighted Performance Measure (WPM) has been used. This is the same as Annual Energy Production (AEP) and is a convenient way of collapsing power curves to single figures for inter-comparison. The wind speed weighting function has been a Weibull distribution with a shape parameter of 2 and a scale parameter of 8.5 m/s.

5.1 Variation of Wind Farm Power Performance With Time

An illustration of how wind turbine performance can vary with time is shown in Figure 5.1. This shows how the power output, averaged over three month periods, varied for Turbine 15 at Carland Cross wind farm. Data has only been used if the wind speed was between 7 and 8 m/s.

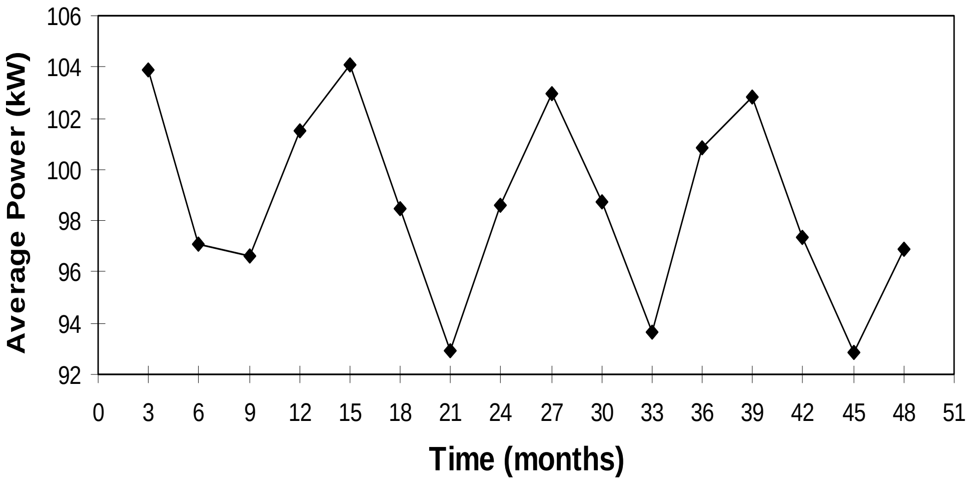

Fig. 5.1. Mean power versus time for turbine 15 at Carland Cross wind farm

The key feature is a strong seasonal pattern.

A very large number of turbines at different wind farms have been analysed and such variation is a common feature.

In terms of the WPM, very similar trends are also apparent with a spread in yield of approximately ±5%..

5.2 Performance Dependence on Secondary Parameters

In the following sections, it is shown that turbine performance has a clear dependency on turbulence intensity, wind shear, flow inclination and turbulence length scale.

More comprehensive details are again given in Refs 5.1 and 5.2.

The basic method used is one of ensemble averaging, where within defined wind speed intervals data are delineated according to values of the specific parameter of interest. Variations caused by other parameters are effectively assumed to average out and to be uncorrelated with the parameter of interest.

5.3 Turbulence Intensity

In what follows, turbulence intensity refers to what is indicated by the nacelle mounted anemometer. Comparison shows that the nacelle anemometer will indicate approximately twice the free field turbulence level.

Figures 5.2, 5.3 and 5.4 show how performance varies with turbulence intensity in the below rated (5 to 9 m/s), at rated (9 to 13 m/s) and above rated (13 to 23 m/s) ranges.

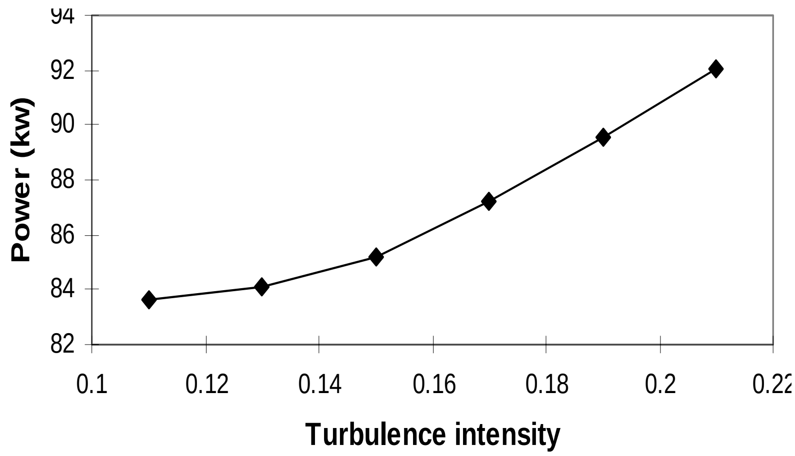

Fig. 5.2. Average power output at Carland Cross (average of all turbines) as a function of nacelle turbulence – below rated conditions 5-9 m/s

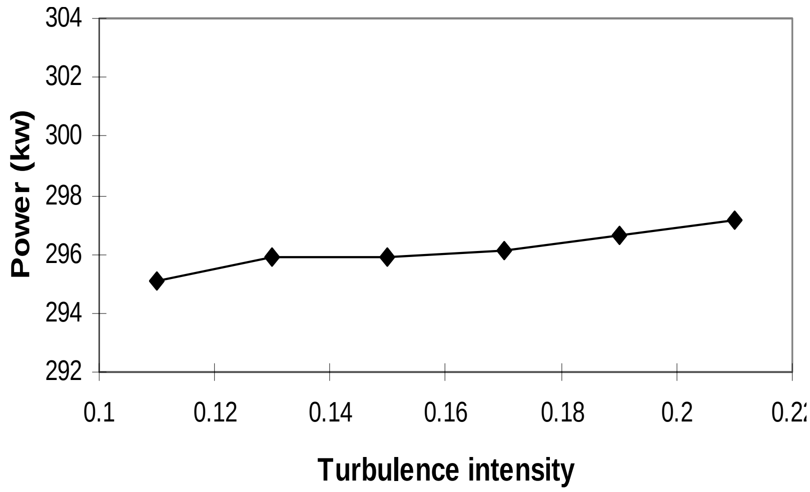

Fig. 5.3. Average power output at Carland Cross (average of all turbines) as a function of nacelle turbulence – at rated conditions 9-13 m/s

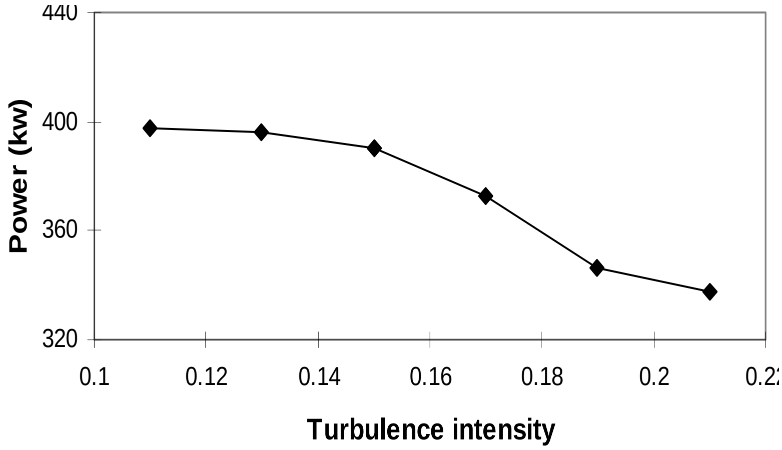

Fig. 5.4. Average power output at Carland Cross (average of all turbines) as a function of nacelle turbulence – above rated conditions 13-23 m/s

The dependency is of the nature that one might intuitively expect. At low wind speeds as turbulence increases, an increasing proportion of higher wind speed data are captured which due to the concave upwards nature of the power curve will result in an increase in the mean value. Similarly in the post-regulation zone, higher turbulence means that an increasing proportion of pre-regulation wind speeds are captured, leading to a fall in the mean power level.

The trends shown are both well defined and of appreciable magnitude, suggesting that such dependencies on turbulence could and should be taken into account when carrying out a performance evaluation.

5.4 Shear

Once again an ensemble averaging approach can be taken.

Figure 5.5 shows for the Carland Cross wind farm the average effect which wind shear has on turbine performance, averaged across all the wind turbines in the farm. To derive shear exponent values for the individual turbines and wind directions, a flow model has been run to transfer shear conditions measured at a site meteorological mast.

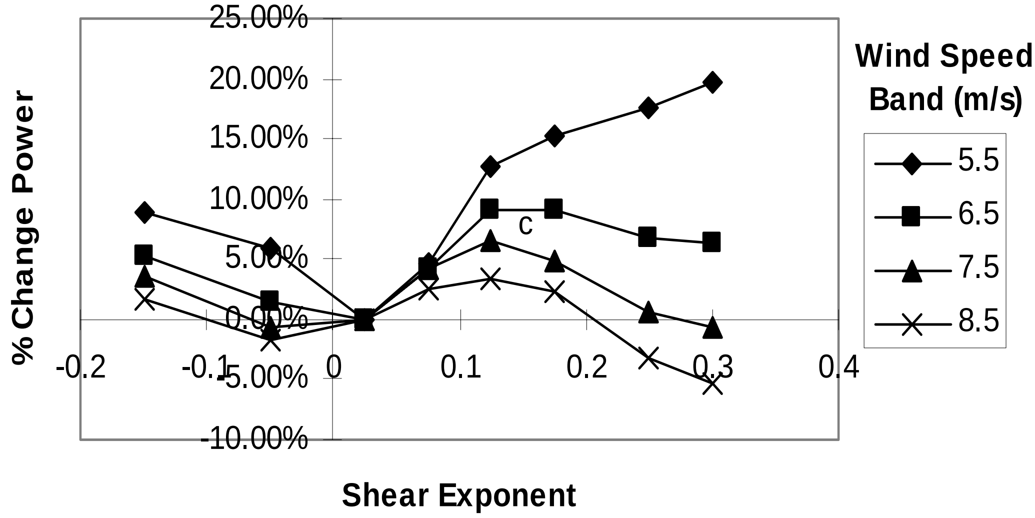

Fig. 5.5. Percentage change in power averaged over all turbines at Carland Cross as a function of shear at below rated power.

Only below-rated conditions have been studied since in the regulation zone, power will clearly remain constant.

Results are plotted relative to power output obtained in the wind shear exponent band 0.0 to 0.05.

The figure shows that shear has a greater effect at lower wind speeds, and can be of very appreciable significance. The trends are once again well defined.

Simple blade-element theory has been used in Figure 5.6 to produce predictions of the shear sensitivity that might be expected.

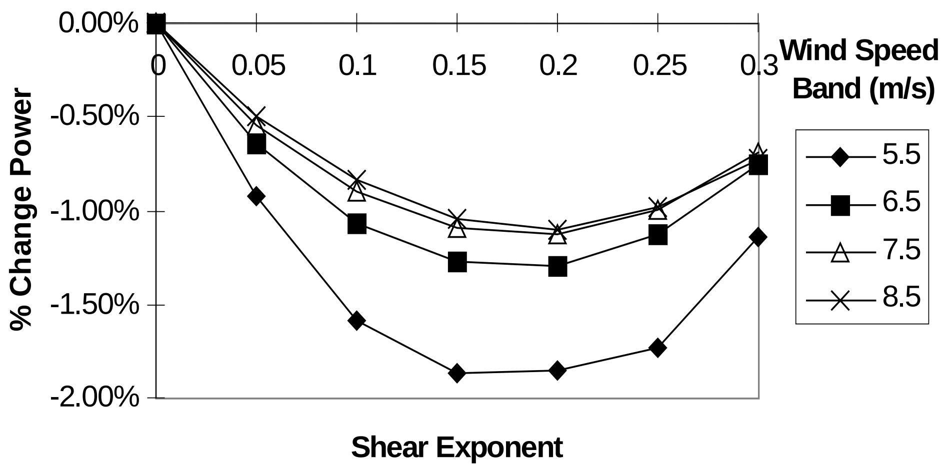

Fig. 5.6. Percentage change in power expected as a function of shear from blade element modelling

It is interesting to note that the nature of the curves are quite different to those derived from the experimental data and that the predicted magnitude of the sensitivity is far smaller than in reality.

5.5 Power Sensitivity to Inclined Flow

Measurement of flow inclination angle is not routinely undertaken. However studies (Ref 5.3) have confirmed that there is a clear, linear relationship between the angle of terrain slope and the angle of inclination of the flow.

In determining slope, a number of definitions can be used. Here slope is based upon the slope of the best-fit Richardson function. Details can be found in Ref 5.1.

Figure 5.7 shows for Carland Cross wind farm the sensitivity of performance to flow (in fact terrain) inclination angle. Once again large quantities (four years) of data have been used.

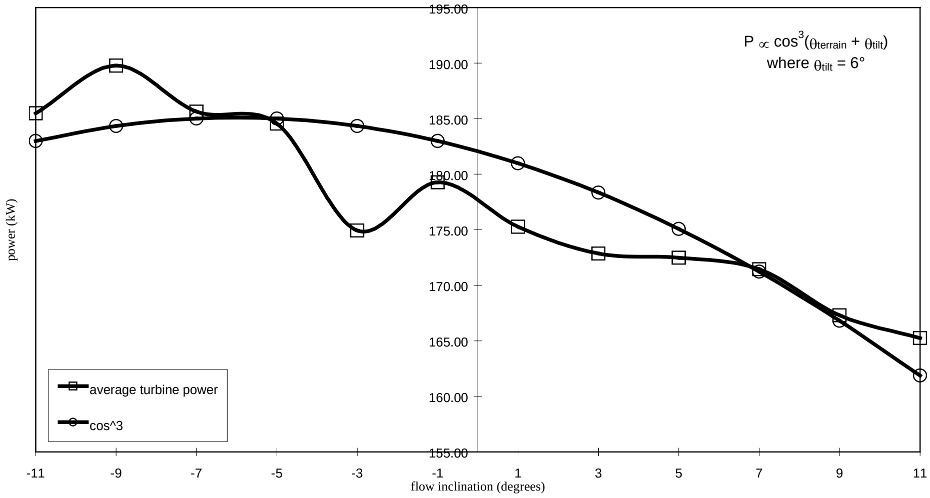

Fig. 5.7. Power versus flow inclination angle for below rated conditions averaged over all turbines at Carland Cross wind farm

Power output from a wind turbine is expected to vary with the cube of the cosine function of the flow inclination angle. The experimental data are loosely consistent with this expectation.

Further analysis confirms, due to the power regulation nature of the turbines, that in above rated conditions there is no dependency,

5.6 Power Sensitivity to Turbulence Length Scale

It can reasonably be expected that a wind turbine should display sensitivity to the length scale of turbulence, particularly for an actively controlled turbine where control action might more readily follow longer than shorter periods. Equally, higher frequency turbulence might be expected to average out over the rotor disc whereas lower frequencies might have more coherence across the disc, again intuitively leading to better energy conversion.

Length scale is not conventionally measured, however it can be reasonably expected that it might be indicated by the ratio of standard deviations of power output and nacelle wind speed. If the ratio is high, good wind following is implied (long length scales) whereas if the ratio is low, poorer wind following is implied (shorter length scales).

Figure 5.8 for 2 years of data from turbine 3 at Coal Clough wind farm and for the 7 to 8 m/s wind speed band, shows how power output is affected by 'length scale'.

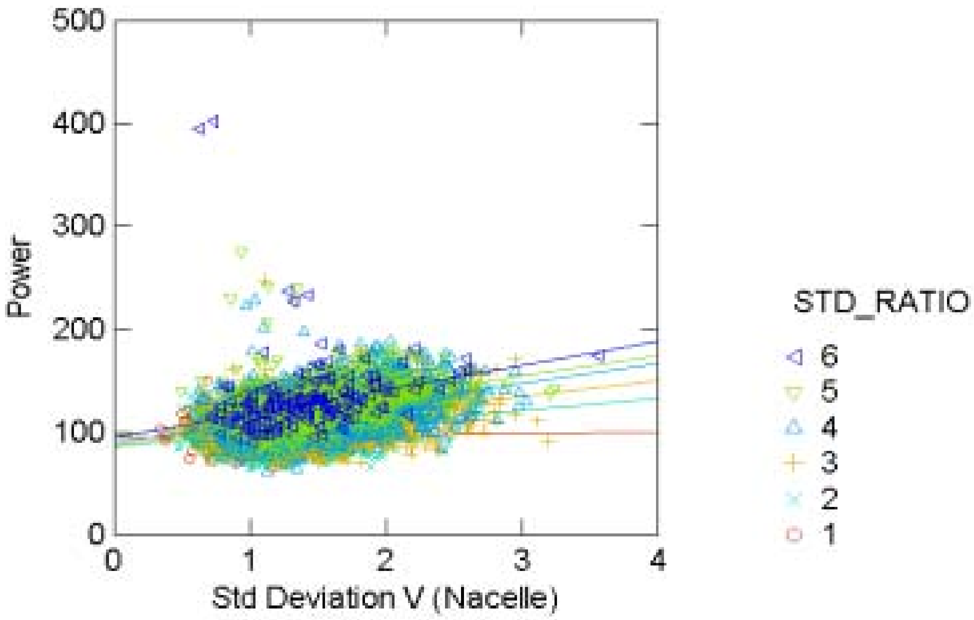

Fig. 5.8. Power as a function of standard deviation of nacelle wind speed, stratified by power to wind speed standard deviation ratio

Despite the extreme data scatter, there is a suggestion that there is a correlation. The results are consistent in trend with the earlier hypothesis.

5.7 Multi-Variate Regression Analysis Methods

In previous sections it has been shown very clearly that wind turbine power performance is not, as is often assumed, solely dependent upon wind speed. A number of important additional parameters and variables have a discernible impact on performance.

It can be hypothesised that if a sufficient number of relevant variables are considered, then a generalised and universally applicable power relationship should be derivable. In this section we look at statistical tools which can be used for unravelling in a mechanistic manner the multi-dimensional relationships which exist.

The aim will be to build up a multivariate model on one turbine and then apply it to other turbines of the same type to check that it is not turbine specific. In addition to mean wind speed, the model uses turbulence intensity, flow inclination, wind shear, standard deviation ratio, air density and standard deviation of wind direction. A regression analysis is applied to these variables with the intention of predicting power more accurately than if just wind speed and air density were used.

The regression model is derived using data from turbine 15 at Carland Cross wind farm (pitch regulated Windane 34, 400 kW turbine) operating between 7 and 8 m/s. The model is then applied to other turbines of the same type to check that it is not turbine specific.

5.7.1 Multiple Regression

A detailed description of multiple regression analysis is given in the fuller report (Ref 5.1). This section will emphasise various assumptions about the data upon which regression relies. These assumptions impose conditions on the data sets used in the model. Regression analysis assumes that all data sets are:

- normally distributed
- mutually independent
- linear in their relation to the predicted variable.

A regression model is also only valid if it is complete. This means that all variables that affect the parameter being predicted must be included in the model. If any of these conditions are not met then the resulting model can be incorrect. The size and even the sign of resulting variable coefficients can be wrong. Within this project it has been found that if these conditions are overlooked then the resulting model does not make physical sense and is also specific to a single data set (Ref 5.4).

Table 5.1 shows that it can be very misleading simply to apply a regression model to a single set of unconditioned data and imply anything from the results. For example one data set, (180° to 210°), gives a value for the inclined flow coefficient of -876.6, whilst the data taken from another sector (240° to 270°) implies a coefficient of 562.6. These values are clearly contradictory and show that results are specific to one data set only.

To check that the results in Table 5.1 are not just a peculiarity of turbine 15 at Carland Cross, data from many other turbines from this and another wind farm, in various wind speed ranges were analysed. The same pattern of results was found in each case and an example is given in Table 5.2. Coefficient values that are not in bold indicate cases where the probability of that coefficient being 0 is higher than 10%, which implies that the variable is not really useful in the model.

Table 5.1: Multiple Regression Results for Turbine 15 at Wind Farm 'B'.

Model = constant + A.$\overline{V}$ + B.σ_v + C.Shear + D.Flow + E.Density)

Direction Sector	Adjusted R^2	Mean speed coefficient	Turb. Intensity coefficient	Shear coef-ficient	Flow coef-ficient	Density coefficient	Constant	Standard Error
30° to 60°								
60° to 90°	**36.4%**	**74.5**	75.2	4.2	-324.3	81.1	-535.8	**7.7**
90° to 120°	**74.1%**	-7.6	-41	**-8.7**	**-1355.1**	-214.8	**358.0**	**2.8**
120° to 150°	**21.9%**	**32.7**	**85.5**	1.1	411.6	174.9	**-336.3**	**6.7**
150° to 180°	**60.2%**	**41.9**	11.9	**32.2**	-108.7	36.5	**-262.6**	**4.5**
180° to 210°	**52.3%**	**49.8**	-3.1	8.2	-876.6	-26.5	**-224.6**	**4.3**
210° to 240°	**42.5%**	**37.8**	**-43.7**	-1.2	**1149.0**	**109.5**	**-322.5**	**4.9**
240° to 270°	**35.4%**	**39.3**	**-59.8**	-3.1	562.6	**154.8**	**-359.7**	**4.9**
270° to 300°	**33.4%**	**39.9**	17.2	**11.5**	**974.8**	166.3	**-375.2**	**6.7**
300° to 30°	Not Enough cases							

Table 5.2: Multiple Regression Results for Turbine 1 at Wind Farm 'B'.

(Model = constant + A.$\overline{V}$ + B.σ_v + C.Shear + D.Flow + E.Density)

Wind Speed Bin (m/s)	Adjusted R^2	Mean speed coefficient	Turb. Intensity coefficient	Shear coef-ficient	Flow coef-ficient	Density coefficient	Constant	Standard Error
5 - 6	**13.3%**	**24.2**	26.5	**-15.9**	**-23.2**	**135.2**	**-254.7**	**20.6**
6 - 7	**16.7%**	**41.9**	**131.2**	**-33.6**	8.25	**405.8**	**-650.4**	**36.3**
7 - 8	**22.7%**	**66.8**	**190.9**	**-68.8**	-28.1	**188.2**	**-613.4**	**48.1**
8 - 9	**24.5%**	**80.1**	**135.1**	**-32.4**	**-47.6**	46.9	**-565.3**	**42.1**
9 - 10	**18.6%**	**67.3**	-22.7	**-20.9**	**-80.1**	22.6	**-403.8**	**41.3**
10 - 11	**10.5%**	**49.8**	15.4	**-44.9**	-12.7	11.1	**-218.6**	**43.8**
11 - 12	**4.7%**	**29.6**	**-172.1**	**-46.6**	20.0	**-218.1**	**263.4**	**48.1**
12 - 13	**4.3%**	-0.4	**-332.89**	**-53.4**	-60.5	**-447.6**	**885.1**	**42.4**
13 - 14	**5.7%**	3.8	**-476.8**	-78.1	119.5	**-655.5**	**1051.0**	**54.3**
14 - 15	**11%**	-6.2	**-514.0**	-56.3	-36.2	**-797.4**	**1348.4**	**41.5**
15 - 16	**37.8%**	**-26.6**	**-1275.7**	**-267.1**	-82.3	**-2454.1**	**3424.2**	**61.3**

5.7.2 Derivation of the model

The candidate variables for use in the model were mean wind speed ($\overline{V}$), turbulence intensity (t), flow inclination (θ_{flow}), wind shear (α_T), standard deviation ratio (σ_{ratio}), air density (D) and standard deviation of wind direction (σ_{dir}). There were two reasons for choosing these variables, firstly it seemed physically likely that variations in these parameters would affect turbine performance and secondly, measurements of these variables were readily available in historical data. There is no guarantee that other, unmeasured variables did not also affect performance, therefore the 'completeness of model' criterion may have been breached. Justification for using the above variables in formulating the model is based upon the results of the earlier ensemble averaging. The model as described has been derived using 4 years of data from turbine 15 at Carland Cross.

5.7.3 Turbine Power Before the Model is Applied

The average power produced by the turbine, between 7 and 8 m/s, over consecutive three month periods, was shown in Figure 5.1. A large amount of variation can be seen in the average power of between 5% and 10%. Using the traditional method of 'modelling' power prediction, it would be expected that the power produced would be nearly constant in a 1 m/s wind speed band. Changes in air density are small at this site and could not account for such a magnitude of variation. The aim of the multi-variate model is to account for these variations using additional variables, as listed above, to describe the wind regime.

5.7.4 Removing Non-Linearities

The relationship between each independent variable and the dependent variable must be linear if a regression model is to give valid results. When there is only one independent variable, linearity can be checked by plotting the residuals from a regression model against the independent variable. If the underlying relationship was purely linear, then this plot should have no pattern or trend and the points would be randomly distributed about the x-axis. If there are multiple independent variables, then it becomes more difficult to test for linearity. Residual and partial residual plots may indicate that a problem exists, but it may not be obvious which variable or variables are affected or what the non-linear relationships are.

Previous sections investigated the relationships between each variable and turbine power. It will be assumed initially that these relationships are correct and the independent variables will be linearised on this basis. From section 5.3, turbulence intensity (t) will be modelled by a second order polynomial fit to the plot of power against turbulence, between 7 and 8 m/s, averaged over all turbines in the wind farm. The polynomial is

$$t_{lin} = 937t^2 - 200t + 110$$

Measured turbulence intensity will be transformed by this equation to try to ensure linearity. Linearised turbulence can no longer be regarded as having dimensions of turbulence (they are more akin to power) and therefore cannot now be interpreted directly as a turbulence.

Using the analysis carried out in section 5.4, wind shear will be transformed by interpolating on the piecewise linear curve shown in Figure 5.9 which is based on experimental data.

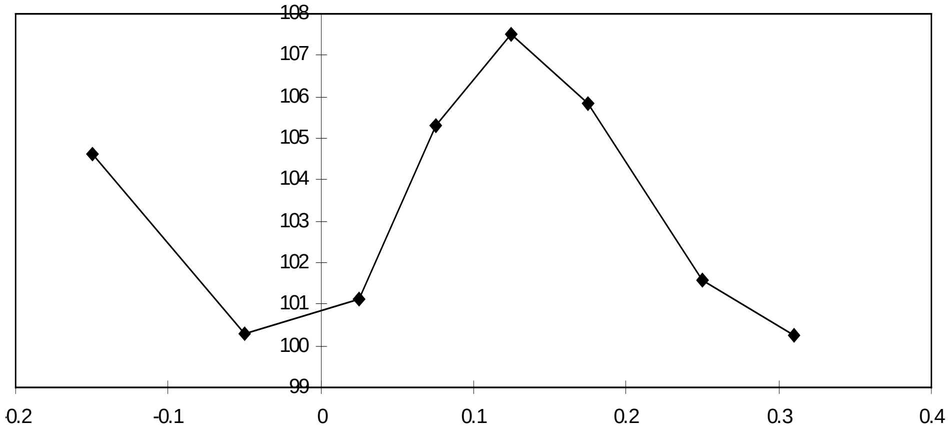

Fig. 5.9. Linearisation of wind shear exponent (average power in kW versus shear exponent) between 7 and 8 m/s for Carland Cross wind farm

Flow inclination will be linearised using the formula:

$$\theta_{flow,lin} = \cos(\theta_{flow} + \theta_{tilt})$$

It is of course possible that these relationships are not valid but influenced by variations in the other independent variables that were not controlled. References to independent variables later in this report refer to linearised independent variables.

5.7.5 Identifying Collinearity

Collinearity arises when two or more independent variables are highly correlated. The presence of collinear variables in a regression model is damaging, as it is difficult for the model to identify the separate effects of each variable. This leads to large standard errors, which in turn signals that the coefficient estimate for the sample may not be close to the true coefficient of the population. Therefore the model becomes specific to a single data set and its variable coefficients may not make physical sense.

The presence of collinearity between independent variables can be identified by a measure known as Tolerance (*T*):

$$T = 1 - R^2$$

Where R^2 is the amount of variance in one independent variable that can be explained by the other independent variables in the model.

Ideally therefore, the Tolerance of each independent variable should be 1. The tolerances of the independent variables from data set 1 (1st three month period) of turbine 15 are given in Table 5.3 below.

Table 5.3. Tolerance of independent variables for first 3 months of data

Independent Variable	Tolerance
Density Ratio (d)	0.897
Nacelle Wind Speed ($\overline{V}$)	0.841
Standard Deviation Wind Direction (σ_{dir})	0.924
Flow Inclination ($\theta_{flow,lin}$)	0.856
Turbulence Intensity (t_{lin})	0.872
Standard Deviation Ratio (σ_{ratio})	0.691
Shear Exponent	0.807

Note that density ratio (d) is the ratio of the measured air density to standard air density (1.225 kg/m^3) and standard deviation ratio is the standard deviation of power divided by the standard deviation of wind speed.

It can be seen that collinearity exists between these variables. However, the level of collinearity (whether it is harmful or not) and the sets of variables which are affected, cannot be determined by T.
A statistic known as a condition index can indicate whether collinearity is distorting the results of a regression model. Condition indices are derived from eigenvalues. The eigenvalues for each independent variable are initially calculated. The condition index of a variable is then the square root of the largest eigenvalue divided by the eigenvalue for that variable. Condition indices larger than 15 suggest a potential problem, and condition indices greater than 30 suggest a serious problem. The condition indices for data set 1 from turbine 15 are given below:

Table 5.4. Condition index for independent variables for first 3 months of data

Independent Variable	Condition Index
Constant	1.000
Density Ratio (d)	5.680
Nacelle Wind Speed ($\overline{V}$)	8.678
Standard Deviation Wind Direction (σ_{dir})	14.906
Flow Inclination ($\theta_{flow,lin}$)	84.627
Turbulence Intensity (t_{lin})	143.790
Standard Deviation Ratio (σ_{ratio})	279.559
Shear Exponent ($\alpha_{T,lin}$)	572.854

On this basis, a serious collinearity problem exists between the independent variables.

5.7.6 Removing Collinearity – Principal Component Analysis

To remove the problem of collinearity that exists between the independent variables, two methods have been considered. The first method is Principal Component Analysis (PCA). PCA produces in a number of orthogonal components, each of which is a linear combination of the independent variables.

The components are completely uncorrelated with one another, each with a tolerance equal to 1. After formation, the components can be used in a regression model to predict turbine power, with no risk of collinearity. An example of the first five components produced by PCA is shown in Table 5.5 for data set 1 from turbine 15. The table gives the weighting of the independent variables for each principal component. For example component 1 is:

$$PC1= -0.20d +0.29\overline{V} +0.38\sigma_{dir} +0.04\theta_{flow,lin} +0.27\, t_{lin} +0.48\sigma_{ratio} +0.1\alpha_{T,lin}$$

Table 5.5. Principal components of data set 1 from turbine 15

	PC 1	PC 2	PC 3	PC 4	PC 5
	Variable Coefficients				
Density Ratio (d)	-0.197	0.373	0.343	0.340	0.750
Nacelle Wind Speed ($\overline{V}$	0.294	-0.112	0.639	-0.279	0.261
Standard Dev. Wind Direction (σ_{dir})	0.380	0.098	-0.447	-0.106	0.402
Flow Inclination ($\theta_{\mathrm{flow,lin}}$)	0.039	0.500	0.252	0.120	-0.719
Turbulence Intensity (t_{lin})	0.267	0.352	-0.276	0.373	0.086
Standard Dev. Ratio (σ_{ratio})	0.482	-0.011	0.216	-0.009	-0.138
Shear Exponent ($\alpha_{T,lin}$)	0.101	-0.385	0.101	0.881	-0.099

A problem with these components is that the underlying physical relationship between the original variables and the dependent variable, turbine power, is not obvious. It is therefore difficult to check whether the model makes physical sense. For this reason an alternative approach, described below, is used.

5.7.7 Removing Collinearity – Partial Residuals Approach

The second alternative method used to remove collinearity problems uses the residuals of the independent variables rather than the variables themselves. Each variable in turn is predicted using a linear combination of the remaining variables. The difference between the original variable and the modelled variable (residual) then becomes the new variable for use in the final regression model. These new residual variables then describe the variance of the original variable that cannot be explained by a linear combination of the other independent variables. The residual variables derived from data set 1 of turbine 15 are described by Table 5.6. For example the residual variable for linearised turbulence is:

$$t_{lin,rsd} = -108.75 + 14.03d - 0.54\overline{V} + 0.64\sigma_{dir} + 89.20\theta_{flow,lin} -1t_{lin} + 0.07\sigma_{ratio}$$

Note that wind shear is not included in Table 5.6, as the coefficients derived for this term varied greatly in sign and direction between data sets and therefore a sensible average value could not be produced. This indicates that the representation of this factor described in the linearisation section is incorrect.

Table 5.6. Residual variables from data set 1 for turbine 15

	New Residual Variables					
	d_{rsd}	$\overline{V}_{rsd}$	$\sigma_{dir\ rsd}$	$\theta_{\mathrm{flow,lin},rsd}$	$t_{lin,rsd}$	$\sigma_{ratio,rsd}$
Independent Variables	Variable Coefficients					
Constant	0.604	8.731	28.645	0.848	-108.75	-69.221
Density Ratio (d)	-1	0.663	-8.169	0.134	14.032	-69.303
Nacelle Wind Speed ($\overline{V}$)	0.001	-1	-0.499	-0.002	-0.535	7.781
Standard Dev. Wind Direction (σ_{dir})	-0.001	-0.021	-1	0	0.643	1.234
Flow Inclination ($\theta_{\mathrm{flow,lin}}$)	0.424	-2.479	-15.449	-1	89.199	109.059
Turbulence Intensity (t_{lin})	0	-0.003	0.09	0	-1	0.146
Standard Dev. Ratio (σ_{ratio})	0	0.02	0.077	0	0.065	-1

To ensure that the residual variables are not specific to one data set, they were derived for each of the available 16 three-month periods and then averaged. Note that where the regression analysis identifies a variable as not significant in a model, then its coefficient is not used in the averaging process. The final formulation of the residual independent variables is given in Table 5.7.

To check that the new independent variables do not damage the model through collinearity, their tolerances and condition indices have been derived from data set 1 of turbine 15 and are shown below in Table 5.8.

It can be seen that a serious collinearity problem no longer exists.

Table 5.7. Residual variables from turbine 15, averaged over all data sets

	New Residual Variables					
	d_{rsd}	$\overline{V}_{rsd}$	$\sigma_{dir\ rsd}$	$\theta_{flow,lin,rsd}$	$t_{lin,rsd}$	$\sigma_{ratio,rsd}$
Independent Variables	Variable Coefficients					
Constant	0.596	7.514	42.131	0.723	-88.467	-4.059
Density Ratio (d)	-1	0.407	-23.995	0.261	-16.394	-49.261
Nacelle Wind Speed ($\overline{V}$)	0.001	-1	-0.587	-0.001	-0.693	6.118
Standard Dev. Wind Direction (σ_{dir})	-0.001	-0.017	-1	0.0	0.573	0.883
Flow Inclination ($\theta_{flow,lin}$)	0.418	-0.877	-11.875	-1	99.823	32.835
Turbulence Intensity (t_{lin})	0.0	-0.003	0.099	0.0	-1	0.166
Standard Dev. Ratio (σ_{ratio})	0.0	0.018	0.084	0.0	0.106	-1

Table 5.8. Collinearity and condition index of the new partial residual independent variables

Independent Variable	Tolerance	Condition Index
Constant	-	1.000
Density Ratio (d_{rsd})	0.716	2.094
Nacelle Wind Speed ($\overline{V}_{rsd}$)	0.987	2.706
Standard Deviation Wind Direction ($\sigma_{dir,rsd}$)	0.782	4.144
Flow Inclination ($\theta_{flow,lin,rsd}$)	0.718	4.814
Turbulence Intensity ($t_{lin,rsd}$)	0.834	8.059
Standard Deviation Ratio ($\sigma_{ratio,rsd}$)	0.815	14.031

5.7.8 Normality of Distribution of Variables

A further condition of regression analysis is that all independent variables are normal. To check this, plots have been produced of each variable against ordered observations from a normal distribution with zero mean. These plots are shown in Figure 5.10. All x-axis labels refer to linearised, residual variables. A diagonal line from the origin to the top right of the graph means that the variable is normally distributed. It was concluded that although no independent variable was totally normal, they were all sufficiently so to require no further transformation. Small deviations from a normal distribution are unlikely to have a damaging effect on the model.

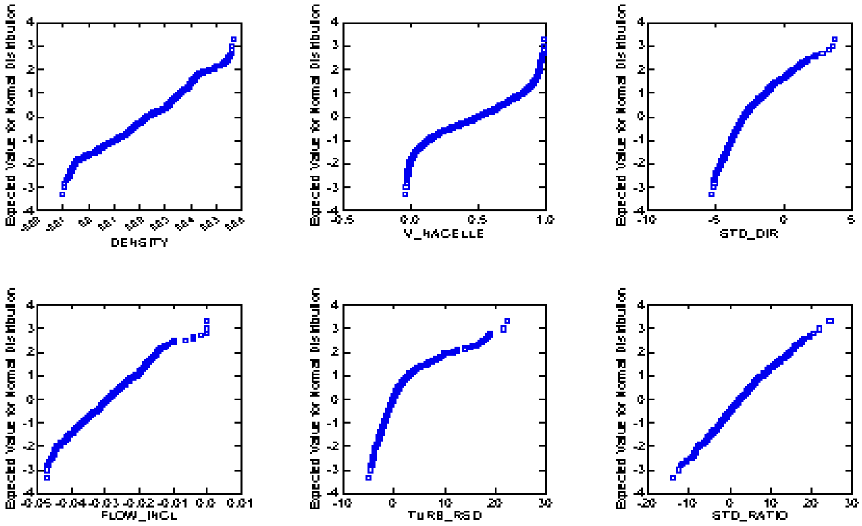

Fig. 5.10. Probability plots of independent variables

5.7.9 Predicting Power

Having dealt with linearity, independence and normality, the next stage is the actual derivation of the regression model of turbine power. Here we use the linearised, residual independent variables described in previous sections. To obtain a model that is general for all of the three month data sets, individual regression coefficients are derived for each data sat and then averaged. The equation for the average model is shown below:

$$\overline{P}_{predicted} = 16685.4 + 0.72.t_{lin,rsd} - 0.39.\sigma_{dir,rsd} + 0.46.\sigma_{ratio,rsd} + 266.1.d_{rsd} + 415.1.\theta_{flow,lin,rsd} + 46.84.\overline{V}_{rsd}$$

Substituting the equations from Table 5.7 into this equation to return to a more physically meaningful representation gives:

$$\overline{P}_{predicted} = 98.71 + 0.73.t_{lin} - 0.92.\sigma_{dir} + 1.37.\sigma_{ratio} + 250.17.d + 434.38.\theta_{flow,lin} + 52.96.\overline{V}$$

This is the final model of turbine power. A further expansion would be possible to undo the earlier linearisation, but this is not done here. Note that wind shear is not included in the model. It was not possible to produce a residual variable of statistical significance, but inclusion of the linearised variable in the model to predict power was attempted. However, as with the process of removing collinearity, the sign and size of the wind shear coefficient varied significantly between 3 month data sets, thus wind shear has not been used.

To evaluate the model, it was applied to each 10 minute data point in every 3 month data set for turbine 15. The average predicted power for each 3 month period is plotted in Figure 5.11, actual average power is also shown for comparison. It can be seen that the model is working and predicting the major fluctuations in turbine power. The correlation coefficient between actual and predicted average power is 84%.

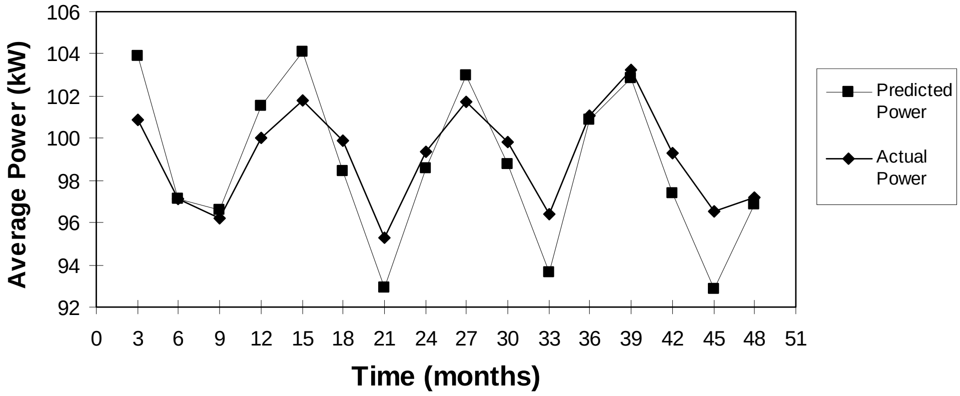

Fig. 5.11. Model results – predicted power turbine 15, Carland Cross

The figure refers to average results. An analysis of the accuracy of the model, in terms of predicting 10 minute average values within each 3 month data set, is given in Table 5.9. Each row of the table refers to a 3 month period. The first column of this table gives the adjusted squared multiple *R* statistic for the relationship between actual 10 minute average power and predicted 10 minute average power, within a 3 month period. This number describes the proportion of variance in the dependent variable (actual power) which can be explained by the variance in the independent variables. It is adjusted to account for the data set being a sample of the population. The second and third columns of the table show the standard deviations of the actual power and of the residual power (predicted minus actual) respectively. If the model were perfect then column three would contain zeroes.

Table 5.9 Model statistics referring to 10 minute data, turbine 15, Carland Cross

	Adjusted R Squared	Standard Deviation	
		Power	Residual
1	80.6%	16.53	7.27
2	79.6%	17.16	7.75
3	76.4%	15.83	7.68
4	76.6%	15.33	7.41
5	81.8%	17.51	8.52
6	77.7%	17.93	8.47
7	76.4%	15.86	7.64
8	76.4%	15.37	7.46
9	78.0%	15.53	7.27
10	77.1%	17.31	8.25
11	80.5%	14.79	6.52
12	79.4%	17.21	7.81
13	77.5%	16.46	7.80
14	82.5%	16.32	6.82
15	84.6%	15.09	5.92
16	83.0%	15.28	6.30
Mean	79.3%	16.22	7.43

5.7.10 Testing the Model

The previous section concluded with a model that successfully predicted turbine power between 7 and 8 m/s. The model was derived from data associated with a single turbine and was tested on that turbine. In this section the model will be applied to other turbines of the same type. There are three, progressively more difficult test cases, the first, turbine 12 from Carland Cross wind farm, is a turbine that is in a similar environment to turbine 15 in terms of terrain and wake effects. The second case, turbine 8 from Carland Cross wind farm, is a turbine in different terrain on the same wind farm, subject to wake effects from different directions. The third test case is for the same make of turbine, but located in a different wind farm, turbine 1 from Coal Clough wind farm. The results are given in Figures 5.12 to 5.14 and Tables 5.10 to 5.12, in the same form as for turbine 15 at Carland Cross.

Figures 5.12 and 5.14 show a data series labelled, “Predicted Scaled”. This refers to a straightforward scaling of the model results, the constant has been modified so the predicted power has the same mean as the actual power. Reasons why this is necessary may be that either turbines have different power curves due to differences in their rotors (pitch angle or blade accretion) or the nacelle anemometers have different calibrations.

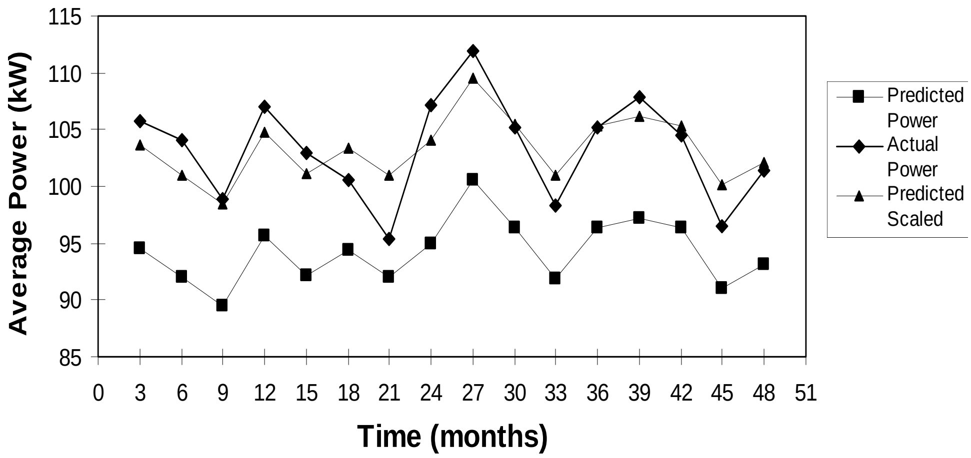

Fig. 5.12. Model results – predicted power, turbine 12, Carland Cross

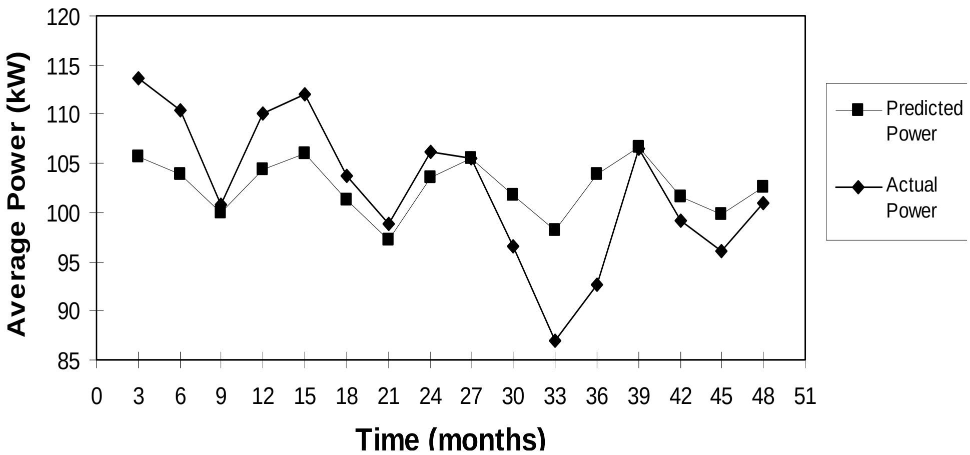

Fig. 5.13. Model results – predicted power, turbine 8, Carland Cross

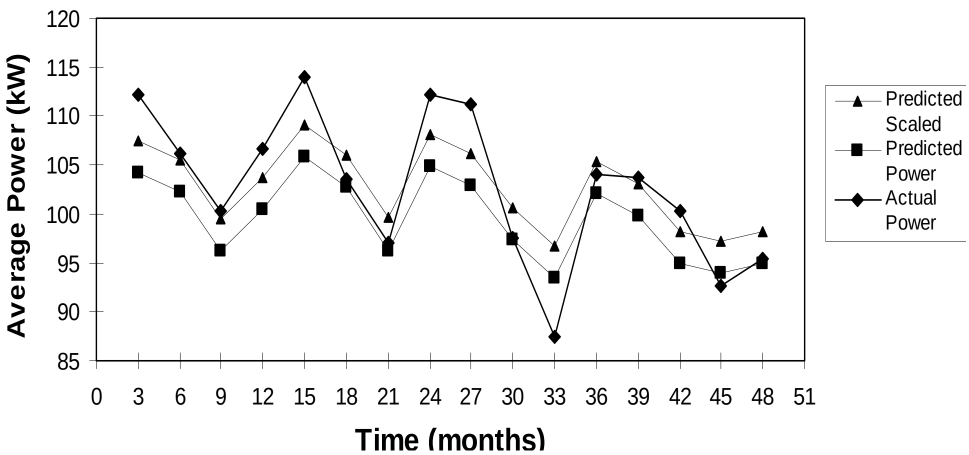

Fig. 5.14. Model results – predicted power, turbine 1, Coal Clough

Table 5.10. Model statistics, 10 minute data turbine 12, Carland Cross

	Adjusted R	Standard Dev.	
	Squared	Power	Residual
1	75.4%	16.87	8.37
2	80.1%	19.32	8.61
3	74.8%	17.05	8.55
4	72.9%	16.81	8.76
5	65.9%	15.83	9.24
6	75.6%	16.59	8.19
7	72.8%	16.80	8.76
8	65.2%	18.74	11.05
9	74.2%	18.52	9.40
10	70.6%	17.63	9.55
11	70.2%	16.80	9.17
12	73.2%	18.54	9.59
13	70.8%	18.31	9.89
14	73.4%	17.91	9.23
15	70.8%	16.32	8.81
16	74.4%	17.25	8.72
Mean	72.5%	17.45	9.12

Table 5.11. Model statistics, 10 minute data turbine 8, Carland Cross

	Adjusted R	Standard Dev.	
	Squared	Power	Residual
1	70.1%	19.09	10.44
2	67.8%	20.18	11.44
3	68.1%	18.09	10.21
4	71.9%	19.31	10.23
5	68.4%	18.12	10.18
6	73.7%	18.60	9.53
7	71.8%	18.07	9.59
8	70.0%	18.86	10.32
9	69.4%	16.91	9.34
10	69.8%	19.50	10.71
11	70.3%	16.44	8.96
12	74.1%	17.12	8.71
13	52.1%	22.33	15.44
14	67.9%	16.43	9.31
15	73.1%	16.79	8.71
16	70.7%	16.47	8.92
Mean	69.3%	18.27	10.13

Table 5.12. Model statistics, 10 minute data turbine 1, Coal Clough

	Adjusted R	Standard Dev.	
	Squared	Power	Residual
1	76.7%	27.44	23.22
2	66.5%	19.33	11.18
3	66.0%	15.80	9.20
4	72.1%	16.96	8.96
5	69.1%	16.53	9.13
6	64.1%	17.90	10.71
7	56.7%	15.99	10.51
8	47.3%	26.51	19.24
9	74.7%	17.30	8.69
10	77.5%	17.81	8.45
11	76.4%	15.15	7.35
12	72.7%	16.97	8.85
13	78.1%	14.55	6.79
14	76.8%	16.55	7.96
15	72.2%	15.11	7.97
16	57.9%	17.58	11.38
Mean	69.1%	17.97	10.60

The results indicate that the model can be applied successfully to turbines other than that from which it was derived. The model explains approximately 70% of the original unexplained variance in the turbine power.

The relative influence of each independent variable on turbine power, can be interpreted using standardised regression coefficients. The standardised regression coefficient is calculated as:

$$\tilde{b} = b\frac{S_x}{S_y}$$

where

$\tilde{b}$	=	standardised regression coefficient
b	=	raw coefficient
S_x	=	standard deviation of independent variable
S_y	=	standard deviation of dependent variable.

The standardised coefficient is interpreted as the number of standard deviations that the dependent variable changes when an independent variable changes by one standard deviation. It is equal to the ordinary or raw regression coefficient which would have been calculated had the variable been converted to a standardised variable, with a mean of zero and a standard deviation of one. Standardised regression coefficients are sometimes known as *Z* scores.

5.7.11 Principal Component Analysis

The following work summarises the key results of Ref 5.5.

In the previous studies, it appeared that shear has a strong influence on performance but that the partial residuals regression technique was not particularly successful in extracting the functional relationship. To tackle this problem, it was decided firstly to apply an alternative regression technique and secondly to use data from very flat sites where the number of parameter dependencies, specifically that of flow inclination angle, could be reduced.

The analysis and results presented here relate to the Vindeby offshore wind farm comprising 450 kW Bonus, stall regulated wind turbines.

To compare directly the effects of different variables on power, variables have been standardised in some cases to a mean of zero and standard deviation of 1.

In principal component analysis (PCA), the various ‘independent’ physical parameters are linearly combined together to create artificial components having no direct physical meaning but which are truly orthogonal.

For this assessment, the physical variables selected were:

- Wind speed at hub height, as measured on the site mast
- Turbulence at hub height, as measured on the site mast
- Wind profile exponent, as deduced from measurements on the site mast
- Wind Direction, as measured at site mast.
- Air density

Additional variables, such as yaw error or difference in direction at two heights have been added where the data are available.

The method of partial residuals used previously is very sensitive to outliers in the data. Additionally, altering the range of the input data can change the derived sensitivity. This implies that the method is not particularly robust, hence the interest in PCA.

For the present purposes, we shall focus on the Vindby data set from 1996 and 1987, with 48 metre elevation wind data restricted to the 7 to 8 m/s range. The wind direction was restricted to a 40 degree sector, giving an overall data set of 89 hours duration.

Principal component analysis was performed using four components. The results are shown in Table 5.13. 86% of the variation in the original variables is explained. The dependencies of power on each variable are shown in the penultimate column. These should be compared with the corresponding partial residuals results shown in the final column.

The results although similar in places are by no means identical and in some instances they are in total conflict.

Table 5.13. Results of principal component analysis on 7-8 m/s data from Vindby (1996/97) and comparison with parallel results from partial residuals analysis

Item	PCA Comp't 1	PCA Comp't 2	PCA Comp't 3	PCA Comp't 4	Dependency of Power from PCA	Depend-ency of Power from Residuals Analysis
Wind Speed at 48m	0.598	0.158	0.238	0.702	0.636	0.708
Wind Direction at 48m	-0.367	-0.106	0.922	-0.01	-0.026	-0.046
Density	0.528	0.622	0.173	-0.265	0.436	0.349
Exponent	-0.606	0.367	-0.187	0.569	-0.264	0.054
Turbulence	0.304	-0.789	-0.028	0.198	0.110	-0.516
Variance explained (%)	24.60	23.59	19.43	18.53	86.25	
Coefficient	0.661	0.162	0.256	0.220		

The analysis was repeated for a more comprehensive data set for various wind speed bins. The sensitivities derived from principal component and partial residuals analysis are compared Table 5.14.

Those entries under partial residuals shown in bold exceed 90% significance.

Once again, the results although similar in places are by no means identical and in some instances they are in total conflict.

Table 5.14. Comparison of parameter sensitivities identified by partial residuals and principal component analyses – Vindby data for 1996, data standardised within each wind speed bin.

Wind Speed Bin	5-6 m/s		6-7 m/s		7-8 m/s	
	Partial	PCA	Partial	PCA	Partial	PCA
Wind Speed at 38m	**0.939**	0.815	**0.945**	0.871	**0.954**	0.880
Wind Direction at 43m	-0.017	0.200	0.024	0.060	0.044	0.000
Density	0.067	0.583	**0.106**	0.154	**0.259**	0.011
Turbulence	0.025	-0.137	-0.007	0.017	0.048	-0.102
Exponent	**0.158**	-0.008	0.002	-0.275	-0.041	0.200
Difference in direction	**-0.178**	-0.175	-0.070	-0.070	-0.059	0.119
Yaw Error	0.024	-0.168	0.018	-0.157	**-0.111**	-0.174
Wind Speed Bin	**8-9 M/S**		9-10 m/s		> 10 m/s	
	Partial	PCA	Partial	PCA	Partial	PCA
Wind Speed At 38m	**0.839**	0.576	**0.946**	0.832	**0.981**	0.742
Wind Direction at 43m	-0.069	-0.540	-0.107	-0.253	-0.000	0.565
Density	0.173	0.071	**0.363**	0.209	**0.066**	0.240
Turbulence	0.105	0.073	-0.108	0.008	-0.025	-0.268
Exponent	-0.066	0.232	-0.009	-0.035	-0.022	0.522
Difference in direction	-0.168	-0.228	**0.167**	-0.372	-0.013	-0.168
Yaw Error	-0.096	-0.074	0.069	-0.308	0.010	-0.351

5.8 Discussion of Results and Conclusions

It is clear from the time-based analysis that the performance of wind turbines does depend upon additional parameters other than hub height wind speed and air density. Many of these parameters would appear to have seasonal trends meaning, if a ‘conventional’ IEC 61400-12 Ed 1 method of performance assessment is adopted,.that turbines will appear to perform better at certain times of year than at others,

Multi-variate regression analysis, although straightforward in concept is not in fact simple to apply and there is significant effort involved in ensuring that the requirements for linearity, independence, normality and completeness are adhered to.

Two methods of application have been studied, these being partial residuals analysis (which is a technique developed as part of this project) and the more recognised principal component analysis.

Partial residuals analysis has been shown capable of explaining the major seasonal changes in performance. However, parameter dependencies are not always consistent between data sets and are also inconsistent with results from principal component analysis.

The work has demonstrated the plausibility of including additional parameters for more accurate power curve measurement. Nevertheless, more refinement is necessary before such methods can be used practically.

Currently, standard power performance measurements made to test manufactures' production warranties encompass horizontal wind speed, air density and turbine power. A more sophisticated test appropriate for complex terrain would require manufacturers to specify their turbine's response to changes in the wind field characterised by variables such as wind shear, turbulence and inclined flow. This would be a complex task, not least because currently most test sites are situated in flat terrain where a suitable range of these variables would be unattainable. Regarding energy yield prediction and siting of turbines for future wind farm sites, it would be useful for manufacturers and developers to consider the effects of these variables on the ability of the turbines to attain their 'normal' warranted power output. It should be possible to make better estimates of energy productivity and thus expected revenue stream. A performance variation of 5%, as seen earlier is very significant and reducing this risk should lead to cheaper financing. To do this accurately a model such as the one described is required. Terrain based wind flow models would be required to predict the behaviour of variables such as turbulence and wind shear across the proposed site. This is not currently possible with the models that are commonly in use.

Notwithstanding these comments, the project has undoubtedly produced significant new knowledge. Although the technique requires large quantities of data and is time consuming and fairly complex to implement, its success and applicability has been demonstrated.

6 Air Density Correction

In the development of the IEC 61400-12 Ed 1 standard for power performance evaluation, there was considerable debate over the ‘correct’ method for normalising power performance data to account for density dependent variations in performance of actively controlled wind turbines.

Density correction seldom reduces scatter in test data, but has some relevance when the power curve measured on one turbine is being used to provide a benchmark for the performance of a similar turbine at a different site of significantly different mean density.

The work reported here has addressed the issue of density correction from two different angles. Firstly the methods described in Chapter 5 for identification of functional relationships using multi-variate regression analysis have been applied to identify whether credible density dependencies can be identified and thereafter used for normalisation. Secondly, a review has been undertaken of the theoretical basis for density normalisation for actively controlled turbines.

6.1 Empirical Relationship Between Power Performance and Density

6.1.1 Stall Regulated Turbines

Before trying to identify density dependencies from actively controlled turbines, it was attempted to demonstrate that regression techniques can extract the known dependency for stall regulated machines.

Data were analysed from two wind farms in Ireland having identical stall regulated Nordtank 500 kW wind turbines.

The analysis method addressed the requirements of independence, normality, linearity and completeness outlined in chapter 5.

The analysis was applied using 10 minute statistics over three wind speed ranges, 6-8 m/s, 8-10 m/s and 10-12 m/s within which the power to wind speed relationships are substantially linear.

The independent variables selected for the model were:

- Mean wind speed
- Density
- Shear as a wind speed ratio or as a wind speed difference, depending upon which gives better regression
- Directional terrain slope, being an indication of flow inclination
- Turbulence intensity derived from mast wind speed
- Wind offset given as unity minus the cosine of the standard deviation of wind direction.

The analysis method used was that of partial residuals as described in chapter 5.

Having carried out the regression analysis and to produce a more visible sign of the relationship between wind speed and density, calculations were carried out to determine what percentage change in power would be predicted for a 1% change in density. The expectation for a fixed speed, stall regulated turbine would of course also be 1%. For the analysis the mean bin values of all parameters were applied to the regression model to give the reference case, and thereafter the density value alone was altered by 1%.

The results are shown below in Table 6.1. The table also shows the coefficient of determination for the model, which indicates the degree to which the data have been explained.

Table 6.1. Regression model prediction of sensitivity of power to changes in density for stall regulated wind turbines

Site	Wind Speed Range (m/s)	Coefficient of Determination	Change in Power for a 1% Change in Density
1	6 – 8	0.902	1.155
1	8 – 10	0.799	0.861
1	10 – 12	0.933	0.778
1	Average		0.931
2	6 – 8	0.865	1.358
2	8 – 10	0.816	0.836
2	10 –12	0.899	0.926
2	Average		1.040

These results, although not being a perfect mirror of physical expectation, are reasonably encouraging and certainly give adequate faith in suggesting that the method may be suitable for application to the less well defined, actively controlled case.

6.1.2 Actively Controlled Turbine

A similar analysis was carried out for a 300 kW actively controlled (pitch regulated) turbine, except that flow inclination angle was not considered.

Table 6.2 gives the key results.

In this instance, rather than calculating the effect on power that a 1% increase in density would have, the wind speed which would produce the same power output for the increased density has been calculated.

Table 6.1. Regression model prediction of sensitivity of power to changes in density for pitch regulated wind turbine

Site	Wind Speed Range (m/s)	Coefficient of Determination	Change in Wind Speed to Maintain Power for a 1% Change in Density
3	6 – 8	0.884	-0.722
3	8 – 10	0.895	-0.306
3	10 – 12	0.896	-4.770
3	Average		-1.933

The wind speed normalisation procedure recommended in the IEC 61400-12 Ed 1 standard suggests that wind speed should be factored by the third power of the density ratio. For a 1% increase in density this implies a 0.33% reduction in wind speed.

The results are not in good agreement particularly at the higher wind speeds where some regulation activity will have been taking place.

6.2 Theoretical Treatment of Density Normalisation for Actively Ccontrolled Turbines

Historically, density normalisation for actively controlled turbines has suggested the application of power normalisation up to 70% of power rating and wind speed normalisation thereafter. This recognised that for a fixed geometry, there should be no difference in behaviour in the rising part of a power curve between a stall and a pitch regulated turbine. This however can introduce an artificial discontinuity in the reported power curve and additionally has no logic for a turbine that is actively controlled in the rising part of the power curve such as for a variable speed turbine. For that reason, the arbitrary decision was taken when developing the IEC 61400-12 Ed 1performance standard to require all actively controlled turbines to have wind speed normalisation applied across the entire operational range.

The purpose of the work reported here is to look at a more justifiable, albeit more complex, normalisation procedure.

A wind turbine's power output has the following dependency:

$$P_{out} = \frac{1}{2} C_p(\lambda, \theta) \rho A V^3$$

where λ is tip speed to wind speed ratio, θ is pitch setting, ρ is air density and P_{out} is electrical output power of the wind turbine. These three variables are independent of each other. However, Cp is a function of λ and θ. Changing density at a given wind speed may activate the system to change its pitch setting or the rotational speed of the rotor in the case of a variable speed turbine.

We shall examine a number of cases:

- Fixed pitch rotor with variable speed
- Variable pitch with fixed rotor speed
- Variable pitch and variable rotor speed.

6.2.1 Fixed Pitch Rotor with Variable Speed

To achieve maximum power output, the rotor speed ω is allowed to vary at a given wind speed so that maximum C_p value is obtained. To perform air density normalisation, the following is relevant for this case:

θ = constant.
$C_p = f(\lambda)$ and is independent of θ.
$\lambda = R\omega/V$.

where

λ = tip speed to wind speed ratio;
ω = rotational speed of rotor;
R = rotor radius .
V = wind speed.
N = index where N=0 at C_{pmax}, N<0 for λ lower than λ at C_{pmax} and N>0 for λ higher than λ at C_{pmax}

For a given wind speed V, $\lambda = f(\omega)$. Thus,

$$C_p = g(\omega) = A + B\omega + C\omega^2 + \ldots$$

For a given wind speed V, power can be re-expressed as:

$$P_2 = \frac{\rho_2}{\rho_m}\{\frac{A + B\omega_2 + \ldots}{a + b\omega_m + \ldots}\}P_m$$

or alternatively (Ref 6.1) as:

$$P_2 = P_m(\frac{\omega_2}{\omega_m})^N(\frac{\rho_2}{\rho_m})$$

where P_2 and ρ_2 are normalised parameters; P_m & ρ_m are measured parameters. For variable rotor speed turbine operating below but close to the maximum C_p, these equations can be further simplified:

$$P_2 \approx P_m\{\rho_2/\rho_m\}, \text{ where } C_p \approx C_{pm}$$

When the maximum C_p is achieved, the power output is also maximised and the rotor speed (rotational) will be fixed. Using the above assumption, C_p is proportional to *V*, and the following relationship applies:

$$V_2 = \{\frac{\rho_m}{\rho_2}\}^{\frac{1}{3-N}} V_m$$

where *P* and ω are constant.

For the turbine operating close to maximum C_p (ie $N \approx 0$), the equation can be simplified.

$$V_2 \approx \{\frac{\rho_m}{\rho_2}\}^{\frac{1}{3}} V_m$$

Note that if the turbine is operating at constant power with wind speed greater than the rated wind speed, the wind speed correction equation is no longer valid. Power output does not increase with the increase of wind speed.

6.2.2 Variable Pitch with Fixed Rotor Speed

This study is based upon earlier work (Ref 6.2).

For variable pitch and fixed rotor speed turbines, $C_p = f(\lambda)$, where θ, ω and *R* are constant.

Thus, $C_p = f(V)$.

Once power output reaches rated power, the output power is independent of wind speed & air density. That is, output power will not be changed by changes in wind speed and air density.

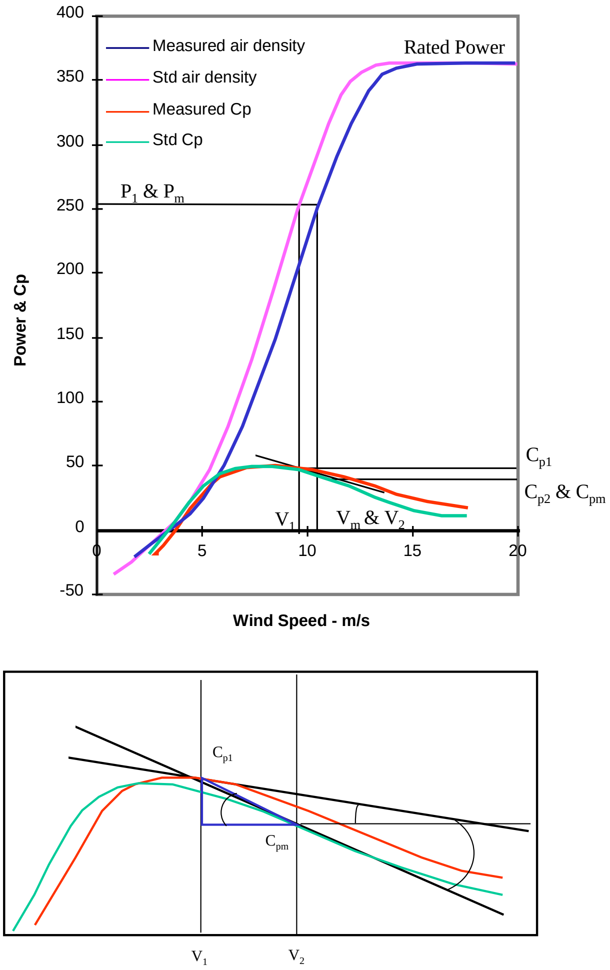

Fig. 6.1. Power and Cp curves for variable pitch with fixed rotor speed

With regard to the above diagram, it is clear that

$$C_{p1} - C_{pm} = dC_p/dV\,(V_1 - V_m)$$

where V_m = measured wind speed; V_1 = normalised wind speed under standard condition.

Combining this equation with the general relationship:

$$\tfrac{1}{2}\rho_1 C_{p1} A D V_1^{\,3} = \tfrac{1}{2}\rho_m C_{pm} A D V_m^{\,3};$$

$$V_1 = V_m \{\frac{\rho_m C_{pm}}{\rho_1 C_{p1}}\}^{\frac{1}{3}}$$

gives

$$V_1 = V_m \{\frac{\rho_m C_{pm}}{\rho_1 [C_{pm} + \frac{dC_p}{dV}(V_1 - V_m)]}\}$$

Having established the above relationship, the relationship between the rate of change of C_p with respect to the change of wind speed can be expressed as follows.

The expression

$$C_p = \frac{P_m}{\frac{1}{2}\rho_m V_m{}^3 A_D}$$

allows C_p to be differentiated with respect to V_m, giving

$$\frac{dC_p}{dV} = \frac{2}{\rho_m A_D} V_m^{-3} \left(\frac{dP_m}{dV_m} - 3\frac{P_m}{V_m}\right)$$

Substituting back into the expression for V_1 gives

$$V_1 = V_m \left\{ \frac{\rho_m C_{pm}}{\rho_1 [C_{pm} + \frac{2}{\rho_m A_D V_m^3}(\frac{dP_m}{dV_m} - 3\frac{P_m}{V_m})(V_1 - V_m)]} \right\}$$

which when rearranged in terms of V_1 gives

$$V_1^4 + AV_1^3 + B = 0$$

where

$$A = \frac{4P_m - V_m \frac{dP_m}{dV_m}}{\frac{dP_m}{dV_m} - 3\frac{P_m}{V_m}} \qquad B = -\frac{\rho_m}{\rho_1} \frac{V_m^3 P_m}{[\frac{dP_m}{dV_m} - 3\frac{P_m}{V_m}]}$$

Note that the P_m vs V_m curve can be obtained by measuring the wind speeds and power outputs of the pitch regulated wind turbine system. The curve $P_m = f(V_m)$ is derived from curve fitting and dP_m/dV_m is calculated by differentiating the P_m vs V_m curve. Having evaluated values A & B, V_1 can be obtained by solving the 4th order polynomial equation for the real root, thus allowing the wind speed normalisation.

6.2.3 Variable Pitch and Variable Rotor Speed.

This work is based on earlier studies (Refs 6.1 and 6.2).

From Ref 6.1 the first correction approach for variable speed turbines is the empirical power law formula that normalises both power and wind speed with air density. The formula is presented below.

$$P_0 = P_m \left\{\frac{\rho_0}{\rho_m}\right\}^x \qquad x = \frac{P_R - P_m}{P_R}$$

$$V_0 = V_m \{\frac{\rho_m}{\rho_0}\}^y \qquad y = \frac{P_m}{3P_R}$$

where P_0 & V_0 are normalised power and wind speed; P_m & V_m are 10 min sample of measured power and wind speed; P_r is rated power.

This ‘twin’ approach was also adopted in Ref 6.2, but with different results.

In this, it is noted that a combined correction will lie between the conventional pitch (subscript 1) and stall (subscript 2) corrections:

$$V_1=V_m(\rho_m C_{pm}/\rho_1 C_{p1})^{1/3}; \quad P_1=P_m$$

$$V_2=V_m; \quad P_2=P_m(\rho_2/\rho_m)$$

There is a linear fraction, k, which allows the normalised data P_3,V_3 to be located on a straight line between the pure speed and pure power corrections

$$k_V= (V_3-V_2)/(V_1-V_2); \quad k_P=(P_3-P_2)/(P_1-P_2)$$

By substituting and assuming that C_p remains constant, we obtain:

$$V_3=V_m(K_V((\rho_m/\rho_0)^{1/3}-1)+1); \quad P_3=P_m(k_P(1-\rho_0/\rho_m)+\rho_0/\rho_m)$$

7 Uncertainty Analysis

The work reported in this document has largely been designed to investigate ‘grey’ areas of performance assessment. The studies have given greater insight in these areas and will allow improved methods to be developed. A parallel output has been improved information on which to base uncertainty estimates.

The earlier items of site calibration, nacelle anemometry and analysis to verify and enhancement of performance assessment method are treated in greater detail, than the remaining issues.

7.1 Approach.

Component uncertainty is best evaluated in terms of the net effect on annual mean power of the plant (*P*). In making this evaluation, a Weibull wind frequency distribution with a scale parameter of 9 m/s and a shape parameter of 2 is assumed.

The annual mean power of the *M* tested units is estimated on a ‘per-unit’ basis:

$$P = \sum_{i=1}^{M} \sum_{j=1}^{25} f_j \cdot p_{ij}$$

where p_{ij} is value of power curve in bin no. j of unit no. i of the M tested wind turbine units. f_i is the bin-centre-value of the wind speed frequency function $f(v)$. 25 wind speed bins are used. If the uncertainty source/component is <not correlated across bins> and is <not correlated from one unit wind turbine to the next>, the summation across the bins and units is:

$$u_i^2 = \sum_{j=1}^{25} f^2(v) \cdot u_{ij}^2, \quad u_C = \sqrt{\sum_{i=1}^{M} u_i^2}$$

where uij is the source/component uncertainty in bin j of unit i (transformed to its effect on power), ui is resulting uncertainty for unit no. i and uC is the integrated uncertainty for the M tested units. The uncertainty uij is the individual uncertainty source resulting from for instance, the nacelle anemometry method.

If the source/component is <fully correlated across bins> and <fully correlated from one wind turbine unit to the next>, the summation across the bins and units is given by

$$u_i = \sum_{j=1}^{25} f(v) \cdot u_{ij}, \quad u_C = \sum_{i=1}^{M} u_i$$

Any deviations from these extreme cases are commented on in the tables in the following sections.

The tables in the following sections summarise uncertainties for the respective uncertainty sources studied earlier in the report. Generally the first rows address uncertainties caused by the specific aspect of the test procedure. At the bottom of the tables, the calibration and other inherent instrument uncertainties are listed. In the last row, the uncertainties are summarised, taking into account, as well as is possible, the correlation between the uncertainty components.

The first (left-most) column specifies the uncertainty component; the second column indicates whether the uncertainty component is expected to be correlated, both within the bin and across bins. The third and fourth column give estimates of the uncertainty as propagated through to mean power output.

7.2 Site Calibration

Site calibration is usually assumed to be a major contributor to the aggregated performance test uncertainty. It is therefore particularly important to obtain an accurate estimate of its uncertainty.

Different types of situation are assessed in the following tables.

7.2.1 Mast, Flat Terrain and Without Site Calibration

In flat, homogeneous terrain site calibration is not required according to IEC 61400-12 Ed 1 because the horizontal wind speed variation is expected to be small. However, even under such conditions a non-negligible uncertainty, 3-4%, must be assumed. In total, when not performing site calibration, the uncertainty will be of the order 5+ %.

7.2.2 Site Calibration with Two Masts

In the following table, uncertainty in the power curve stemming from site calibration is evaluated. The terrain is assumed to be moderately complex. The analysis of the component uncertainties leads to a total uncertainty of approx. 5% or more.

Table 7.1. Site calibration uncertainty assessment – performance assessment using a met mast in flat terrain without site calibration

Uncertainty Source/ Component	Type (A/B)	Corre-lated (Y/N)	Magni-tude u_C/P	Comments
Uncertainty due to variability of power curve data	A	N	0.2%*	*) derived from Enercon 40 turbine in flat terrain.
Site effect*	B	Y	**3-4%***	*Uncertainty due to difference of wind conditions between mast and turbine location (flat terrain, no site calibration assumed)
Anemometer effects (overspending etc.)	B	Y	1%	
Instruments' Type B				
Anemometer wind tunnel calibration	**B**	Y	2%	
Anemometer mounting effects	B	Y	2%	
anemometer signal recording	B	Y	0.2%	
Power transducer	B	Y	2%*	*)Assuming 0.5% accuracy in respect to measuring range of 250% of rated power
Current transformer	B	Y	0.5%	
Power signal recording	B	Y	0.6%	
Temperature sensor calibration	B	Y	0.3%	
Temperature sensor mounting	B	Y	0.3%	
Temperature signal recording	B	Y	0.3%	
Air pressure sensor calibration	**B**	Y	0.2%	
Air pressure sensor mounting	B	Y	0.1%	
Air pressure signal recording	B	Y	0.1%	
Total Uncertainty A+B				
Flat terrain without site calibration	A+B	N	5%	

Table 7.2. Site calibration uncertainty assessment – performance assessment using a met mast moderately complex terrain with experimental site calibration

Uncertainty Source/ Component	Type (A/B)	Corre-lated (Y/N)	Magni-tude u_C/P	Comments
Statistical uncertainty of site calibration correction factors	B*	Y**	0.2%	*)although the uncertainty is of type A when the site calibration is derived, it turns to a type B uncertainty when applying the correction **)correlated over wind speed bins, but uncorrelated over wind direction bins
Uncertainty due to wind speed dependence of site correction factors	B	Y*	0.1%	*)Value for uncertainty derived from difference in AEP associated to power curves based on wind speed dependent site calibration and non wind speed dependent site calibration
Uncertainty due to dependence of site calibration on turbulence intensity	B	Y*	0.4%	*)Value for uncertainty derived from difference in AEP associated to power curves based on turbulence dependent site calibration and non turbulence dependent site calibration
Uncertainty due to variability of power curve data	A	N	0.3-0.4%*	*)Enercon 40 machine in moderately complex terrain
Anemometer effects* (over-speeding, sensitivity to vertical inflow etc.)	B	Y	2%	*) Only relevant for anemometer at the wind turbine location. Effects on the anemometer at the reference mast are (at least partly) included in the correction
Instruments' Type B				
Anemometer wind tunnel calibration (mast anemometer)*	B	Y**	3%*	*)two anemometers **)uncorrelated between anemometers
Anemometer Mounting effects*	B	Y	2%	*) Only relevant for anemometer at the wind turbine location. Effects on the anemometer at the reference mast are included in the correction
Anemometer signal recording*	B	Y**	0.3%	*) two anemometers **) uncorrelated between anemometers
Power transducer	B	Y	2%*	*) Assuming 0.5% accuracy in respect to measuring range of 250% of rated power
Current transformer	B	Y	0.5%	
Power signal recording	B	Y	0.6%	
Temperature sensor calibration	B	Y	0.3%	

Temperature sensor mounting	B	Y	0.3%	
Temperature signal recording	B	Y	0.3%	
Air pressure sensor calibration	B	Y	0.2%	
Air pressure sensor mounting	B	Y	0.1%	
Air pressure signal recording	B	Y	0.1%	
Total Uncertainty A+B				
Moderately complex terrain with experimental site calibration	A+B	N	5%*	*)observed difference to AEP of same turbine in flat terrain: 7%

7.2.3 Site Calibration, Mast and Parked Wind Turbine

Here, the power curve evaluation is based on site calibration using a nacelle anemometer on a parked turbine. The basic assumptions are: 1) A model of the nacelle has been investigated in a wind tunnel to identify appropriate positioning of the nacelle anemometer, 2) there is optional establishment of a correction at the nacelle position to account for vertically inclined air flow, 3) the turbine yaw system ensures alignment of the nacelle to the wind direction within +/- 20°, and 4) the nacelle anemometer has been calibrated in wind tunnel.

The total uncertainty is in this case estimated to be 6-8%, the highest value applying if no correction is made for inclined flow and/or if the nacelle does not track the wind direction.

Table 7.3. Site calibration uncertainty assessment – performance assessment using a met mast with experimental site calibration using a nacelle mounted anemometer on the parked wind turbine

Uncertainty Source/ Component	Type (A/B)	Correlated (Y/N)	Magnitude u_C/P	Comments
Lateral inclination of inflow (impact of nacelle body on nacelle anemometer during site calibration due to yaw hysteresis or systematic yaw offset during site calibration)	B	Y	1-2%*	*)According to wind tunnel measurements a yaw offset of 10° will result in an error of wind speed below 1% (2% in AEP). The uncertainty can be reduced by selecting only data without yaw error according to a measurement of the yaw position. An uncertainty of order 1 % in AEP remains due to a possible offset of the wind vane or the yaw signal and possible differences of the wind direction at the vane and the wind direction incident to the turbine.

Vertical inclination of inflow during site calibration (impact of nacelle body on nacelle anemometer during site calibration)	B	Y	1-6%*)	*) 6% uncertainty in AEP is valid for vertical flow inclination of about 20°. The uncertainty can be reduced by establishing a correction of the nacelle disturbance dependent on the vertical flow inclination from the wind tunnel measurements and to apply this correction during the site calibration according to measurements of the flow inclination. An uncertainty of order 1-2 % in AEP remains because the flow inclination at the turbine location might differ from the measured flow inclination (e. g. if measured at the met mast) and because of uncertainties of the correction established in the wind tunnel.
Systematic impact of nacelle body on nacelle anemometer during site calibration (apart from effect of nacelle misalignment or vertical inflow)	B	Y	2%*	*) position of nacelle anemometer should be chosen in a way that systematic flow disturbance is below 1% in wind speed according to wind tunnel investigation of nacelle model
Height difference between nacelle anemometer and hub	B	Y	2%	
Wind tunnel blockage (during investigation of nacelle model)	B	Y	0.3%	
Uncertainty also present at site calibration with two masts; results derived from measurements at Enercon 40turbine in moderately complex terrain				
Statistical uncertainty of site calibration correction factors	B*	Y**	0.2%	*)although the uncertainty is of type A when the site calibration is derived, it turns to a type B uncertainty when applying the correction **)correlated over wind speed bins, but uncorrelated over wind direction bins
Uncertainty due to wind speed dependence of site correction factors	B	**Y***	0.1%*	*)Value for uncertainty derived from difference in AEP associated to power curves based on wind speed dependent site calibration and non wind speed dependent site calibration

Uncertainty due to dependence of site calibration on turbulence intensity	B	Y*	0.4%	*)Value for uncertainty derived from difference in AEP associated to power curves based on turbulence dependent site calibration and non turbulence dependent site calibration
Uncertainty due to variability of power curve data	A	N	0.3-0.4%*	*)Enercon 40 machine in moderately complex terrain
Anemometer effects* (overspeeding, sensitivity to vertical inflow etc.)	B	Y	2%	*) Only relevant for anemometer at the nacelle. Effects on the anemometer at the reference mast are (at least partly) included in the correction
Instruments' Type B				
Uncertainty also present at site calibration with two masts; results derived from measurements at Enercon 40 turbine in moderately complex terrain				
Anemometer wind tunnel calibration (mast anemometer)*	B	Y**	3%*	*)two anemometers **)uncorrelated between anemometers
Anemometer mounting effects*****	B	Y	2%	*) Only relevant for anemometer at the nacelle. Effects on the anemometer at the reference mast are included in the correction
Anemometer signal recording*	B	Y**	0.3%	*)two anemometers **)uncorrelated between anemometers
Power transducer	B	Y	2%*	*) Assuming 0.5% accuracy in respect to measuring range of 250% of rated power
Current transformer	B	Y	0.5%	
Power signal recording	B	Y	0.6%	
Temperature sensor calibration	B	Y	0.3%	
Temperature sensor mounting	B	Y	0.3%	
Temperature signal recording	B	Y	0.3%	
Air pressure sensor calibration	B	Y	0.2%	
Air pressure sensor mounting	B	Y	0.1%	
Air pressure signal recording	B	Y	0.1%	
Total Uncertainty A+B				
If neither the nacelle position is detected nor a correction for vertical inflow is applied during site calibration	A+B	N	8%*	*)20% flow inclination assumed

If no nacelle position is detected but a correction for vertical inflow is applied during site calibration	A+B	N	6%	
If data with yaw misalignment are sorted out and a correction for vertical inflow is applied during site calibration	A+B	N	6%	

7.2.4 Performance Assessment, Applying Numerical Site Calibration (WasP)

When applying numerical site calibration the total uncertainty of the performance assessment is expected to as low as 4% in moderately complex terrain when uncertainties in different measurement sectors 'average out', and as high as 20% in complex terrain, where the model directly fails or sector-wise uncertainties do not average out. For higher total uncertainties, the action of numerical site calibration becomes the only significant source of uncertainty.

Table 7.4. Site calibration uncertainty assessment – performance assessment using a met mast with theoretical site calibration using a wind flow model

Uncertainty Source/ Component	Type (A/B)	Correlated (Y/N)	Magnitude u_C/P	Comments
Flow modelling	B	Y	1%-20%*	*) WASP modelling tested in moderately complex terrain against site calibration with two masts (Enercon 40 machine in Eifel mountains). The difference in AEP of the resulting power curves over the whole measurement sector (width=124°) is only 1%. The terrain effects are averaged out over the measurement sector. The sector with about the largest terrain slope showed also the largest difference between the WASP modelling and the site calibration with two masts of about 12 % in wind speed. The corresponding uncertainty in AEP within this sector is 20%.
Uncertainty also present at site calibration with two masts; results derived from measurements at Enercon 40turbine in moderately complex terrain				

Uncertainty due to wind speed dependence of site correction factors	B	Y*	0.1%*	*)Value for uncertainty derived from difference in AEP associated to power curves based on wind speed dependent site calibration and non wind speed dependent site calibration
Uncertainty due to dependence of site calibration on turbu-lence intensity	B	Y*	0.4%	*)Value for uncertainty derived from difference in AEP associated to power curves based on turbulence dependent site calibration and non turbulence dependent site calibration
Uncertainty due to variability of power curve data	A	N	0.3-0.4%*	*)Enercon 40 machine in moderately complex terrain
Instruments' Type B				
Uncertainty also present at site calibration with two masts; results derived from measurements at Enercon 40turbine in moderately complex terrain				
Anemometer wind tunnel calibration	B	Y	2%	
Anemometer Mounting effects	B	Y	2%	
Anemometer signal recording	B	Y	0.2%	
Power transducer	B	Y	2%*	*) Assuming 0.5% ac-curacy in respect to measuring range of 250% of rated power
Current transformer	B	**Y**	0.5%	
Power signal re-cording	B	Y	0.6%	
Temperature sensor calibration	B	Y	0.3%	
Temperature sensor mounting	B	Y	0.3%	
Temperature signal recording	B	Y	0.3%	
Air pressure sensor calibration	B	Y	0.2%	
Air pressure sensor mounting	B	Y	0.1%	
Air pressure signal recording	B	Y	0.1%	
Total Uncertainty A+B				
	A+B	N	4%-20*	*)4% if site effects cancel out over differ-ent wind direction sec-tors, 20% in steep slopes if WASP model-ling fails

7.3 C – Transducer Uncertainty

The uncertainties related to calibration of transducers are small compared to the uncertainties related to test procedures and methods. The application of the international standard IEC 61400-12 Ed 1 includes measurement of three primary quantities: wind speed, electric power and air density. Of these wind speed usually has the largest uncertainty attached, of the order 1-2% (in terms of power 2-6%). Assuming quality transducers are used, electric power and air density each have uncertainties less than 1%.

In terms of anemometer uncertainty, calibration need not any longer have major uncertainty. The bigger problem relates to in-service uncertainties caused by flow distortion and response to turbulent and inclined flows.

7.4 D – Analysis to Verify and Enhance Performance Assessment

The following table summarises the key uncertainty associated with the multi-variate performance assessment approach whilst the ensuing text gives commentary.

Table 7.5. Uncertainty sources inherent in multi-variate performance assessment

Uncertainty Source/component	Type (A/B)	Correlated (Y/N)	Magnetude u_C/P	Comments
Statistical uncertainty in multivriate approach	*A*	*Partially (the technique identifies covariances between variables)*	*Not evaluated as part of project*	'Conventional' power performance assessment is typically carried out over a three month period and it is assumed that the derived power curve is representative of the long-term. This is generally an invalid assumption, but the magnitude of the implied uncertainty is generally ignored. Multivariate analysis provides a method of both handling this phenomenon and of estimating associated uncertainty.

In Chapter 5 it was demonstrated that the power performance of a wind turbine depends upon more variables than are currently considered when establishing the conventional 'power curve' which only shows power as a function of wind speed, normalised for air density.

In reality, performance depends upon additional factors such as turbulence intensity, turbulence length scale, deviation of the mean wind vector from the rotor plane etc.

It has been demonstrated in Chapter 5 that a multi-variate 'model' of power performance characteristics can be developed which gives significantly better explanation of the performance data than is possible using the conventional approach.

This more comprehensive model allows relationships to be uncovered that can be used to create power curves that would apply to longer, more typical time scales, to different seasons or to different sites. For conventional power curve evaluation, there is no recognition that the climatic distributions encountered during the test can skew or bias the power curve.

The multi-variate model is based upon the application, on a wind speed bin-wise basis, of least squares regression analysis. To ensure validity of the model careful conditioning of the data is required. Relevant issues are normality of all data distributions, independence of the selected dependent variables, linearity of relationships and completeness of the model.

As for any regression analysis, the derived best-fit parameters are only approximations of the 'true' values and have associated statistical uncertainty. This means that any prediction based upon the model will also have uncertainty.

Assume the power performance process can be described by the relationship:

$$y(x) = +a_1 x_1 + a_2 x_2 + ... + a_M x_M$$

where y is power , x_i are the significant independent variables and a_i are the sensitivities.

The results of the parameter optimisation analysis can be used to estimate values of the dependent variable y from measurements of the independent variables x:

$$\hat{y}_k = +\hat{a}_1 x_{1,k} + \hat{a}_2 x_{2,k} + ... + \hat{a}_M x_{M,k}$$

where $\hat{y}$ is the best estimate of power based upon measurements of x and previously derived best estimates, $\hat{a}_{1..M}$, of the sensitivities.

The uncertainties in a are of type A and can be readily evaluated (details are not given here, but are included as an Annex to Ref 7.2) and can be represented by the covariance matrix $\sigma^2(a_{ij})$ of the fitted parameters. The diagonal elements are the variances of the individual parameters whereas the off-diagonal elements are the co-variances.

The statistical uncertainty involved in subsequently estimating the dependent variable, y_k, from a set of measurements $x_{1,k}$, $x_{2,k}$ … $x_{M,k}$ is given by

$$\sigma_y^2(k) = \sum_{j=1}^{j=M} \sum_{i=1}^{i=M} x_{ik} x_{jk} \sigma^2(a_{ij})$$

Within this project, these uncertainties have not been numerically assessed, but it is clear that a substantial improvement in explanation and a corresponding reduction in uncertainty is possible. The following figure, extracted from Ref 7.2 shows how real changes in power output for the same wind speed bin can be explained by a model having a multi-variate composition. Conventional power curves would predict an essentially horizontal line.

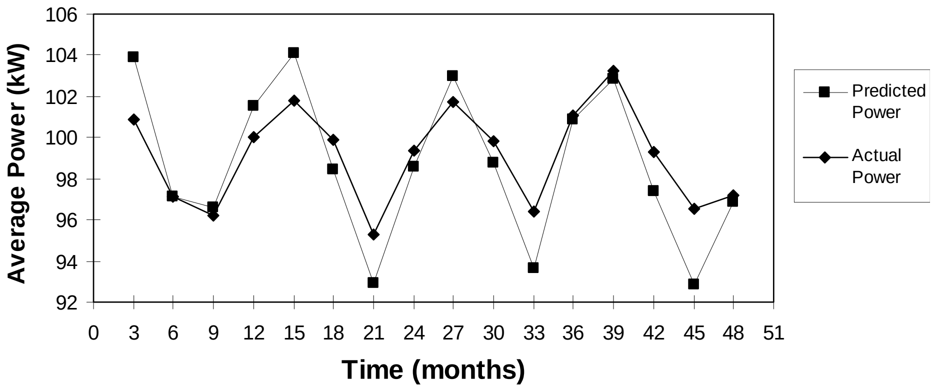

Fig. 7.1. Reduction in uncertainty possible with multi-variate analysis compared with the fixed level associated with conventional performance assessment

The multi-variate regression analysis studies undertaken in this project highlight an important point which is either not widely appreciated or conveniently forgotten, that being that conventional power performance curves change with time, not because the machine characteristics change, but because the distribution of the independent climatic variables do.

To use a power curve derived over a finite period of time or at one location in order to estimate performance over a longer period of time or at a different site is a fundamentally uncertain process.

By identifying a fuller power performance characteristic based upon additional significant variables in principle will allow a better quality extrapolation to be made either to different time periods or to different locations.

7.5 E – Density Correction

Of the variables, additional to hub height mean wind speed, that influence power output, air density is often the most important. This variable is the only additional variable already treated in standards, basically assuming that power is proportional to the weight of air. No improvement as to how to adjust for air density variations is proposed in the present work.

7.6 Summation

The uncertainties identified in the previous sections are summarised in the following table.

Table 7.6. Summary of uncertainty levels associated with various aspects of performance assessment

Method/component	Uncertainty in AEP
Mast, flat terrain and without site calibration	5+%
Site calibration with two masts	5+%
Site calibration, mast and parked wind turbine	6-8%
Numerical site calibration; WasP	4-20%
Nacelle anemometry	5-7% or more
Transducer uncertainty alone	<2%
Analysis to verify and enhance performance assess. (excl. air density)	?? 1-5%
Density correction (uncertainty after correction)	<1%

The results of the present analysis may be compared with those from previous analyses, (Ref. 7.2). There is a good match.. The new analyses performed in the present project do support conclusions made in the earlier work regarding current obtainable accuracy and to the future improvement of performance assessment methods.

7.6.1 Lowest Possible Uncertainty in 1999.

Employment of the procedures and methods outlined in this document opens up possibilities for reduction in uncertainties relative to “common practise”. The following proposals would help lower the upper uncertainty limit for a range of uncertainties in complex terrain.

- Rational estimation of reference power of a large fraction or all of the units in the wind farm would open up the possibility of a less uncertain estimate of the population mean of the plant power. The potential improvement depends on to what extent the per-unit estimates can be made independent. Assuming the per-unit uncertainties to be of the same size and to be uncorrelated, the uncertainty of the population mean estimate can be reduced to a small number (best case). On the other hand, assuming the per-unit uncertainties to be of the same size but fully correlated, the uncertainty of the population mean will be equal to the per-unit uncertainty (worst case).

- Numerical site calibration can potentially be improved, by applying numerical tools with the utmost care, and by calibrating the models with two or three met masts at the site. If financially feasible, experimental site calibration would improve results significantly.

- Especially in complex terrain, inclusion of a number of input variables in addition to wind speed will reduce uncertainty significantly. To obtain this effect, proper regression analysis tools must be applied.

- The plant blockage effect is not accounted for in present-day practise (and not described here; for further information, see Ref 7.1. For typical separations between met tower and wind farm, a correction can be made by means of numerical simulation.

It would seem difficult to reduce further the lower limits of the ranges for total uncertainty.

7.6.2 Future Improvements

It is suggested that the following actions would significantly improve accuracy of performance assessment:

- Identification of ways of ensuring that the per-unit uncertainties of reference power effectively are uncorrelated.
- Improvement of analytical/numerical methods for site calibration.
- Refinement and streamlining of multi-variate sensitivity analysis.
- Improvement of quality of design, manufacturing and understanding of the operation of the (cup) anemometer.
- Introduction of remote-sensing anemometry, which from the top of each wind turbine can measure wind speed at a freely chosen point in space in front of the machine.

Component	Uncertainty range 1999 (%)	Lowest possible in 1999 (%)	Potential, Future (%)
With separate met mast:			
Sensitivity analysis, experimental (Type A)	1-2%	1-2%	1-2%
Sensitivity analysis, numerical (Type B)	--	--	1-2%
Site calibration, experimental, homogeneous→complex	1-2% → 2-5%	1-3%	0-2%
Site calibration, numerical, homogeneous→complex	2-4% → 10-20%	2-10%	0-5%
Blockage effects, numerical, 5D→2D	2-4% → 6-8%	1-3%	0-2%
Instrument – anemometer, good practise→bad practise	2% → (20%)	2%	1%
Instruments – others, good instruments→poor instruments	1% → 2%	1%	0.5%
Method deficiencies	1-2%	1%	1%
Limited input variables, several variables→ U_{hub}	1-10%	1-3%	1-2%
Wake effects	--	--	--
TOTAL: Experimental methods	4-13%	3-6%	2-5%
Numerical methods	5-20%	4-11%	2-7%
With nacelle anemometer:			
+Nacelle anemometer blockage effects,	1% → 50%	--	--
+Wake effects on nacelle anemometer	1-2% → 5-10%	--	--
- site calibration	1-2% → 5-10%	--	--
TOTAL: experimental	5-30%	--	--

8 Recommendations

The following recommendations can be given as a result of the work described in Chapters 2 to 6.

8.1 Site Calibration

The following procedural recommendations can be given.

8.1.1 Site Calibration with Two Masts

When carrying out a site calibration with two masts as described in IEC 61400-12 Ed 1, the following suggestions are given.

- the sector size should be no greater than 10°; this should be reduced if the gradient of the correction factors from bin to bin is larger than 2%

- the minimum measuring period per 10° wind direction sector should be 24 hours in the wind speed range 4-16 m/s; there should be at least two hours of data sets above 8 m/s

It is suggested that future work should address whether site calibration can be improved by taking into account factors other than hub height wind speed, such as turbulence intensity. A solution could be to derive site correction factors for different wind speed bins at different turbulence levels. The width of the data classes should be matter of future investigations. It may well be that a very extensive data set might be needed to fully delineate such effects, and this may not always be practical. The use of multi-variate analysis should be considered.

8.1.2 Alternative Site Calibration with Parked Turbine

The following recommendations are given.

- Before undertaking a site calibration using an anemometer mounted on the nacelle of a parked turbine, the flow around a scale model of the nacelle should be investigated in a wind tunnel, preferably with Laser Doppler Anemometer to find a suitable anemometer position. If possible a position should be found where flow distortion is less than 1% of the free tunnel flow. If this is not possible, a correction factor for the nacelle anemometer should be derived. The flow should be examined at incident angles to the nacelle both in the horizontal and the vertical direction.

- According to IEC 61400-12 Ed 1, the vertical displacement of the cup anemometer from hub height should be ±2.5% of hub height. As these limits cannot normally be met with nacelle anemometers, the vertical wind speed profile as measured at the reference mast should be used to correct the wind speed measured by the nacelle anemometer to hub height. Alternatively, deviations from hub height larger than 2.5 % should be taken into account in form of an uncertainty calculation.

- During the open-field site calibration test the wind turbine's yaw system should allow to follow the wind direction. Only measurements within the yaw misalignment limit found to be acceptable from the wind tunnel test should be used.

- The nacelle anemometer readings, if necessary corrected according to the wind tunnel measurements and the vertical wind speed profile, should be regressed against the wind speed at the reference met mast by a linear regression forced through the origin. Any deviations from unity during the site calibration are now due to terrain effects.

- The model of anemometer used on the nacelle should be the same as on the reference mast.

8.1.3 Site Calibration via Flow Modelling

Site Calibrations should not be based on modelling

8.1.4 Self Consistency Test

The method described in Chapter 2 should be applied to gain confidence in the integrity of the test data.

8.2 Nacelle Anemometry

From the work outlined in Chapter 3 on the potential of nacelle anemometry, the following recommendations can be given.

The major aims of the investigations described in Chapter 3 were to clarify whether, and under what conditions, the relation between the met mast and the nacelle anemometer remains the same or whether it deviates by a known and predictable amount.

Before giving advice on this, some comments are provided on the basic methods recommended for establishing nacelle-to-free-wind-speed relationships.

8.2.1 Defining the Basic Correction Factors

The following advice is given:

- Data should be collected in a manner that follows the experimental principles of IEC 61400-12 Ed 1in terms of definition of free wind speed seen by the turbine.

- To define the base relationship, free field wind speed averaged over ten minutes should be binned against the wind speed measured with the nacelle anemometer

- The correction should be established with one of the following techniques depending upon the nature of the data:

i. (Non linear) regression of the bin averaged wind speed - the method gives good results but since the choice of function can be highly subjective, it is best avoided

ii. Rather than binning wind speed, the ratio of met mast to nacelle wind speed can be binned giving a binwise correction factor. Binwise corrections are to be preferred since they make no assumptions regarding the physical relationship. A disadvantage is that neighbouring data points, which belong to different bins, could be corrected by very different amounts.

iii. A refinement of the binwise correction of the nacelle anemometer is to use a linear interpolation of the correction factors between bins.

- The correction procedure should be chosen according to the associated uncertainty. A criterion for this choice can be based on a statistical comparison between the corrected nacelle anemometer readings and the mast measurements. The corrected nacelle anemometer should reproduce the wind speed measured at the mast with a standard error of below 0.1 m/s in the most important wind speed range (e.g. 4-16 m/s). In the case of a regression, the statistical uncertainty of the regression coefficients should be considered. In the case of a binwise correction the statistical uncertainty of the bin averages should be considered (<1% is desired in the wind speed range 4-16 m/s).

- Where the number of data points within a bin is limited, and this obviously affects the calculations, the two neighbouring bins can be used to produce an interpolated, inferred and revised figure.

8.2.2 Transferability of Nacelle Anemometer Corrections to Other Turbines of the Same Type

For the successful application of the nacelle anemometer method for power curve verifications, a number of requirements must be fulfilled:

- All individual anemometers should be calibrated according to Measnet procedures (Ref 8.1).

- The mounting arrangement and the type of the nacelle anemometer should be identical at the turbine to be tested and at the turbine that was used for the determination of the correction to the ambient wind speed.

- The signal conditioning of the nacelle anemometer signal should be calibrated and documented.

- It is best to use nacelle anemometers that are insensitive to vertically inclined airflow.

- The position of the anemometer on the nacelle should be chosen carefully. It should always be assumed that the manufacturer’s normal position for the anemometer is non-ideal and better options should be explored.

8.2.3 Limitations of Nacelle Anemometry

It has been demonstrate that the nacelle-to-free-wind-speed relationship can be sensitive to the wind turbine settings (e.g. different pitch angles) and to inclined airflow in complex terrain. It has also been shown that operation in wake situations can produce distortions in the results.

To overcome these problems, the following recommendations are offered:

- The sensitivity to wind turbine setting should be determined by operating the turbine for short periods with different rotor settings (e.g. pitch angle). For stall regulated turbines at least two different blade angles should be used.

- In terms of terrain induced, vertical inclination effects, it may be possible to minimise any influence by finding a position where the effect is negligible. Another solution is to reduce the valid wind direction sector for the power curve evaluation to reflect acceptable limits in the terrain slope.

- Sectors in which the wind turbine operates in the wake centre of nearby wind turbines should be excluded. A useful method for choosing valid sectors is to delineate the performance data into narrow sectors and to exclude those in which apparent performance is obviously unrealistic or deviant.

8.2.4 Self Consistency Checks

The need to limit directional sectors in nacelle based performance verifications was outlined above.

- In confirming that the sectors chosen are consistent, it is recommended that a checking procedure is applied wherein wind speed is inferred from power measurements according to the following method:

- As a first step a temporary and density normalised power curve is evaluated from an open sector preferably having gentle terrain slopes.

- The data measured during the power curve verification is then re-analysed. The wind turbine itself is used as an anemometer (with the power to wind speed relationship being as defined by the temporary power curve) and wind speeds for each ten minute period are calculated. A reverse density normalisation is applied. The wind speed can only be calculated in the below rated power range.

- The ratio of corrected nacelle anemometer wind speed to wind speed inferred from electrical power are evaluated by bin averaging or regression analysis within narrow wind sectors (5°-10°).

- In the sectors valid for power curve evaluations the wind speed ratio should be near unity (within 2%). Deviation of the ratios from unity directly indicates a terrain or wake induced error in the wind speed determination.

- The final power curve should then be re-calculated from the sectors in which agreement is good.

8.3 Transducer Uncertainty

From the work reported in Chapter 4, the following brief recommendations can be given.

8.3.1 Identification of Anemometer Performance Characteristics Under Influences of Non-Horizontal Wind and Shear Wind Regimes

Measurement errors introduced by cup anemometer(s) due to unknown sensitivity to vertical flow inclination angle can be corrected using cup inclination test data.

Similarly, if horizontal shear wind tests were carried out for defining errors introduced by cup anemometer under shear wind regimes, this error type could also be quantified as part of the anemometer calibration procedure.

8.3.2 In-service Evaluation of Anemometer Uncertainty

From the 3-dimensional modelling studies outlines in Chapter 4, it is clear that evaluation of the in-service uncertainty of cup anemometers is possible. Although the process is not simple, it has been shown that tests and simulations can be carried out to provide a realistic estimate of uncertainty.

It is recommended that a system be set up for anemometers which will allow manufacturers and users alike to classify the uncertainty levels for anemometers.

8.3.3 Evaluation of Voltage, Current and Power Uncertainty

The 0.5 class index for current and voltage transducers represents 0.5% voltage and current error at standard room temperature. It does not reflect the power measurement uncertainty, which has been calculated to be around 1% due to thermal effect. For an accurate assessment, the uncertainty should be expressed in terms of percentage of power uncertainty within the operating temperature range.

8.3.4 Determination of Power Quality Using Power Spectrum Analyser

It has been shown using a power quality analyser that the average loss of power due to filtering of harmonic voltages and currents could be up to 0.2%. For accurate assessment of power output from wind turbines, it is helpful to compare the turbine’s power quality characteristics against the specifications for the instruments to be used for the performance assessment

8.4 Method to Enhance Performance Assessment - Multivariate Measurement of a Wind Turbine Power Curve

As shown in Chapter 5, wind turbine power performance is not solely dependent upon wind speed. A number of important additional parameters and variables have a discernible impact on performance. A basic hypothesis is that if a sufficient number of relevant variables are considered, then a generalised and universally applicable power relationship should be derivable. In addition to mean wind speed, the power curve is a function of turbulence intensity, flow inclination, wind shear, standard deviation ratio, air density and standard deviation of wind direction. A procedure, based on regression analysis, that can be used to derive the power curve, is given below. Great care must be taken when applying regression tools as misleading results are easily obtained if the fundamental assumptions of multiple regression are not adhered to.

8.4.1 Measurement of Secondary Independent Variables

All variables should be measured concurrently. The analysis is based on average measurements and the averaging period for each variable must be the same, a maximum averaging period of 10 minutes is recommended. Ideally a meteorological mast calibrated for the test turbine should be used, however this is not always practical and alternative measurement methods are given below. Measurement of mean horizontal wind speed, the most important parameter and of power, the dependent variable, are dealt with elsewhere in this report.

The derivation of a multivariate model for turbine power is complex and a significant amount of data is required. In each 1 m/s wind speed bin, a minimum of 2000 samples is required. The data in each bin must also adequately cover the range of all the secondary variables.

8.4.2 Turbulence Intensity

Turbulence intensity is measured as the standard deviation of the mean horizontal wind speed divided by the mean wind speed. If measured on a meteorological mast a calibration should be applied to account for the difference in turbulence between the meteorological mast and the wind turbine. This correction should be measured during site calibration. Alternatively, turbulence can be measured using a nacelle mounted anemometer.

8.4.3 Flow Inclination

Flow inclination is defined as the deviation of the wind flow from the horizontal. Ideally, it should be measured directly on a meteorological mast using an inclinometer or a sonic anemometer, for example. Such measurements should be corrected for differences in flow angle between the mast and the test turbine. The correction should have been previously derived during site calibration. Alternatively, an estimate of flow inclination can be made based upon the terrain slope local to the wind turbine. Use of the Richardson model is recommended.

8.4.4 Wind Shear

Wind shear should be measured on a meteorological mast using at least two measurement heights. As usual the measurements should be corrected to account for terrain affects between the mast and the turbine. Ideally this correction should be derived from measurements obtained during site calibration. However if the turbine is remote from the mast and such measurements are unavailable, then a wind flow model such as WAsP or MS3DH can be applied at each measurement height.

8.4.5 Standard Deviation Ratio

Standard deviation ratio is defined as the ratio of the standard deviation of power to the standard deviation of wind speed. It represents the extent to which the turbine can respond to rapid changes in wind speed and arises as a parameter due to the mismatch between the bandwidth of a turbine and the bandwidth of a cup anemometer. To obtain this parameter the standard deviation of turbine power is measured and divided by the standard deviation of wind speed.

8.4.6 Air Density

Measurement of air density is covered elsewhere in this report and it is thought to be adequate to have a single measurement for the whole site.

8.4.7 Standard Deviation of Wind Direction

This variable is the mean standard deviation of the wind direction over the averaging period. It will be measured on the met mast and it is currently not known how to correct such data for terrain effects. However, a wind flow model has been developed that may be appropriate.

8.4.8 Completeness

Not all variables described above will necessarily be important at the test site, moreover there may be additional variables that describe the wind environment that are not listed above. For example on a very flat site, flow inclination will probably not vary. In general, the more complex the terrain, the more parameters there are that are important. It is important in the regression analysis that all variables that effect the dependent variable are included in the model. Otherwise the resulting model can be incorrect. Unless a variable is obviously be redundant, then it should be considered, if at a later stage it turns out to be insignificant then it will not be used in the final model of the power curve.

8.4.9 Linearisation of Independent Variables

An assumption in regression analysis is that the underlying relationship between each individual independent variable and the dependent variable is linear. It is important that this rule is obeyed, otherwise an incorrect model can result. It is obvious that turbine power is not a linear function of all the independent variables under consideration, therefore each variable in turn needs to be assessed and possibly transformed.

Initially, produce a scatter-plot of the data and look for obvious non-linearities. It is often difficult to see whether there is a non linear relationship and a residuals plot may highlight any curvature. A residuals plot is produced by performing a regression and plotting the residuals. If there is no linear relationship then the residuals will be randomly distributed around the x-axis in a horizontal band. If there is any pattern, then there may be non-linearity.

Identifying non-linearity is made more difficult as inevitably some of the independent variables will be correlated. Ideally, any collinearity should be removed before attempting to identify non-linear relationships. However, methods to remove collinearity are also based on the assumption of linearity between the independent variables! A solution is to produce a scatter-plot of each independent variable against power, keeping all other independent variables constant. This requires an enormous amount of data, so practically compromises may need to be made by using and verifying known physical relationships and empirical relationships derived form historical data.

After identifying non-linearities, the independent variables should be transformed so that their relationship to power is linear.

8.4.10 Removing Collinearity

At this point a set of linearised independent variables has been obtained. The analysis should now continue by dividing the data into 1 m/s wind speed bins and deriving a separate model for each wind speed bin. It may be that in the future when more experience has been gained that computation can be reduced by dividing the power curve into three sections, below rated, at rated and above rated and linearising wind speed within each section.

Collinearity arises when two or more independent variables are highly correlated. The presence of collinear variables in a regression model is damaging as it is difficult for the model to identify the separate effects of each variable. This leads to large standard errors, which in turn signals that the coefficient estimate for the sample may not be close to the true coefficient of the population. Therefore the model becomes specific to a single data set and its variable coefficients may not make physical sense.

The presence of collinearity between independent variables can be identified by a measure known as Tolerance (T):

$$T = 1 - R^2$$

Where R^2 is the amount of variance in one independent variable that can be explained by the other independent variables in the model.

Ideally therefore, the Tolerance of each independent variable should be 1. Tolerances less than 1 mean that collinearity exists between the variables. However, the level of collinearity (whether it is harmful or not) and the sets of variables which are affected, cannot be determined by T.

A statistic known as a condition index can indicate whether collinearity is distorting the results of a regression model. Condition indices are derived from eigenvalues. The eigenvalues for each independent variable are initially calculated. The condition index of a variable is then the square root of the largest eigenvalue divided by the eigenvalue for that variable. Condition indices larger than 15 suggest a potential problem and condition indices greater than 30 suggest a serious problem.

To remove the problem of collinearity that exists between the independent variables, two methods can be considered. The first method is Principle Component Analysis (PCA). PCA results in a number of orthogonal components each of which is a linear combination of the independent variables. The components are completely uncorrelated each with a Tolerance equal to 1. The components can then be used in a regression model to predict turbine power, with no risk of collinearity. All components should be taken forward into the final model of power and significance tests can be performed at a later stage to establish whether some components can be discarded

A problem with principle components is that the underlying physical relationship between the original variables and the dependent variable, turbine power, is not obvious. It is therefore difficult to check whether the model makes physical sense. For this reason an alternative approach, described below, can be used.

The second method used to remove collinearity problems uses the residuals of the independent variables rather than the variables themselves. Each variable in turn is predicted using a linear combination of the remaining variables. The difference between the original variable and the modelled variable (residual) then becomes the new variable for use in the final regression model. These new residual variables then describe the variance of the original variable that cannot be explained by a linear combination of the other independent variables.

In order that the residual variables are not specific to one data set, they should be derived for at least 10 distinct data sets and then averaged. Standard significance tests should be applied when deriving each residual variables to determine which of the remaining independent variables are important.

Tolerances and condition indices should be calculated for the new independent variables to check that collinearity has been successfully removed.

8.4.11 Normal Distribution of Variables

A further condition of regression analysis is that all independent variables are normal. To check this, plots can be produced of each variable against ordered observations from a normal distribution with zero mean, known as a probability plot. A diagonal line from the origin to the top right of the graph means that the variable is normally distributed. If it is concluded that an independent variable is not normally distributed then it should be transformed at this stage.

8.4.12 Regression Model of Turbine Power

At this stage, the independent variables should have been linearised, rendered independent and normalised, therefore as long as all the important parameters have been included, all the conditions of regression have been met. A multiple regression analysis should now be performed with power as the dependent variable and the normalised principle components or residual variables as the independent variables.

It is important to derive a model that is not specific to any one data set. Although every effort will have been made to transform the data to a form that is appropriate for regression, practically certain compromises will have been necessary. A further technique that can be used to ensure that the model is robust and generic is to divide the data into at least 10 distinct sets. Each set should have at least 200 points. A multiple regression is then performed on each data set. The resulting coefficients from each data set should then be compared. If they differ greatly then this is an indication of a problem with the data, either non-linearity, collinearity or an incomplete model. Small discrepancies between coefficients are expected and differences in just one or two data sets can be ignored. Overall, the resulting regression coefficients should be similar between data sets, indicating the same underlying relationships.

Coefficients for the final model of turbine power, are derived by averaging the regression coefficients across all data sets. Significance tests should be carried at with each calculation, it may be that one or more of the independent variables or principle components are found to be non-significant and can be discarded. Care should be taken when averaging the coefficients so that extreme values or rogue results are not included. Finally the model for predicting power should be simplified by substituting the equations for the residual variables or principle components form sections 4.0 and 5.0 into the final regression equation for turbine power.

8.4.13 Assessing the Relative Importance of Independent Variables

The relative influence of each independent variable on turbine power, can be interpreted using standardised regression coefficients. The standardised regression coefficient is calculated as:

$$\tilde{b} = b\frac{S_x}{S_y}$$

where h

$\tilde{b}$ is the standardised regression coefficient
b is the raw coefficient
S_x is the standard deviation of the independent variable
S_y is the standard deviation of the dependent variable

The standardised coefficient is interpreted as the number of standard deviations that the dependent variable changes when an independent variable changes by one standard deviation. It is equal to the ordinary or raw regression coefficient which would have been calculated had the variable been converted to a standardised variable, with a mean of zero and a standard deviation of one. Standardised regression coefficients are sometimes known as Z scores.

8.5 Density Correction

Brief recommendations from the work described in Chapter 6 are given below.

8.5.1 Air Density/Wind Speed Normalisation Procedure for Wind Turbines

The proposed normalisation equations should not be used for small wind turbines (i.e. machines below 10 kW). This is because small machines are more sensitive to turbulence and local effects, which have not been taken into account in this study. For stall regulated machine, the existing IEC 61400-12 equation is well established. For pitch regulated (fixed speed) machines, new equations as given in Chapter 6 for wind speed normalisation are recommended. For pitch regulated (variable speed) machines, the equation recommended by the IEC should be used as it is conservative and simple. However, other equations as given in Chapter 6, which combine air density and wind speed normalisation, can be used as an alternative for validation purposes.

8.5.2 Establishment of Empirical Relationship Between Wind Climate and Power Performance

Results presented in Chapter 6 suggest that there is an empirical relationship between air density and power performance.

Given the requirements for multi-variate regression analysis, significant quantities of data are likely to be required before full dependencies, including those involving air density, can be extracted confidently.

9 Acknowledgements

The work described in this report was made possible by Directorate General XII of the European Commission. The financial assistance is gratefully acknowledged by the participants in the project.

10 References

2.1 Albers, A., Klug, H., Westermann, D. European wind turbine testing procedure developments. Activities of DEWI within project task 3.1A – site calibration. DEWI. 1 Dec 1998.

2.2 Albers, A., Klug, H., Söker, H. Wind speed, turbulence and wake evaluation based on wind turbine data. European wind energy conference 97. Dublin. 1997

3.1 Albers, A., Klug, H., Westermann, D. European wind turbine testing procedure developments. Activities of DEWI within project task 3.1A – site calibration. DEWI. 1 Dec 1998.

3.2 Antoniou, I., Pedersen, T. F., Frandsen, S. Activities within the projects I) Wind turbine testing procedure development, task 1 SMT4-CT96-2116 and ii) Power performance assessment JOR3-CT96-0114. Report Risø-I-1420(EN). Risø National laboratory, Denmark. April 1999.

4.1 Lee, W.K., McCourt, M., Davy, W., Noble, D. European wind turbine testing procedure, task 1C instrumentation accuracy, sub-task 1C1 – review of uncertainty sources for cup anemometers and definition of characteristics for particular instruments. Report 219/99. National Engineering Laboratory, United Kingdom. May 1999

4.2 Lee, W.K., Kakaiya, S. European wind turbine testing procedure, task 1C instrumentation accuracy, sub-task 1C.2 - simulation of anemometer responses in a 3-D wind regime. Report 255/99. National Engineering Laboratory, United Kingdom. June 1999

4.3 Lee, W.K., Davy, W. European wind turbine testing procedure developments, task 1C instrumentation accuracy, sub-task 1C.3 – uncertainties in other transducers. Report 114/99. National Engineering Laboratory, United Kingdom. May 1999.

4.4 Mann, J., Simulation of 3-D wind velocity vector as a function of time. Risø National Laboratory, Denmark. May 1999.

4.5 Mann, J., Models in Micrometeorology, Risø National Laboratory, Denmark, March 1994

4.6 Pedersen, T.F. A Procedure for classification of cup-anemometers. Risø National Laboratory, Denmark

5.1 Ruffle, R. Wind turbine performance assessment. ETSU agreement W/11/00429/00/00. Report 067/RES/2004 Issue 01. RES, United Kingdom. March 1999.

5.2 Frandsen, S. et al. Power performance assessment. Contract JOR3-CT96-0114. Final report. Chapter 4 – Wind turbine sensitivity to variables. Risø National Laborator, Denmark. Dec 1998.

5.3 Hannah, P. Investigation of upflow on escarpments. Report W/36/00281/35/REP. Energy Technology Support Unit, United Kingdom. 1997.

5.4 Ruffle, R. Twelve monthly progress report on power performance analysis of historical wind farm data. Report 067/RES/1022 Issue 1. Renewable Energy Systems Ltd, United Kingdom. Dec 1997.

5.5 Dunbabin, P. Regression analysis of data from Vindeby and Alsvik. Report 067/RES/2002 Issue 1. Renewable Energy Systems, United Kingdom. Dec 1998.

6.1 Albers, A. Air density correction of power curves. German Wind Energy Institute (DEWI), Germany. Dec 1995.

6.2 Pedersen, T.F. Air density normalisation. Risø National Laboratory, Denmark. March 1996.

8.1 Frandsen, S. et al. Power performance assessment. Final report under contract JOR3-CT96-0114. Risø National Laboratory, Denmark. June 1999.

8.2 Ruffle, R. Wind turbine performance assessment. Final report. 067/RES/2004 Issue 01. Energy Technology Support Unit, United Kingdom. March 1999.

8.3 MEASNET Measurement procedure for cup anemometer calibrations. 1997

Bibliographic Data Sheet **Risø-R-1209(EN)**

Title and authors

European Wind Turbine Testing Procedure Developments

Part 1 Measurement Method to Verify Wind Turbine Performance Characteristics

Raymond Hunter, RES Task coordinator
Troels Friis Pedersen , RISØ Project coordinator
Penny Dunbabin, RES
Ioannis Antoniou, RISØ
Sten Frandsen, RISØ
Helmut Klug, DEWI
Axel Albers, DEWI
Wai Kong Lee, NEL

ISBN	ISSN
87-550-2752-0 87-550-2753-9 (Internet)	0106-2840
Department or group Wind Energy Department	Date January 2001
Groups own reg. number(s)	Project/contract No(s) CMT4-CT96-2116
Sponsorship	

Pages	Tables	Illustrations	References
120	28	72	20

Abstract (max. 2000 characters)

There is currently significant standardisation work ongoing in the context of wind farm energy yield warranty assessment and wind turbine power performance testing. A standards maintenance team is revising the current IEC (EN) 61400-12 Ed 1 standard for wind turbine power performance testing. The standard is being divided into four documents. Two of them are drafted for evaluation and verification of complete wind farms and of individual wind turbines within wind farms. This document, and the project it describes, has been designed to help provide a solid technical foundation for this revised standard. The work was wide ranging and addressed 'grey' areas of knowledge, regarding existing methodologies or to carry out basic research in support of fundamentally new procedures.

- The work has given rise to recommendations in all areas of the work, including site calibration procedures, nacelle anemometry, multi-variate regression analysis and density normalisation.

Descriptors INIS/EDB

ANEMOMETERS; CALIBRATION; DATA COVARIANCES;
PERFORMANCE TESTING; PERFORMANCE; RECOMMENDATIONS;
SITE CHARACTERIZATION; VERIFICATION; WIND; WIND TURBINE ARRAYS;
WIND TURBINES

Available on request from Information Service Department, Risø National Laboratory,
(Afdelingen for Informationsservice, Forskningscenter Risø), P.O.Box 49, DK-4000 Roskilde, Denmark.
Telephone +45 4677 4004, Telefax +45 4677 4013, email: risoe@risoe.dk